DOCTORAL (PhD) DISSERTATION

UTILIZATION OF THE BAUXITE RESIDUE TO RECOVER SCANDIUM RARE EARTH ELEMENT

Compiled within the framework of the

University of Pannonia

Doctoral School of Chemical Engineering and Material Sciences

Written by:

Ali Dawood Salman

MSc in Chemical Engineering

Supervisor:

Dr. habil. Tatjána Juzsakova

Associate professor

DOI:10.18136/PE.2023.843

Sustainability Solutions Research Lab

Research Centre for Biochemical, Environmental and Chemical Engineering

Faculty of Engineering

University of Pannonia

Veszprém, Hungary

2023

Utilization of the Bauxite Residue to Recover Scandium Rare Earth Element

Thesis for obtaining a PhD degree in the Doctoral School of Chemical Engineering and Material Science of the University of Pannonia in the branch of Bio, Environmental and Chemical Engineering Sciences

Written by Ali Dawood Salman

Supervisor(s): Dr. habil. Tatjána Juzsakova

propose acceptance (yes / no)

(supervisor/s)

As reviewer, I propose acceptance of the thesis:
Name of Reviewer: …..... …..... yes / no

(reviewer)

Name of Reviewer: …..... …..... yes / no

(reviewer)

The PhD-candidate has achieved ….....% at the public discussion.

Veszprém

…….

(Chairman of the Committee)

The grade of the PhD Diploma …..... (…….. %)
Veszprém

(Chairman of UDHC)

ABSTRACT

Bauxite residue, better known as red mud (RM), is an industrial waste generated during alumina production containing residual minerals of bauxite ore. Stockpiling of huge amounts of residue can create environmental problems. Red mud comprises iron, aluminium, titanium, sodium and even more interestingly, valuable rare earth elements (REEs) such as scandium, lanthanum, yttrium. The REEs, and scandium in particular, are generally more enriched in residues originating from karst bauxites. Scandium holds 95% of the rare-earth economic value in the red mud and is associated with hematite, goethite, and anatase. This work devoted to recovery of scandium from Ajka, Hungarian red mud by liquid-liquid/solvent extraction (SX), ion exchange (IX) and solid-liquid extraction (SLE). The presence of a high iron content (~40 wt%) in red mud makes it difficult to recover scandium due to the similarity of their physicochemical properties. In this study, hydrometallurgy methods (leaching and solvent extraction) were used to recover Sc and remove dissolved, co-extracted elements such Fe, Al, Ti, La, Y from RM leachates. Five protocols for the Sc extraction and purification based on organophosphorus compounds (OPCs) namely bis(2-ethylhexyl) phosphoric acid (D2EHPA), tributyl phosphate (TBP) and trioctylphosphine oxide (TOPO) were proposed and evaluated. The results showed that the SX by using two cycles of diethyl ether was efficient to extract 99% of Fe(III) from hydrochloric red mud leachate as $HFeC1_4$ prior to scandium extraction. Among the suggested five Protocols, the Protocol C, multi solvent extraction by TBP extractant, showed exceptional performance in terms of 81 % Sc recovery efficiency from leachate. To improve and develop the scandium selectivity, several macrocyclic compounds were investigated such as dicyclohexano-18-crown-6 (DC18C6), kryptofix 2.2.2 (K 2.2.2) and diaza-18-crown-6 (C 2.2) as novel extractants for scandium using response surface methodology (RSM). The results of optimization obtained using STATISTZICA and WinQSB softwares showed the maximum Sc extraction efficiency by K 2.2.2, C 2.2 and DC18C6 can be obtained under the following optimum conditions: 0.006 mol/L concentration of K 2.2.2, C 2.2 and DC18C6, 11 min contact time, pH 4 of the aqueous solution and 75 mg/L initial Sc concentration are 99%, 97% and 15%, respectively.

In a step towards applying the concepts of green chemistry, elimination of organic solvent used, three Fe_3O_4/SiO_2/OPCs solid phase for Sc extraction were synthesized by sol-gel method involving organophosphorus compounds such as D2EHPA, TOPO and TBP. The successes immobilisation of OPCs was confirmed by a variety of characterisation techniques, including FTIR, SEM, and EDX. The results revealed that, the preliminary findings were harmonized with the results of SX systems. Among the prepared SP nanocomposite, Fe_3O_4/SiO_2/TBP showed superior selectivity (97 %) toward Sc removal from leachate compared with other elements and remaining elements were extracted in smaller amount (5% Al, 0.4% Fe, 12% Ti, 22% La and 7% Y).

Keywords: bauxite residue, scandium, organophosphorus extractants, macrocyclic extraction compounds, extraction Fe_3O_4/SiO_2/OPCs solid phase

الملخص

مخلفات البوكسايت او مايعرف بالطين الاحمر هي مخلفات صناعية تنتج أثناء عملية إنتاج الألومينا وعادة تحتوي على المعادن المتبقية من خام البوكسايت. يمكن أن يؤدي تخزين هذه الكميات الهائلة من النفايات إلى مشاكل بيئية عديدة . بشكل عام تتألف مخلفات البوكسايت بشكل أساسي من الحديد والألمنيوم والتيتانيوم والصوديوم بالاضافة الى العناصر الأرضية النادرة ذات القيمة الاقتصادية مثل سكانديوم ، اللانثانم ، الإيتريوم. عادة ما تكون العناصر الأرضية النادرة والسكانديوم على وجه الخصوص أكثر تركيز في المخلفات الناشئة من البوكسايت بعد عملية انتاج الألومينا .من بين هذه العناصر المهمة هو السكانديوم بسبب تطبيقاته الصناعية الحديثة حيث يشكل السكانديوم 95٪ من القيمة الاقتصادية لعناصر الارض النادرة في مخلفات البوكسايت. بناءا على ما سبق

تم تخصيص هذا العمل لاستعادة عنصر السكانديوم من مخلفات البوكسايت المجري عن طريق دراسة الاستخلاص المذيبي بالمذيبات العضوية (SX) ، والتبادل الأيوني (IX) والاستخلاص بواسطة السائل الصلب (SLE). من اهم المشاكل التي تمت مواجهتها في عملية الاستخلاص هي وجود نسبة عالية من الحديد (حوالي 40٪ بالوزن) في مخلفات البوكسايت وهذا يجعل من الصعب استعادة عنصر السكانديوم بسبب تشابه خواصهم الفيزيائية والكيميائية. وبناءا على ذلك ، تم استخدام طرق المعالجة (الترشيح والاستخلاص بالمذيبات) لاسترداد العناصر المذابة والمستخرجة بشكل مشترك مثل Fe، Al، Ti، La، Y من راشح مخلفات البوكسايت. حيث تم اقتراح وتقييم ولاول مرة خمسة بروتوكولات لاستخلاص وتنقية السكانديوم بواسطة مركبات الفسفور العضوية (OPCs) وهي حمض الفوسفوريك (2-إيثيل هكسيل) (D2EHPA) وفوسفات ثلاثي بيوتيل (TBP) وأكسيد ثلاثي أوكتيل فوسفين (TOPO). أظهرت النتائج أن مرحلتين من الاستخلاص بواسطة ثنائي إيثيل الإيثر كان فعالاً ازالة 99٪ من الحديد الثلاثي Fe(III) من محلول راشح مخلفات البوكسايت على شكل $HFeC1_4$ قبل الشروع باستخلاص السكانديوم. من بين البروتوكولات المقترحة ، أظهر البروتوكول C ، وهوالاستخلاص المذيبي المتعدد بواسطة مستخلص TBP ، أداءً استثنائيًا من حيث كفاءة الاسترداد التي وصلت الى 81٪ من السكانديوم الموجود في المحلول الحامضي . كأتجاه بحثي أخر ولتحسين انتقائية السكانديوم وتطويرها ، تم اختبار الاستخلاص من محاليل قياسية بأستخدام عدد من المركبات متعددة الحلقات لاول مرة تستخدم قي استخلاص السكانديوم مثل dicyclohexano-18-crown-6 (DC18C6) و kryptofix 2.2.2 (K 2.2.2) و diaza-18-crown-6 (C 2.2) باستخدام منهجية الاختيار الامثل . أظهرت نتائج الاختيار الافضل التي تم الحصول عليها باستخدام البرامج الاحصائية STATISTZICA و WinQSB ان أقصى كفاءة استخلاص للسكانديوم بواسطة K 2.2.2 و C 2.2 و DC18C6 يمكن الحصول عليها في ظل الظروف المثلى التالية: 0.006 مول / لتر تركيز K 2.2.2 و C 2.2 و DC18C6، 11 دقيقة من وقت الاستخلاص ، ودرجة الحموضة 4 للمحلول المائي وتركيز للسكانديوم الأولي 75 مجم / لتر 99٪ ، 97٪ و 15٪ على التوالي.

في خطوة نحو تطبيق مفاهيم الكيمياء الخضراء والتخلص من المذيبات العضوية المستخدمة سابقا، تم تصنيع ثلاث انواع من المتراكبات النانوية الصلبة Fe_3O_4 / SiO_2 / OPCs تتضمن مركبات الفوسفور العضوية مثل D2EHPA و TOPO و TBP. تم تأكيد نجاح تثبيت هذه المركبات من خلال مجموعة متنوعة من تقنيات

التوصيف ، مثل FTIR و SEM و EDX. أظهرت النتائج أن النتائج الأولية ان من بين المتراكبات النانوية المصنعة ، Fe_3O_4 / SiO_2 / TBP اظهر انتقائية فائقة وصلت الى (97٪) استخلاص نحو عنصر السكانديوم من المادة المحلول الحامضي مقارنة بالعناصر الأخرى .

الكلمات الدالة: مخلفات البوكسايت , سكانديوم , مستخلصات الفسفور العضوية , مستخلصات المركبات متعددة الحلقات, متراكبة الطور الصلب $Fe_3O_4/SiO_2/OPCs$

LIST OF CONTENT

List of Tables

List of Figures

LIST OF SYMBOLS

C_i	Initial concentrations of element in solution	mg/L
C_f	Final concentrations of element in solution	mg/L
C_L	Concentration of metal ions in the leachate solution	mg/L
C_T	Total concentration of metal ions in leachate solution	mg/L
D	Distribution ratio between organic and aqueous phase	-
K	Extraction equilibrium constant	-
M	Molarity	mol/L
ppm	Parts per million	mg/L or mg/kg
Vo	Volume of organic phase	mL
V_a	Volume of aqueous phase	mL
V	Volume of solution	L
V_{micro}	Volume of micropores (< 2 nm)	cm^3/g
$S_{1.7\text{-}300}$	Pore volume having a diameter between 1.7 and 300 nm	cm^3/g
S_{BET}	Specific surface area	m^2/g
S_{micro}	Specific surface area of micropores (< 2 nm)	m^2/g
S	Stripping efficiency	%
R	Recovery efficiency	%
E	Extraction efficiency	%
L	Leaching efficiency	%

LIST OF ABBREVIATIONS AND ACRONYMS

A/O	Aqueous-to-organic volume ratio
BET	Brunauer-Emmett-Teller surface area determination method
BJH	Barret–Joyner–Halenda pore size distribution determination method
C2.2	Diaza-18-crown-6
CCRD	Central composite rotatable design
D2EHPA	Di-2-ethylhexylphoshoric acid
DC18C6	Dicyclohexyl-18-crown-6
EDX	Energy dispersive X-ray analysis
FTIR	Fourier transform infrared spectrometry
ICP-OES	Inductively-coupled plasma optical emmission spectroscopy
IL	Ionic liquid
K2.2.2	Kryptofix 2.2.2
L/S	Liquid-to-solid ratio
MC	Macrocyclic compounds
OPCs	Organophosphorus compounds
REEs	Rare earth elements
RM	Red mud
SEM	Scanning electron microscopy
SLE	Solid−liquid extraction
SPE	Solid phase extraction
SRL	Sulfation-roasting-leaching
SX	Solvent extraction
TBP	Tri-n-butylphosphate
TEOS	Tetraethylorthosilicate
THF	Tetrahydrofuran
TOPO	Tri-n-octylphosphine oxide
XRD	X-ray diffraction
XRF	X-ray fluorescence

Acknowledgement

Completing this thesis has been a long but a fruitful journey. I feel deeply indebted to many people who have greatly inspired and supported me during my PhD study at University of Pannonia.

First and foremost, I would like to express my thanks and appreciation to my supervisors, Prof. Ákos Rédey, his family and Dr. Tatjána Juzsakova, for their invaluable guidance, encouragement, academic stimulus and generous help, but most of all for giving me the opportunity to learn the rigorous scientific approach and the dedicating spirit for work. Prof. Ákos Rédey, yes of course he left for another world but for me his beautiful soul is still with us.

Special thanks to Dr. Moayyed G. Jalhoom, for his encouragement and kindness who provided me the full support and help. I would like to thank all the members of the Hungarian GINOP-2.2.1-15-2017-00106 project: Complex utilization of red mud and recovery of rare earth metals from red mud., who influenced my scientific work in a different way. I give special thanks to Mr. János Lákó, Dr. Veronika Vagvolgyi, Dr. Balázs Zsirka and Dr. Viktor Sebestyén, for their kindness, availability, and support. I would like to acknowledge my colleagues (but moreover friends), Ms. Gvendolin Kulcsar, Ms. Katalin Győrfi, Ms. Rebeka Borsfai, Ms. Kinga Berta, Mr. Béla Varga, for their help and kindness. Special thanks to, Dr. Endre Domokos, head of Research Centre for Biochemical, Environmental and Chemical Engineering, for his help and support.

Also, I would like to praise all the research fellows Dr. M. Al Asadi, Mr. Thamer Adnan Abdullah and Dr. Phuoc-Cuong Le, whom I had the opportunity to exchange ideas and knowledge. I could never thank enough to my family, especially to my lovely wife, and my beloved sisters for all their unconditional love, support, encouragement.

1 INTRODUCTION

1.1 Background

Red mud (RM) or Bauxite residue (BR) is a by-product that originates through the Bayer method of alumina (Al_2O_3) manufacture from the bauxite mineral ores [1]. Yearly, almost two tonnes of BR is produced for each tonne of Al_2O_3 mined from the Bayer method. It's assessed that around 160 million tonnes of BR are manufactured each year, whereas almost four billion tonnes have already been stored. The disposal and lasting storage of the waste volumes occupy a big land. In turn, and this causes higher costs and obligations for Al_2O_3 manufacturers [2]. The high alkalinity of BR (i.e. pH=10–13) is a main environmental concern, as shown in Fig. 1. Moreover, spills have led to major environmental incidents [2, 3]. In 2015, the collapse of a tailing dam in the state of Minas Gerais in Brazil was evidenced as well the serious ecological and socio-economic impact of storing solid waste residue at large scale [4]. A huge amount of BR has been disposed, and is still generating in all over the world. In October 2010, an extremely serious environmental catastrophe occurred in Ajka, Hungary [5]. This disaster focused the attention of the governmental people and scientists on the possibility of the processing and reutilization of the BR and decreasing drastically the storage volume of wet red mud [6]. BR comprises considerable concentrations of Rare Earth Elements (REEs), but their retrieval being a challenge. REEs are the fifteen metallic elements of the lanthanides series, together with yttrium and scandium [7].

They're today regarded as strategic elements due to their significance for the contemporary technology as well as the clean-tech uses. The subject of REEs has become a hot industrial and strategic issue due to its core role in the current and emerging technologies, particularly in light for their rarity [8, 9]. The rarity of REEs is determined not only by their occurrence in the earth’s crust, but also by the balance between their demand and supply [10]. Nowadays, the management of BR represents a major issue for the aluminium industry because of its high alkalinity and the large quantities produced annually [11]. Despite the potential for recycling, the metal extraction at industrial scale has not been practiced so far, due to the low concentration of some elements, which makes the recovery of these metals not economically feasible [12]. The recovery of these and perhaps

additional metals combined with the utilization of the leftover residue could partly solve both the supply problem of REEs and the storage problem of BR [13].

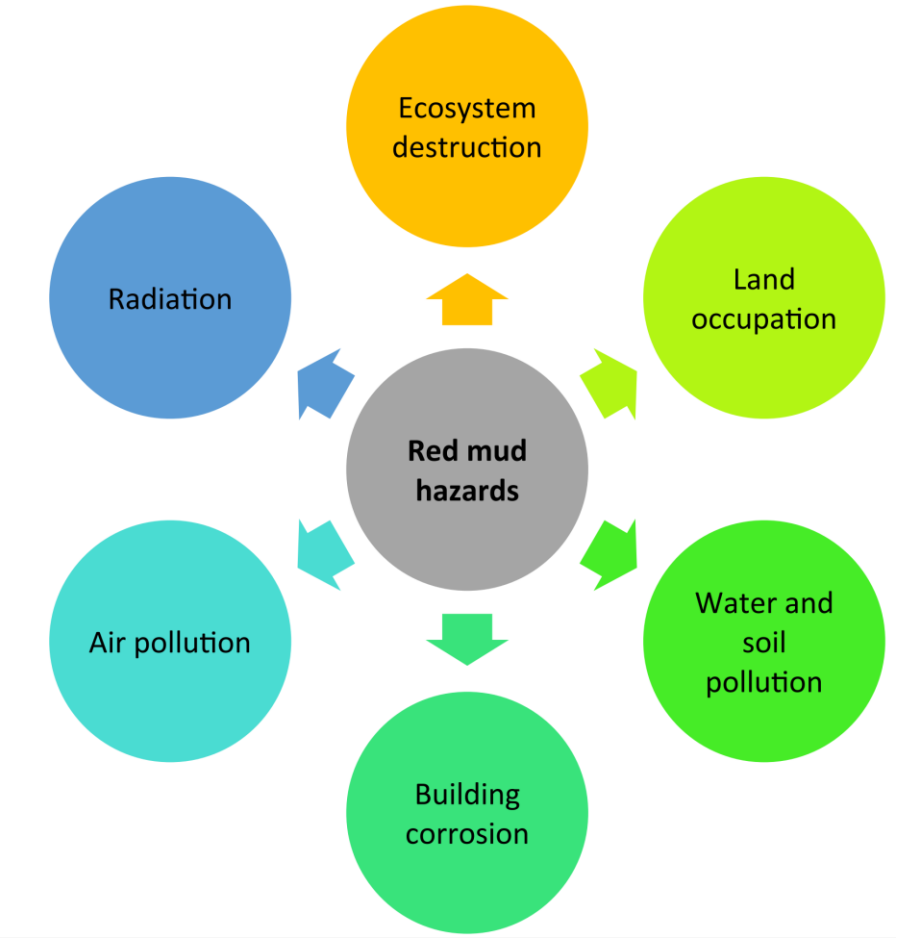

Fig.1. Representation of the risks of red mud **[14, 15]**

1.2 Nature of Red Mud

The manufactured RM has been verified to be hard for dealing with due to its features. And the intricacy is increased owing to the great variety in every produced product of RM. There're different phases that being characteristically existing in RM, as manifested in the Table (1). This table shows an overview of the general phases and their ranges of RM that make it thixotropic, difficult to settle because of its fine particle size and extreme alkalinity [16].

The RM from Ajka (Hungary) is composed mainly of fine particles of silica, aluminium, iron, calcium, and titanium oxides along with economically interesting components, like vanadium and nickel. In addition, the RM contains valuable minor metal elements, such as cobalt, cerium, scandium, lanthanum, praseodymium, and yttrium [17].

Table 1. Mineralogical composition range in red mud [2, 17]

Red mud in general			**Ajka Red mud**	
Mineral Phase	**Chemical composition**	**Concentration, wt%**	**Chemical composition**	**Concentration, wt%**
Hematite	Fe_2O_3	5 – 30	Fe_2O_3	40–45
Goethite	FeOOH	0 – 25	Al_2O_5	10–15
Magnetite	Fe_3O_4	0 – 8	SiO_2	10–15
Diaspore	α-AlOOH	0 – 5	CaO	6– 10
Boehmite	γ-AlOOH	0 – 20	Na_2O	5-6
Gibbsite	γ-$Al(OH)_3$	0 – 5	TiO_2	4–5
Quartz	SiO_2	2 – 5	MgO	0.5–1
Rutile	TiO_2	2 – 5	**Trace elements (ppm)**	
Anatase	TiO_2	0 – 11	V	1000
Ilmenite	$FeTiO_3$	0 – 10	Ni	250
Muscovite	$K_2O{\cdot}3Al_2O_3{\cdot}6SiO_2{\cdot}2H_2O$	0 – 15	Co	100
Sodalite	$3Na_2O{\cdot}3Al_2O_3{\cdot}6SiO_2{\cdot}Na_2SO_4$	4 – 40	**REEs content in red mud (ppm)**	
Cancrinite	$Na_6Ca_2(AlSiO_4)6(CO_3)_2$	0 – 50	Sc	54-100
Calcite	$CaCO_3$	1 – 20	La	100-150
Perovskite	$CaTiO_3$	0 – 22	Y	60-110
Imogolite	$Al_2SiO_3(OH)_4$	0 – 32	Ce	100-400
			Cr	500-1000
			Sr	150-240
			Pr	50-100

1.3 Complex Utilization of Red Mud

RM is a polymetallic material comprised basically compounds that aren't soluble in the concentrated solutions of NaOH, such as Fe and Ti minerals, undigested minerals of Al, calcium compounds, sodium Al hydrosilicates, and significant concentrations of REEs [2, 18]. The chemical composition of RM depends on the origin of the bauxite ore and the operational conditions during the Bayer process. However, during the processing of bauxite by the Bayer process, all the REEs end up in the RM [19]. Therefore, RM is a remarkable origin not only for the main elements, like Al, Fe and Ti, but also for the rare earth elements (REEs) [20].

Many efforts are being made globally to find suitable uses for RM, so that the alumina industry may end up with less or even no residue at all. In this context, Agrawal and co-authors suggested several steps that could be taken for the complex utilization of RM involving several metals recovery, as shown in Fig. 2. The concentrations of REEs in the RM compared to bauxite are approximately in two times higher [21]. In 2020, the European Union updated the list of critical raw materials that include titanium, zirconium, and REEs. Among the REEs, scandium represents up to 95% of the economic value of the RM [2, 11, 22]. As a consequence of its big quantities as well as the ease of mining and leaching, RM can be an important origin of scandium (Sc) [23], which is a rare and costly metal because of its limited accessibility and the tasks linked to its retrieval and purification; the Sc_2O_3 (99.99%) present price is (3800 US$/kg) [24]. The biggest challenges to scandium beneficiation remain the low natural abundance of the element in mineral deposits as well as its association with other elements having very similar chemical properties as previously stated [25-27].

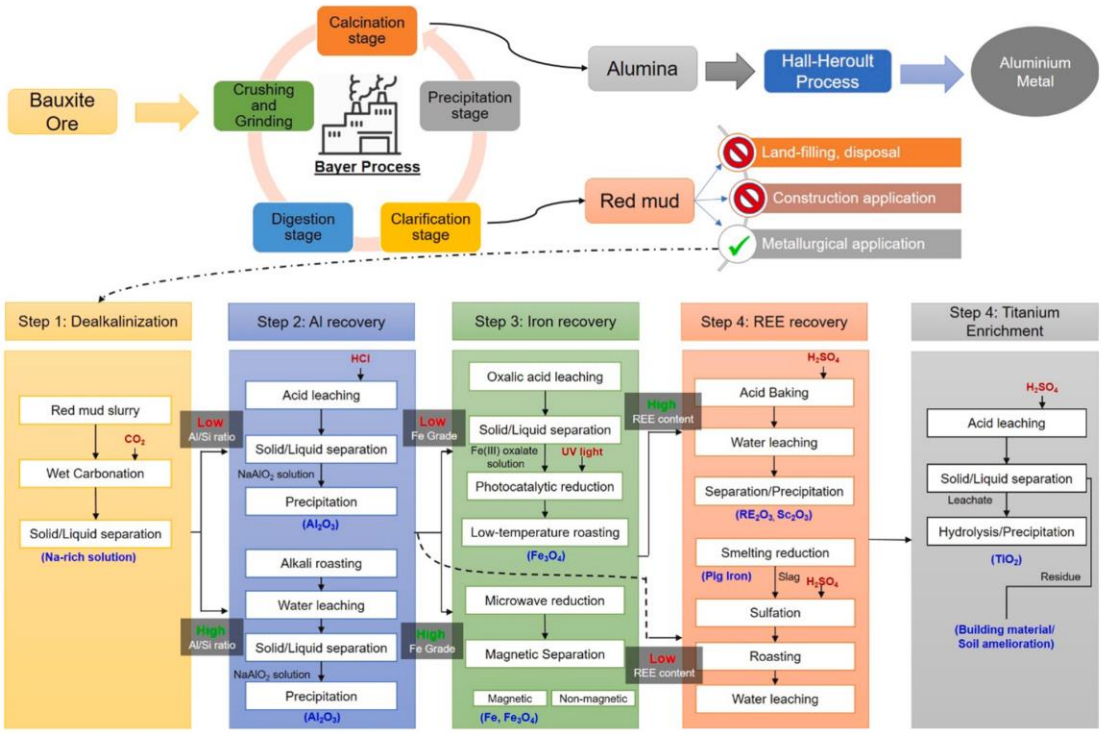

Fig.2. Proposed flowsheet for multiple metal recovery from red mud [28]

1.4 Rare Earth Elements and Their Chemistry

Fifteen lanthanides in addition to Sc and yttrium are pointed to as EERs. Figure 3 evinces the rare earth elements in the periodic table [29]. Nevertheless, Sc is a considerably slighter cation (0.745 Å) than the yttrium and lanthanides as well as has a various chemical behavior**,** and thus it is occasionally not contained within in the set of rare earth [30].

It is mainly observed naturally in a trivalent cationic state, Sc^{3+}, and although reduction can occur, there are few examples of Sc^{2+}.

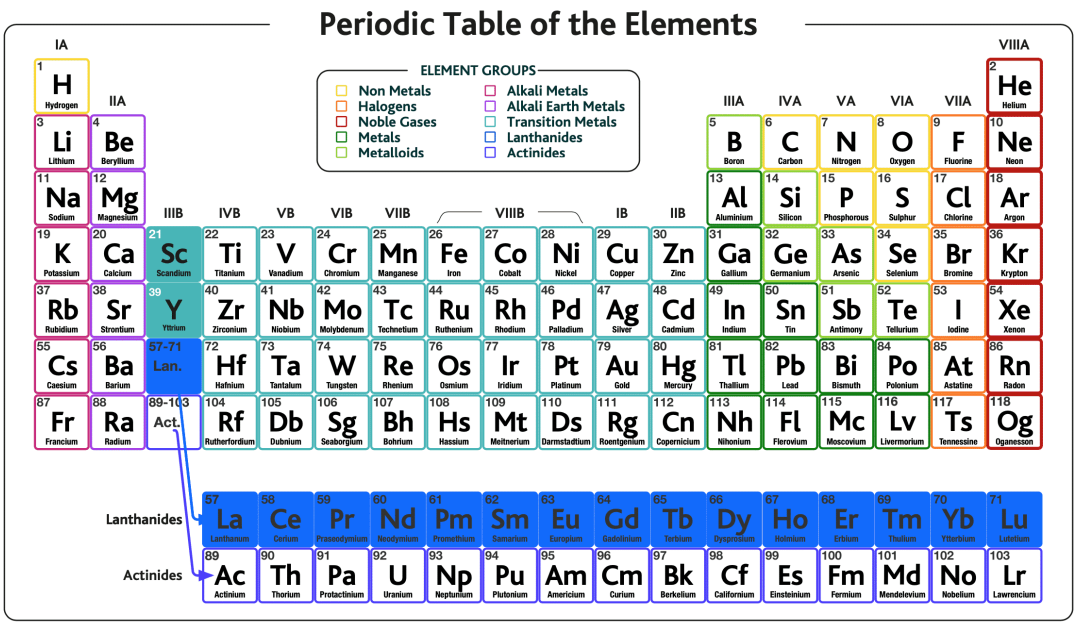

Fig. 3. Rare earth elements in the periodic table of elements [29]

REEs possess alike chemical properties and in nature, they're usually obtained collected in the similar minerals [31]. They're totally categorized as metals and always very reactive. And, they tarnish in touch with air to form oxides. The range of the metals melting point is from 799℃ for Ce to 1663℃ for Lu. Also, the lanthanides (Ce-Lu) being f-block elements, and scandium, lanthanum and yttrium being d-block elements. Normally, such elements take place as trivalent ions [32]. Nevertheless, praseodymium, cerium, and terbium can likewise take place in the tetravalent condition, and ytterbium, europium, and samarium take place in the divalent condition [33]. Lanthanides (Ln) coordination numbers are elevated, characteristically within (6) and (12). The ionic radii are the key factor for understanding the Ln^{3+} coordination chemistry, and the minor variations in the atomic radii highly influence the REEs' chemical characteristics. Across the lanthanides series (Ce-Lu), the electrons are positioned in the (4f) shell. The lanthanides contraction is due to the poor shielding of nuclear charge by the electrons in the 4f shell. Such shell possesses a slight influence upon the bonding, and the important discrepancy between two lanthanides is frequently merely their ionic or atomic radius. And, the lanthanide trivalent ions' radii (for a coordination no. of 8) reduce stably from 1.16 Å for La^{3+} to 0.98 Å for

Lu^{3+}. The yttrium ionic radius (0.9 Å) is alike to those for the elements from the dysprosium forwards. Yttrium frequently interpolates in a series of characteristics in the neighbourhood of erbium, dysprosium or holmium. Nevertheless, in certain states, yttrium elucidates further likenesses toward other rare earth elements; for example, in the series of stable constants by certain chelating agents. Whether the properties of Y are more like the lighter or heavier of the lanthanides depend on the level of covalent character of the chemical bonds. The REEs have a vigorous trend for forming compounds in aqueous solution throughout a broad range of pressure and temperature. Owing to their chemical likeness, the rare earth elements are hard to detach from each other. Based upon their ability to detach, the rare earth elements are categorized as Middle Rare Earth Elements (MREEs), Heavy Rare Earth Elements (HREEs) or Light Rare Earth Elements (LREEs). The rare earth elements categorization comprising some of their properties [34-36] is summarized in Table (2). And, according to such categorization, Scandium is a HREE.

Table 2. Properties and classification of REEs [34, 37]

Element	**Ionic radius (Å)**	**Classification [34]**	**Classification [34]**
La	1.04	**LREEs**	**LREEs**
Ce	1.01		
Pr	0.997		
Nd	0.983		
Pm	0.97		
Sm	0.958		**MREEs**
Eu	0.947		
Gd	0.938	**HREEs**	
Tb	0.923		**HREEs**
Dy	0.912		
Ho	0.901		
Er	0.89		
Tm	0.88		

Yb	0.868		
Lu	0.861		
Sc	0.745		
Y	0.9		

1.4.1 Scandium Applications

Sc is initially utilized for making the alloys of Al–Sc that are characteristically include 2%wt.% Sc [38]. Such alloys are considerably tougher than the traditional high-strength alloys, with an elevated strength, a high grain refinement, without welds' hot cracking, and outstanding resistance to corrosion resistance [39]. Moreover, scandium was utilized in certain contemporary uses, like fuel cells, oil well tracer, electronic parts, analytical standards, and high-intensity metal halide lamps [40]. And, the Sc participation in the Solid Oxide Fuel Cells (SOFC) formation is also too appealing owing to the vigorous O_2-ion conductivity of the Sc_2O_3-stabilized ZrO_2 materials [11]. Gadolinite, thortveitite and euxenite are the minerals of Sc containing important Sc quantities [11, 41]. And, it also co-exists in small quantities in the ores of Al, Co, Fe, Mo, Ni, P, Ta, Sn, W, Ti, , Ur, Zn, and Zr [12, 27, 42]. Scandium ore with a Sc content that ranges from (0.002%) to (0.005%) can be regarded the resources of scandium and has to be utilized [42]. The states with the highly resources of scandium are USA, Ukraine Australia, Russia, Norway, Madagascar, Kazakhstan and China [43]. Sc is highly found in Ur, Ta, Al, and Zr ores in America; the ores of Ni laterite in Australia; the ores of Fe, Sn, and W in China; the ores of Ur in Kazakhstan; the ores of iron in Ukraine and Russia and, and pegmatite rocks in Norway and Madagascar [37].

And, the Sc commercial uses have been restricted owing to the shortage of stable and long-lasting manufacture in addition to its expensive cost [46, 47]. In the Sc oxide form, the worldwide Sc output is about two tons yearly [48]. The ores of Sc with a high content of Sc can be recuperated employing the pyrometallurgical methods. The consumption of energy, from the other side, is considerable. Sc is often enriched in remains, waste liquors, tailings, liquors, and slags, and it's mainly manufactured as an ore treating by-product [49]. And, the simplest method for recovering the Sc is via precipitation; that means the

insoluble compounds of Sc scandium from Sc that contains solutions [50]. Also, even in such state, the else metals co-precipitation doesn't permit solutions with big amounts of metals to be recuperated [51].

1.4.2 REEs Recovery Methods

Hydrometallurgy is a well-built method to extract the rare earth elements from the REE-carrying materials, like normal ores as well as the else secondary origins [44]. It involves two main stages: leaching and separation [45]. In the stage of leaching, rare earth elements are separate from the REE-carrying materials employing chemical substances in aqueous solution. After that, various detaching procedures are utilized for recovering the rare earth elements from the aqueous solution. REEs separation as well as retrieval from the aqueous solution found through hydrometallurgy being, in general, conducted via many traditional methods comprising co-precipitation, precipitation, adsorption, liquid membrane (LM), ion exchange (IX), liquid-liquid extraction (LLE), or solvent extraction (SX) [27, 28]. The SX and the IX are the high broadly utilized methods for the REEs retrieval from the residues such as RM [46]. The SX provides virtuous split-up parameters as well as the likelihood for treating big amounts of RM leachate solution. Nevertheless, it's related to many ecological topics owing to the big organic solvents volumes utilized, such as kerosene and hexane [47]. The ionic liquids (IL) have been introduced as a greener substitution to the traditional solvents, like bis(2-ethylhexyl) phosphoric acid (commercial names D2EHPA or P204) tributyl phosphate (TBP) [9]. Ionic liquids such as betainium bis(trifluoromethylsulfonyl)imide, abbreviated as betainium bistriflimide or [Hbet][Tf2N] are produced the from organic salts with a 100 ºC melting point below [9, 48]. Their chief benefits are their decreased the flammability as well as lesser danger of air contamination in comparison to traditional organic solvents, though few of them, for example fluorinated IL ([CnC1Im][$C_4F_9SO_3$]) can be hurtful [49]. Nevertheless, they're, in general, costly and need elevated temperatures, which can also raise the prices from a manufacturing point of view [50]. Molecular recognition technology (MRT) is known as a very selective chemistry process depending upon MRT that was implemented for the separate REEs separation [51]. Nevertheless, the procedure makes use of cryptands and crown ethers, which are somewhat costly [52, 53]. And, for the Sc retrieval, the hydrometallurgical

procedures (leaching, solvent extraction as well as precipitation) currently used in industrial scale [54, 55]. It is noteworthy, the process design of scandium recovery flow sheets depend on the type, nature, origin of source (ores or waste) and number of contaminants [56]. Manufacturing the neat Sc metal from low-grade ores, secondary sources, such as BR with the content of Sc about 50-250 g/t is a challenging task [42]. SX is the highly efficient technique for the Sc split-up as well as the purification from aqueous solutions owing to its elevated enrichment, selectivity, efficiency of separation, elevated capacity of extraction, and capability for operating upon a big scale [57, 58]. Many commercially extractants are commonly used for Sc recovery from the aqueous phase, such as organophosphorus extractants D2EHPA, Cyanex 272 and TBP [59, 60]. Moreover, varying the balanced pH in the system of SX may cause an elevated selectivity toward the targeted rare metal ions, resulting in the impurities [17, 61, 62]. To make up for its low concentration, scandium is often recuperated as an undesirable by-product through the processing of remains as well as tailings from a broad range of origins, like Ti pigment producing, procedure of Ur leaching, chlorinating magneto-vanailmenite dust, and waste liquor [42, 63]. And, over the previous some decades, the investigators have placed much work to purify the leach liquor for separating the Sc [23, 64-66].

1.4.3 Limitations and Challenges for Sc Recovery from Red Mud

The co-dissolution and co-extraction of metal impurities such as iron, titanium, zirconium, uranium, thorium, and rare earths could interfere the scandium extraction. Hydrometallurgical processes are in most of the cases characterised by their high acid consumption due to the presence of multiple alkaline solids, remaining after the Bayer process, which render the pH of the residue very high, pH >12. Consequently, part of the acid must be used for the neutralization of the alkaline products left behind after the alumina production (i.e. after digestion in the Bayer process). Although high acid concentration can lead to the high recovery of REEs, this can make the process less efficient as the other elements can be dissolved as well [42].

The presence of major metals in the leachate, in particular iron and/or aluminium represents a serious drawback during the further separation process, namely solvent extraction, or ion exchange. Such elements are hard for separating from the rare earth

elements because they share the same condition of trivalent oxidation and can be mined simultaneously with the REEs in most of separation processes. In addition, the presence of silicate compounds (e.g., cancrinite, sodalite) in BR, and their potential decomposition during the acid leaching, is a major problem in RM leaching, because silica tends to polymerize once it is in solution. The formation of this polymer (or silica gel) can significantly reduce the filtration efficiency of the leach liquor before the separation process [2, 67].

1.5 Recovery of Sc from the Red Mud

The process of recovering Sc typically consists of three important steps that begin with the solid waste or ores: (1) acid leaching to convert the solid to the ionic form; (2) solvent extraction step to extract metal ions from leachate and enrichment the concentration of Sc ions; (3) scrubbing step to remove some unwanted co-extracted metal ions, such as Fe, Al, Ti, Ca, etc.; (4) stripping step to recover the desired Sc extracted ions by appropriate acid solution; and finally (5) purification of the produced solution using various processes, such as precipitation and then calcination. Figure 4 depicts a schematic flow diagram of the major stages in the processing of scandium and others REEs [12, 68, 69].

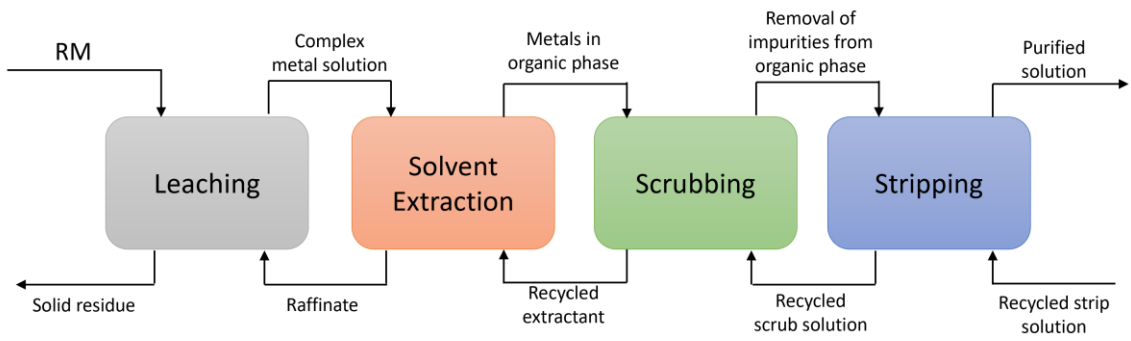

Fig. 4. General process for scandium recovery from red mud leachate [70]

1.5.1 Acid Leaching

The bauxite waste, also named red mud, is frequently treated with acids to recover the scandium and other REEs. The process is called as acid leaching. Many researchers [71-76] have investigated the leaching process of scandium from red mud. Zhang and

collaborators [74] used hydrochloric acid to leach scandium from the red mud, and the best leaching conditions were found to be the following: HCl concentration of 6 mol/L; liquid per solid ratio (L/S) of 4; temperature of 50 °C, and leaching time of 1 h, for which a Sc_2O_3 leaching rate of 82% was obtained. Wang and collaborators [77] also extracted scandium from the RM by leaching it with HCl, and they discovered that the most critical parameter impacting the scandium extraction was the L/S ratio, whereas the HCl concentration had a significant effect on the iron dissolution. The scandium leach rate was higher than 85% in the following operational conditions: HCl concentration of 6 mol/L, L/S ratio of 5, temperature of 60 °C, and reaction time of 1 h. In addition, acid consumption during the leaching process was estimated around 21.2 mol of HCl used per kg of RM. Scandium was recovered by Xu et al. [78] using HCl as a leaching agent at an acid concentration of 7 mol/L, an L/S ratio of 8, and an 80 °C leaching temperature for 1.5 h. In another study carried out by Tang et al. [79], it was shown that the scandium leaching from RM with a particle size distribution of 65–80 µm at a sulfuric acid concentration of 50%, L/S ratio of 3, and 90°C for 3 h was above 85%. A series of leaching studies using different acids, such as hydrochloric, nitric, sulfuric, acetic, methane sulfonic, and citric acids was carried out on Greek RM by Borra et al. [21]. Where several variables, including varying acid concentrations, L/S ratios, leaching time, and temperatures were investigated for their effects. The scandium content of the Greek RM utilized was approximately 120 ppm, which was a high concentration. Their findings revealed that acid was utilized during the initial leaching stage for the purpose of increasing the pH value, neutralizing of alkalinity of RM, and dissolving the aluminosilicates in the RM. The percentage of REEs extracted improved as the acid concentration, L/S ratio, and leaching period were increased. For mineral acids at a low concentration of 0.5 mol/L, the leaching temperature had a little effect on the extraction, while for citric acid leaching, the extraction of rare earth elements increased as the temperature was increased. Finally, they found that the hydrochloric acid leaching had the highest REEs extraction rate when compared to other acids [75]. Moreover, they identified the following leaching conditions: 24 h of leaching time at the room temperature with a 6 mol/L HCl concentration, and an L/S ratio of 50:1, the extraction rate of Nd, Dy, and Y was found to be greater than 80%, while that of La, Ce, and Sc was around 70–80%.

At the above leaching conditions, the dissolution of iron increases with increasing acid concentration from 5% at 0.5 mol/L HCl to about 60% at 6 mol/L HCl. As a result, the Sc dissolution increased. According to these findings of Borra et al., iron and scandium are the highly associated elements in bauxite residue, and they present in the iron (III) oxide lattice [7, 75]. Liu et al. [80] observed that RM was constituted of hematite, goethite, quartz calcite, anatase, zeolite and gibbsite as the mineral phases of the red mud. Time of flight-secondary ion mass spectrometry (TOF-SIMS) and electron probe micro analysis (EPMA) were employed to check the affinities of Sc and Ga with the primary elements found in the red mud, which included Fe, Al, Si, Ti, and Ca. Scandium leaching in the RM was assumed to be primarily regulated by diffusion from the outermost surface of the iron particles. It was also discovered that the hydrochloric acid concentrations less than 3 mol/L were favourable for maximum scandium leaching and less Fe dissolution into the solution. Because Fe is easily decomposed in the acid digestion process, hematite (Fe_2O_3) is a major chemical component of RM, and different hydrometallurgical methods were developed for the extraction of Sc and other precious metals from RM [81]. For the pre-treatment procedures, a reduction–sintering method was used, in which the RM was mixed with a carbon source, $CaCO_3$, and Na_2CO_3 at 800-1000 °C. After that, brown mud was obtained by re-leaching alumina with hot water at 65 °C [81]. The brown mud produced a 90% yield for reduced iron and a 99% yield for pig iron, resulting in a clear distinction between the pig iron and the residue. Scandium (420 g/t) was found in the residue as well as TiO_2 (19.4 wt.%), La (1470 g/t), and Y (180 g/t) [82]. Afterwards, the pig iron was separated from the residue, which was dissolved with sulphuric acid, and the Ti was recovered by hydrolyzing the leaching solution at 140 °C [81]. Following the recovery of Ti, the Sc can be extracted further by SX or precipitation from the solution depending on the circumstances. Ochsenku et al. [83] extracted Sc, La, and Y from RM by selective leaching with dilute nitric acid under normal circumstances and without the use of any pre-treatments. Their findings revealed that the best Sc (80%) and Y (96%) recoveries were obtained by using nitric acid leaching for 24 h at 0.5 mol/L of concentration, an L/S ratio of 50, and the room temperature. Scandium has the highest leaching selectivity over Fe under these conditions, with 3% dissolution of Fe. It was observed that the preparation steps of the RM, such as screening, magnetic separation, and thermal treatment were

unnecessary because most of the major components, particularly Fe, in the RM were not significantly dissolved by this selective leaching method. The dilute nitric acid leaching approach was subsequently scaled up to a pilot plant running at the room temperature and pressure, as illustrated in the proposed flowsheet in Fig. 5 [72]. Economically, for the red mud which includes a high content of hematite as Fe_2O_3 (>30 wt.%), the pre-treatment (carbo-thermal reduction) is appropriate to recover or eliminate the iron content first [84, 85].

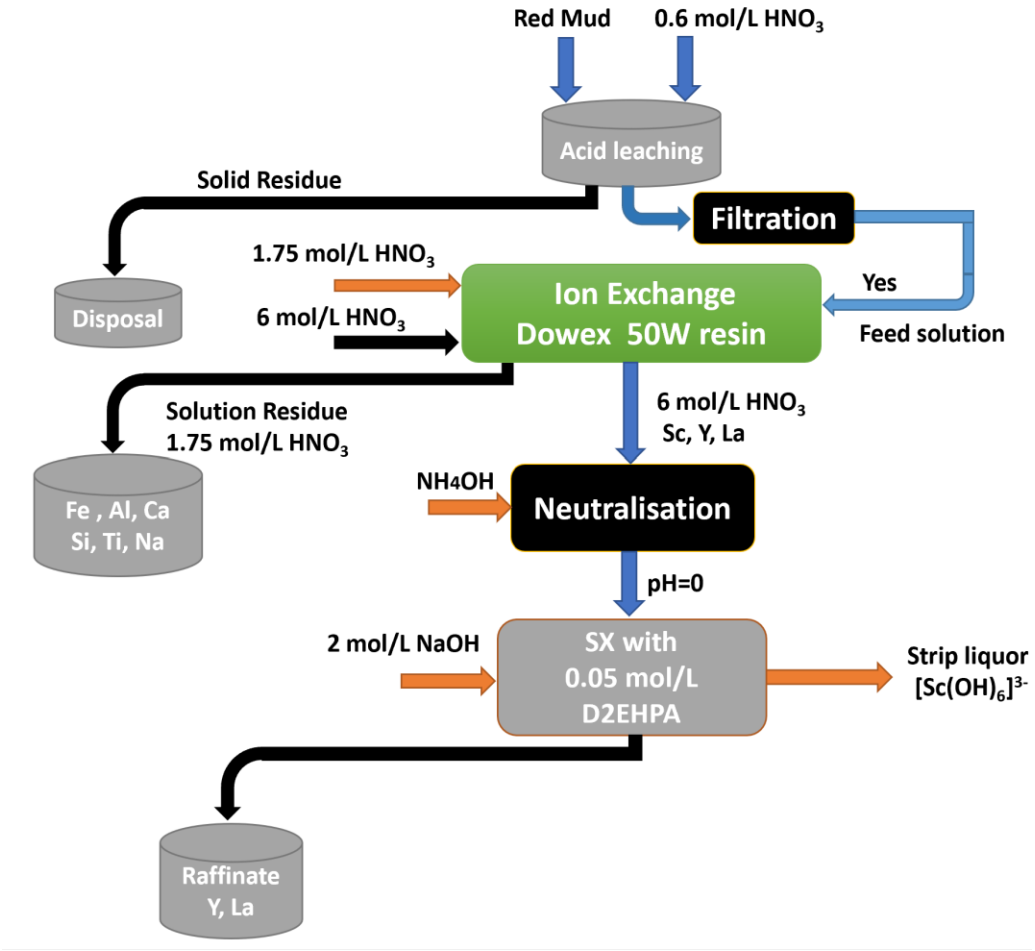

Fig. 5. Proposed flowsheet for scandium recovery from RM applying leaching, ion exchange and liquid extraction steps [72]

1.5.2 Solvent Extraction

Solvent extraction (SX) is a frequently utilized process for scandium recovery from acidic solutions. Organophosphorus compounds, such as D2EHPA, TBP, HEHEHP (another commercial names Ionquest801or P507), and Cyanex 272 are mostly used for scandium recovery [86]. Several studies investigated the extraction of scandium from leachate solutions of red mud using the extractants mentioned above [41]. In this context, Xu et al. [78] used 8 vol% of D2EHPA in order to extract scandium from the real HCl leachate solutions of RM, achieving a 97.9% extraction efficiency at the following conditions: A/O phase ratio of 10, an extraction period of 2.5 min, and 4 vol.% concentration of the alcohol additive. When Zhang et al. [87] used 1 vol% of P507 in kerosene as an extractant, they recovered scandium from RM-HCl leachate solutions (scandium content of 7 ppm). Consequently, with an O/A phase ratio of 1 and an extraction time of 15 min, the extraction efficiency of scandium was greater than 90%. Following the SX, the organic layer was scrubbed twice with 6 mol/L of HCl and distilled water, respectively, at an O/A phase ratio of 3. Moreover, the recovery process was carried out at the following conditions: 2 mol/L of NaOH, 15 min contact time, O/A phase ratio of 3, and 50 °C. Following that, the $Sc(OH)_3$ was additionally dissolved by 6 mol/L of HCl, and the pH of the produced solution was adjusted to 1.5 with the ammonium hydroxide prior to the precipitation step. Finally, a material-enriched Sc_2O_3 with a purity of 66 wt% was achieved through the use of oxalic acid precipitation followed by thermal decomposition at ~ 800 °C. Liu et al. [88] evaluated the extraction performance of Sc from the synthetic leachate of sulfation-roasted RM using OPCs (D2EHPA, P507) and carboxylic acid based reactant. As a result, it was observed that D2EHPA has high extraction ability when it comes to Sc. Furthermore, D2EHPA can be directly applied to the real leachate of H_2SO_4-roasted RM with a low concentration of Fe^{3+} and Si^{4+}, and 96.5% Sc can be recovered from the organic phase (D2EHPA/sulfonated kerosene). In another study [89], a solution of (6 mol/L) HCl was used to dissolve the RM for 4 h using a solid/liquid volumetric ratio of 4 at 60 °C. After extraction, the following composition was obtained: 8 ppm of scandium, 9 g/L of sodium, 7 g/L of iron, 12 g/L of calcium, 15 g/L of aluminum, and 3 g/L of titanium. Scandium was subsequently extracted by adsorption on the TBP-modified activated carbon. However, due to the co-adsorption of titanium, the low adsorption

efficiency of scandium was observed. Based on the acid leaching and solvent extraction procedure, Li et al. explored the feasibility and mechanism of recovering Sc from a Sc-rich material. It was observed that H_3PO_4 outperformed HCl, H_2SO_4, and HNO_3 in separating Sc from impurities.

It was also shown that if H_3PO_4 concentration was 6–8 mol/L and the leaching temperature was 120–140°C, the leaching period was 60–90 min, the L/S ratio was 10–12 mL/g, and the leaching of Sc approached 90% (345 ppm) [23]. The majority (98.6%) of scandium could be further extracted via solvent extraction under the conditions of a D2EHPA concentration of 2%, a pH value of 1.8 and an aqueous-organic ratio of 3:1. Botelho et al. looked towards recovering scandium and zirconium from RM after being leached with 20% of H_2SO_4. Separation studies were conducted out utilizing Cyanex 923, D2EHPA, Alamine 336, and TBP, and their mixes. It was found that at all pH values, Cyanex 923 and Alamine 336 were more selective for Zr than for Sc. At pH 1.5 and 2.0, D2EHPA was more selective for scandium extracting 89% and 40% of Zr, respectively [90]. Wang et al. [91] performed the SX experiments for scandium recovery from a synthetic solution based on Australian RM. This solution, which contained 5.53 mg/L scandium, was prepared by mixing the sulphuric acid (1 mol/L) with the Australian RM at an L/S ratio of 10, heating it to 50 °C, and allowing it to leach for 2 h. Different extractants were investigated to separate scandium from other metals in the synthetic leach solution, such as an acidic OPCs (D2EHPA, Ionquest 801 and Cyanex 272), a primary amine (Primene JMT), a carboxylic acid (Versatic 10), and two chelating materials (LIX 984 N and LIX54-100). Scandium was extracted using D2EHPA, Ionquest 801, Cyanex 272, and Primene JMT with an extraction efficiency of over 99%. On the other hand, the mentioned OPCs (D2EHPA, Ionquest 801) and amine compound (Primene JMT) presented enough high Fe co-extraction rates, which could be higher than 54%. As a phase modifier, TBP was added to these three OPCs extractants (D2EHPA, Ionquest 801, Cyanex 272) because their phase separation was poor when they are used individually. Through further optimization, it was found that the organic system composed of 0.05 mol/L D2EHPA and 0.05 mol/L TBP in Shellsol D70 as a diluent at A/O ratio of 5, temperature of 40 °C and pH of 0.25 performed the best scandium extraction. The loaded organic system was scrubbed twice and then stripped from the D2EHPA/TBP system with NaOH to obtain $Sc(OH)_3$ product. Based

on these results, Wang et al. developed a potential flowsheet for the scandium recovery from the H_2SO_4 leachate solution of the RM, as evinced in Fig. 6.

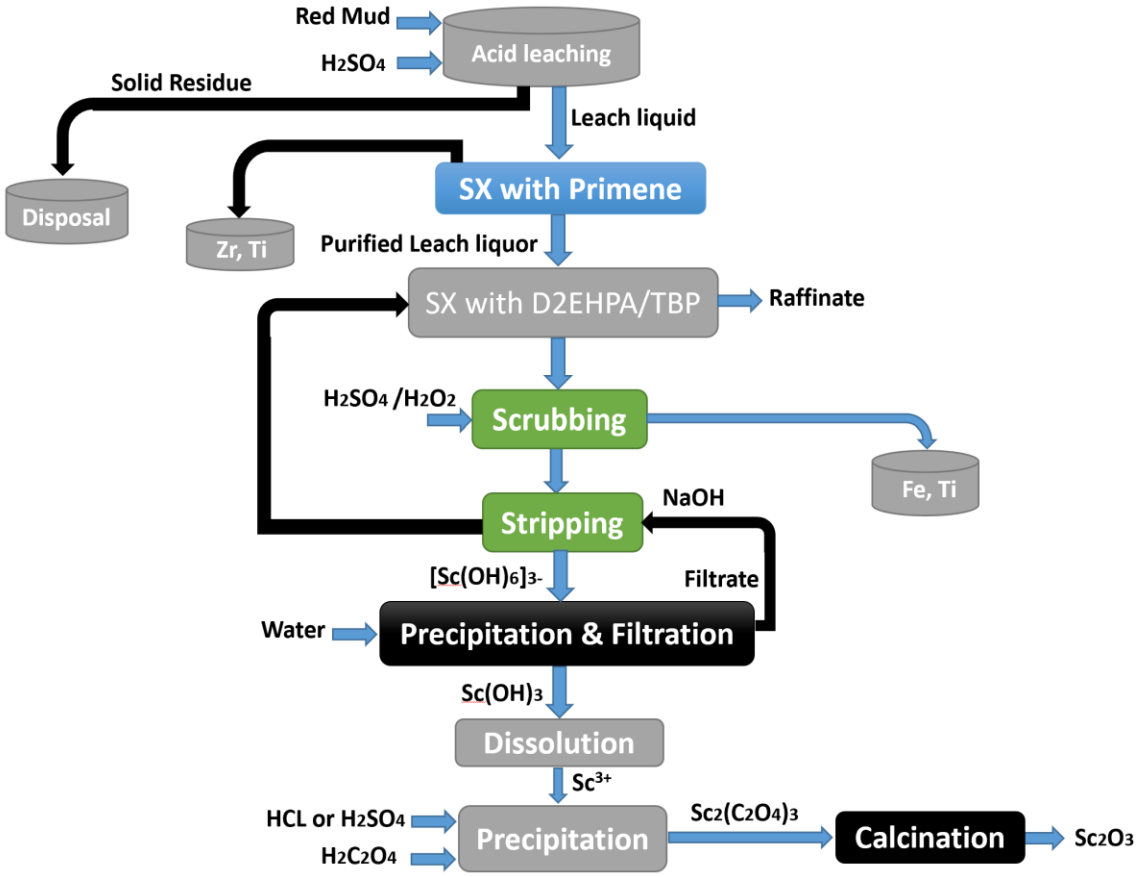

Fig. 6. The proposed flowsheet of scandium separation from Australian RM applying leaching, double liquid extractions, scrubbing, stripping, precipitation and calcination steps [91]

According to previous findings, D2EHPA is commonly used for the scandium extraction from RM solutions due to its efficiency and capacity. Furthermore, a higher scandium recovery rate can be obtained by combining D2EHPA with TBP. Although acidic OPCs can achieve high scandium extraction from leachate solutions, the impurity metals, particularly Fe, may be co-extracted depending on the leaching conditions. As a result, it is critical to investigate the best conditions for SX in order to maximize the scandium recovery from RM while minimizing other metals. The selective extraction of scandium

from the Greek RM was studied by Ochsenkuhn et al. [92], and the flowsheet of the complete system is manifested in Fig. 7.

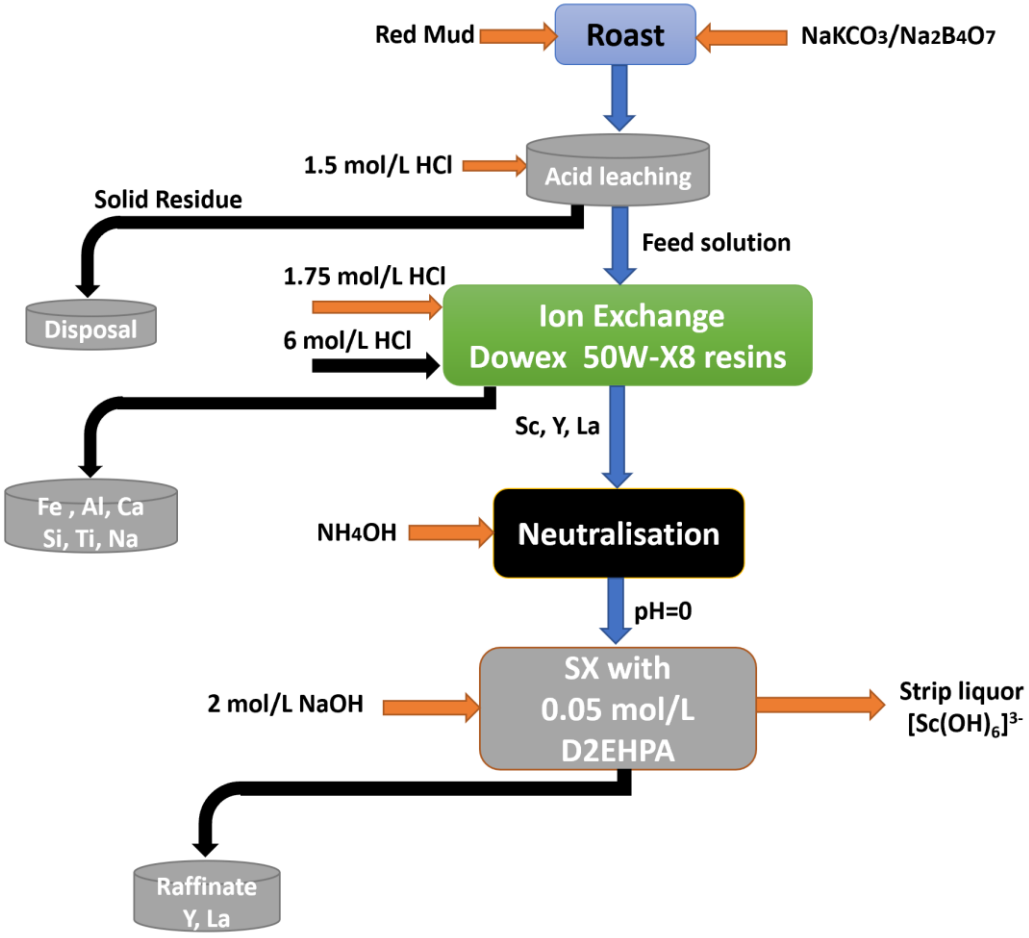

Fig. 7. The proposed flowsheet of scandium separation from Greek RM applying roasting, leaching, ion exchange and liquid extractions steps [92]

The dried RM powder was sintered at 1100 °C for 20 min with sodium potassium carbonate and sodium tetraborate, then dissolved in concentrated hydrochloric acid (1:1), and diluted with 1.5 mol/L hydrochloric acid. The ion exchange column loaded with Dowex 50 W-X8 cation type of resin pre-treated with 2 mol/L hydrochloric acid was used to pass the leachate solution. The ion exchange process was followed by 1.75 mol/L hydrochloric acid elution of major impurity metals, such as Fe, Al, Ca, Si, Ti, and Na and

minor elements, like Ni, Cr, Mn, and V followed by 6 mol/L hydrochloric acid sequential elution of Sc, Y, and La. The Sc, Y, and La eluate solution was adjusted to a pH value around zero with NH_4OH before SX using 0.05 mol/L of D2EHPA in hexane at an A/O ratio of 10. An extraction efficiency of 99% (0.28 ppm) was obtained, which resulted in the scandium extraction into the organic phase, while most of the other elements were allowed to remain in the aqueous phase. Scandium was then recovered from the strip liquor and purified as mixture of $[Sc(OH)6]^{3-}$ and $Sc(OH)_3$ using 2 mol/L NaOH at an O/A ratio of 1:1. For the overall process, 94% of the scandium was recovered from the RM using a sequence of roasting, acid digestion, IX, SX, and back extraction. The recovered scandium solution obtained would next be dissolved with hydrochloric acid before being precipitated with oxalic acid. Following that, pure Sc_2O_3 could be produced by calcining $Sc_2(C_2O_4)_3$.

1.5.3 Recovery of Sc by Macrocyclic Compounds

Macrocyclic polyethers (crown ethers) and aminopoly ethers (cryptands) were introduced by Lehn, Charles Pedersen and Donald Cram [93]. Macrocyclic compounds and their open-chain analogy produce stable complexes with many metals and behave as good liquid extractants for their isolation and separation. However, the factors affecting the efficiency of systems on their basis are not yet well understood. Study of complications' processes in the extraction systems and design of high-technology processes using these extractants for the isolation of valuable products are extremely urgent [94]. In recent time, there has been much interest in the extraction of rare-earth elements (REEs) with macrocyclic polyethers. Several studies used crown ethers components, such as 12-crown-4, dibenzo-18-crown-6 and 15-crown-5 to extract individual REEs from aqueous solutions into organic solution [95, 96]. Many authors have concluded that the relative sizes of the macrocycle cavity and the metal ion are important factors in controlling the stoichiometry of any resulting complex [95]. Tsay et al. [97] used crown ethers, such as 15-crown-5, 12-crown-4 and dibenzo-18-crown-6, and extracted the individual rare earth ions from aqueous picrate solutions into nitrobenzene solution. It was observed that Tb^{3+}, Eu^{3+}, Gd^{3+}, Nd^{3+} and Yb^{3+} can be easily extracted using 15-crown-5; however, the extraction of $Ce^{4+,}$ Sm^{3+}, Dy^{3+} and Lu^{3+} was more difficult.

Macrocyclic polyethers compounds elucidated rather high extractive power toward lanthanides, and the main characteristics of extraction systems were determined. However, there are few data in the literature on scandium extraction with such compounds [98, 99]. However, there are few data in the literature on scandium extraction with such compounds [94, 95]. In this context, G. V. Kostikova et al. [94] performed a systematic study for scandium extraction with benzo-15-crown-5 in chloroform from trichloroacetate solutions. It was found that the optimal conditions for selective scandium recovery with the use of benzo-15-crown-5 in chloroform as diluent are lithium trichloroacetate concentration in an aqueous solution of 1–2 mol/L in pH range 3–5 and concentration of the organic solution 1 mol/L of benzo-15-crown-5. Therefore, the search for macrocyclic compounds showing high extractive power toward scandium and suitable for the efficient processes of the extractive separation of scandium and rare earth elements is an urgent task.

1.5.4 Recovery of Sc by Solid Phase Extraction

The Solid-Phase Extraction (SPE) is recognized as an encouraging method exhibiting many main benefits, like cheap and period saving, convenient, high parameter of pre-concentration, and the capability of combining with various detection methods. And as an ecologically friendly alternate technology, the technology of adsorption can efficiently simplify the procedure of the extraction of Sc and decrease the procedure expenses in comparison with the conventional technique of the extraction of solvent as well as the technique of the extraction of liquid film [100]. Nevertheless, it has to be observed that the efficacy of extraction and the selectivity of such method are vigorously reliant upon the utilized sorbent material. Up to now, different solid phase adsorbents, comprising resin [92], silica gel [101], functionalized biochar [100], functionalized nonporous silicon [102]. Roosen et al. [103] synthesized chitosan–silica particles functionalized with the chelating ligands diethylenetriamine pentaacetic acid (DTPA) and ethyleneglycol tetraacetic acid (EGTA) and tested these for scandium recovery from bauxite residue leachates. And, it was noticed that merely EGTA-functionalized chitosan–silica seemed to be greatly selective for Sc over Fe. As a result, a remarkable separation between scandium and other major elements in BR leachate has been conducted by method of

column chromatography with a HNO_3 as eluting solution at pH 0.50. In another study, a macroporous silica-polymer saturated via trialkyl phosphine oxide (RPO/SiO_2-P) has been utilized for recovering the scandium (90 mg/L) from an synthetic multi-metal ion solution that contains Y, Ce, La, Sc, Al, and Fe elements in 5 M H_2SO_4 medium [104]. The mesoporous silica without functionalization (KIT-6) was utilized for separating the scandium from the solution that REEs, Al, Fe, Al metal ions, and Sc at the pH 3. And, the material's capacity of adsorption was (1 mg/g) in the present investigation, which manifested a virtuous selectivity toward the scandium compared to aluminium as well as the rare earth elements but not iron in the solution if the whole metals possess equal the first concentration (50 μg/L). Nevertheless, the efficiency of the adsorption of scandium was alike to that for iron. Solvent-impregnated resins are widely used in hydrometallurgical processing [105]. The promises impregnated resins class materials known as TVEX (first letters from Russian words meaning “solid extractants”) in the former USSR, which amalgamated the characteristics of solvent extractants and ion-exchange resins, are progressively utilized for the recovery of Sc as well as sorption and solvent extraction. These impregnated resins materials were prepared by the polymerization of styrene and divinylbenzene in the presence of selective extractant [106]. Scandium extraction by TVEX containing di-isooctyl methyl phosphonate (DIOMP), TBP and D2EHPA was studied in detail in a number of papers [107-109]. It was found that the TVEX porous matrix influences both extractant capacity and Sc complex formation in organic phase depending on extraction mechanism. Thus, scandium was extracted [10] by TVEX containing 50% TBP from sulfuric solutions by hydrate-solvate mechanism. Authors of [110, 111] measured the steadiness and kinetic factors of extraction of Sc via impregnated resins depending upon the hypercross-connected polystyrene and included D2EHPA as well as various radical phosphine oxide from the acidic sulphate-chloride solution. The extraction of Sc has been investigated [112] from the sulphuric solution of (6 mol/L) via micro-encapsulation extractants included different compounds such as D2EHPA/DB18C6, TBP/DB18C6, 18-crown-6, dibenzo-18-crown-6.D2EHPA, and tributyl phosphate. Among the investigated above materials, the extractant systems containing organophosphorus compounds were the highly convenient

and encouraging materials for the selective retrieval of Sc from the ores as well as manufacturing waste.

1.6 Scope of Work

This PhD dissertation aims to introduce a new, efficient, and sustainable approach/technique for Sc recovery from RM by applying liquid-liquid and solid-liquid extraction processes. Thus, the main objectives of the dissertation can be given as follows:

- Optimisation of several parameters of the acid leaching process, such as the type of acid leaching agents, contact time, temperature and solid (S: red mud) to liquid (L: leachate) ratio;
- Investigation the selectivity of different organophosphorus liquid extractants, such as bis-2-ethylhexyl phosphoric acid (D2EHPA), tributyl phosphate (TBP), and trioctylphosphine oxide (TOPO) for extraction of Sc from red mud leachate;
- Study the ability of ion exchange technique (50Wx8 resin) for advanced purification as complementary stage for solvent extraction process.
- Investigation the effect of various parameters, such as the concentration of extractants, temperature and pH of solution, aqueous to organic (A/O) volume phases ratio, and shaking-extraction time on Sc extraction efficiency from red mud leachate;
- Study of the extraction ability of liquid macrocyclic compounds towards Sc (III) by liquid–liquid extraction from model solution using response surface methodology (RSM) and the determination of the optimum conditions of extraction process; and
- Preparation, characterization and application of Fe_3O_4/SiO_2/OPCs (OPCs = D2EHPA, TOPO, TBP) solid phases for the separation of Sc from red mud leachate by solid-liquid extraction process.

Fig.8 shows the representation of experimental work in terms of block diagram.

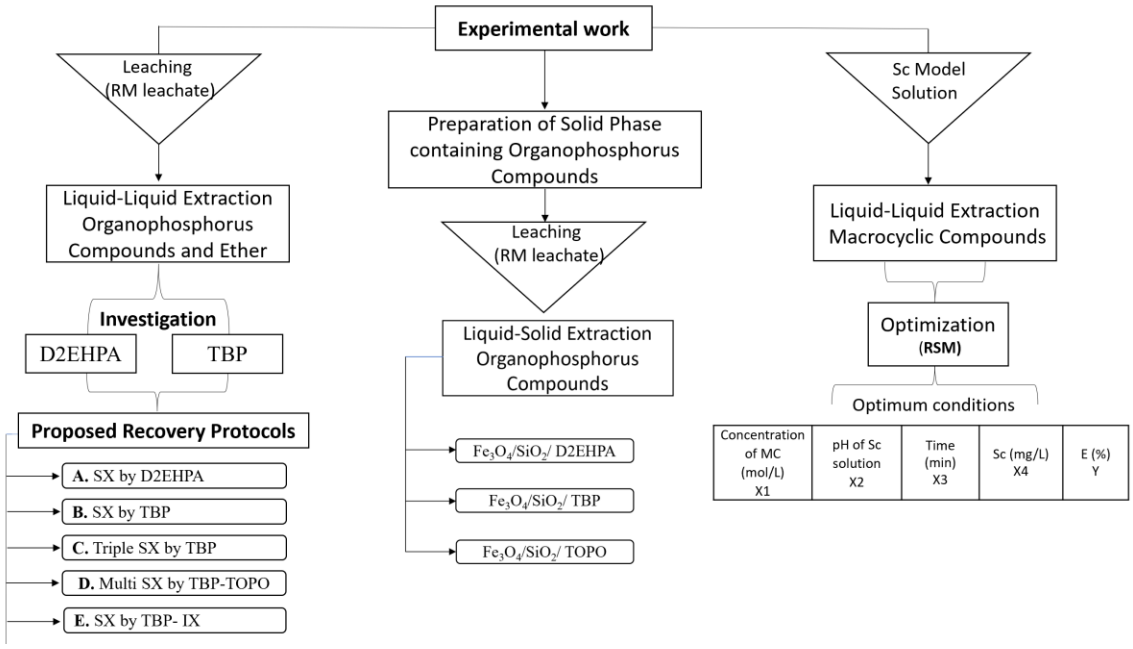

Fig. 8. Block diagram represent the experimental work

2. EXPERIMENTAL

2.1 Materials and Methodology

All chemicals were of analytical reagent grade. Milli-Q, ultra-pure water (G=1.408 μS/cm) was used throughout the study. Table 3 shows the chemicals and reagents used in this work.

Table 3. The chemicals and reagents

Chemical name (commercial name, abbreviation)	Chemical formula, purity	Provider company
Bis-2-ethylhexyl phosphoric acid (D2EHPA)	$C_{16}H_{35}O_4P$, 95%	Sigma–Aldrich Co., Ltd (Germany)
Trioctylphosphine oxide (TOPO)	$C_{24}H_{51}OP$, 97%	Sigma–Aldrich Co., Ltd (Germany)
Tributyl phosphate (TBP)	$C_{12}H_{27}O_4P$, 97%	Sigma–Aldrich Co., Ltd (Germany)
Di-cyclohexano-18-crown-6	$C_{20}H_{36}O_6$, 98%	Sigma–Aldrich Co., Ltd (Germany)
1,7,10,16-tetraoxa-4,13-diazacyclooctadecane (C2.2)	$C_{12}H_{26}N_2O_4$, 96%	Sigma–Aldrich Co., Ltd (Germany)
4,7,13,16,21,24-hexaoxa-1,10-diazabicyclo ([8.8.8] hexacosane or Kryptofix 2.2.2 (K 2.2.2)	$C_{18}H_{36}N_2O_6$, 98%	Sigma–Aldrich Co., Ltd (Germany)
1,2-dichloroethane	$C_2H_4Cl_2$, 99.8%	Sigma–Aldrich Co., Ltd (Germany)
Dichloromethane	CH_2Cl_2, 98%	Sigma–Aldrich Co., Ltd (Germany)
Chloroform	$CHCl_3$, 99%	Sigma–Aldrich Co., Ltd (Germany)
Chloroacetic acid	$ClCH_2CO_2H$, 99%	VWR Chemicals BDH Co, (Leuven, Belgium)
Sodium hydroxide	NaOH, 97%	VWR Chemicals BDH Co, (Leuven, Belgium)
Acetic acid	20 vol%	Sigma–Aldrich Co., Ltd (Germany)

Hydrochloric acid	HCl, 37%	VWR Chemicals BDH Co, (Leuven, Belgium).
Diethyl ether	$C_4H_{10}O$, 99%	VWR Chemicals BDH Co, (Leuven, Belgium)
Tri-n-octylamine, (N_{235})	$C_{24}H_{51}N$, 98%	Sigma–Aldrich Co., Ltd (Germany)
Octyl alcohol	$C_8H_{18}O$, 98%	Sigma–Aldrich Co., Ltd (Germany)
Xylenol orange tetrasodium salt	$C_{31}H_{28}N_2Na_4O_{13}S$, 90%	Sigma–Aldrich Co., Ltd (Germany)
Petroleum	For analysis	Supelco-Merck Kft., (Budapest, Hungary)
Tetraethyl orthosilicate (TEOS)	$SiC_8H_{20}O_4$, 98%	Sigma–Aldrich Co., Ltd (Germany)
Ferric chloride hexahydrate	$FeCl_3 \cdot 6H_2O$, 99%	Merck Kft., (Budapest, Hungary)
Ferrous chloride tetrahydrate	$FeCl_2 \cdot 4H_2O$, 99%	Merck Kft., (Budapest, Hungary)
Ethanol	C_2H_5OH, 100%	VWR Chemicals BDH Co, (Leuven, Belgium)

2.2 Red Mud Acid Leaching

Different leaching methods were applied in the present study to optimize the leaching process, maximize the Sc, and minimize the major elements, such as Fe, Ti and Al content. Mechanical, microwave (MW)-assisted, high-pressure leaching (HPL), and Sulfation–Roasting–Leaching (SRL) digestions processes were used to transform the metals content of the RM into ionic form. Among these methods, the mechanical digestion process was chosen for its cost and efficiency compared with the other methods. The RM samples used in this study were obtained from the Ajka RM disposal facility in Hungary, and these samples were further dried at 105 °C for 24 h. The main chemical composition of the dried RM was determined using X-ray fluorescence spectroscopy (XRF) (Table 6). The concentrations of elements in aqueous phase were measured by an ICP–OES (Table 6).

All digestion experiments were initiated by mixing approximately 1 g of RM with different leaching conditions (acids, concentrations, and S/L ratios).

In the mechanical digestion, the following protocol was chosen: the red mud sample of 1 g weight was leached by HCl acid solution of volume 30 mL, and the main as well as rare earth elements were transferred into the acidic solution as ionic form. The leaching process was carried out in a reflux system equipped with 100 mL pot with a magnetic stirrer at 100 rpm. A thermostat controlled the temperature of the electrically heated silicone oil bath, which ranged from the room temperature to 80 °C. The leaching process was carried out at the following conditions (7 mol/L) of HCl concentration, 3 and 5 h of leaching time, and 30 solid to liquid ratio (S/L). The pot was removed after leaching and cooled in the water to the room temperature. To separate the pure leachate from residue, the suspension was filtered. The leachate was then collected and subjected to a solvent extraction processes. Furthermore, the leaching efficiency of red mud, L%, has been calculated according to Eq. (1).

$$L(\%) = \frac{C_L}{C_T} \times 100 \qquad (1)$$

Where, C_L and C_T are the concentration of metal ions in the leachate solution and the total concentration of metal ions in the red mud, respectively. The total concentration of the elements was calculated based on XRF analysis. The description of mechanical digestion practical steps is presented in Fig. 9.

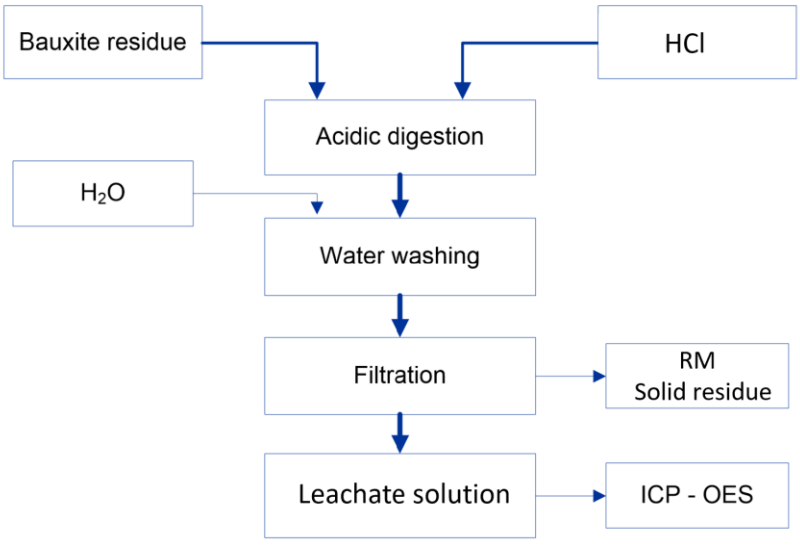

Fig. 9. Flow sheet of digestion of red mud (bauxite residue)

2.3 Iron Content Removal from Red Mud

The removal trivalent iron from the obtained leachate solutions was investigated by two proposed extractants by solvent extraction techniques. The red mud was leached by 7 mol/L of HCl acid solution before the solvent extraction. Two extractants tri-noctylamine (N235) of 10 vol% (or 20 vol.%, and 30 vol.%) in kerosene or pure diethyl ether were used. The extractants structure is shown in Fig. 10. Equal volumes (10 mL) of the organic phase (N235 or diethyl ether) and aqueous phase (red mud leachate solution) were mixed for 15 min in a separation funnel. In solvent extraction by diethyl ether, the extraction cycle was repeated two times for the same leachate sample to achieve better iron removal efficiency. The separated aqueous phase was investigated by ICP-OES instrument.

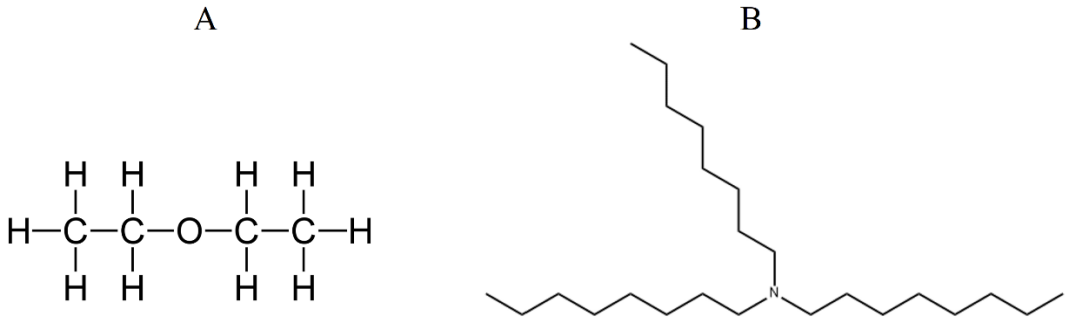

Fig. 10. Chemical structures of organic extractants for iron removal: (A) diethyl ether, (B) tri-noctylamine (N_{235})

1.4 Liquid-Liquid Extraction by Organophosphorus Compounds

Two main organophosphorus compounds as extractants were investigated involving D2EHPA and TBP. The third one (TOPO) was suggested for purification step. The following parameters have been chosen to be the key variables in D2EHPA and TBP systems: concentration of extractant, A/O phase ratio, concentration of stripping solution, pH value, extraction time and temperature. The chemical structures of D2EHPA, TBP and TOPO extractants are depicted in Fig. 11.

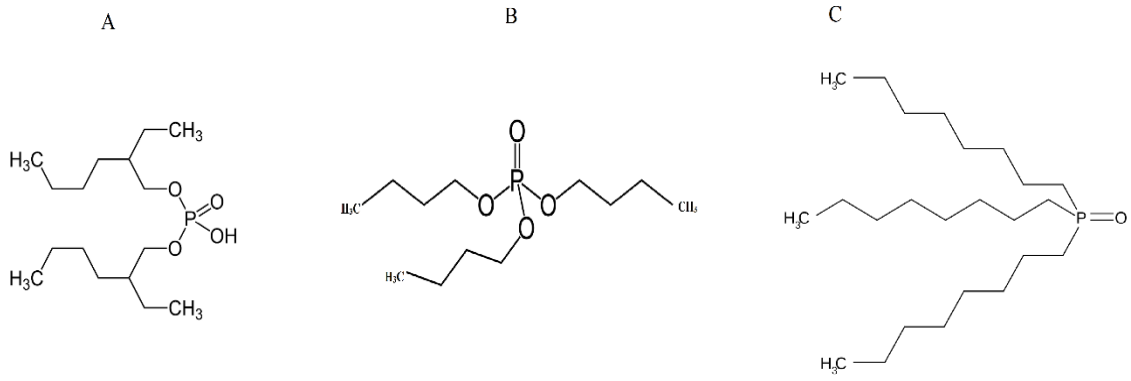

Fig. 11. Chemical structures of organophosphorus extractants compounds: (A) D2EHPA, (B) TBP and (C) TOPO

2.4.1 Liquid-Liquid Extraction by DE2HPA

The obtained solution after SX by diethyl ether "free iron" was treated with DE2HPA extractant. The following parameters have been recognized as key parameters in the scandium extraction process: 0.05 M DE2HPA in kerosene, aqueous to organic volume ratio A/O (1:5), pH (0-1), concentration of alkaline solution (0.5-3 mol/L NaOH) as stripping agent, time of extraction (5-25 min), and temperature (25-75 °C).

To achieve equilibrium in liquid-liquid system, 10 mL of aqueous phase and 10 mL of extractant were added to a 50 mL mixing separation funnel and shaken for 15 min. After that, the caustic solution was used for stripping the extracted target Sc metal ions from the organic extractant. Due to the organic extractant that is some extent soluble in aqueous phase, the complete phase separation is difficult to achieve. 2.5 mol/L NaOH solution was used to back extract the Sc from the Sc-loaded DE2HPA organic phase so that Sc can react with OH^- ions, and form the $Sc(OH)_3$ precipitate. For better separation of extractant from the aqueous phase, 60 °C was used as the stripping temperature. The precipitated particles were separated from the solution by centrifugation. The separated partials that were (hydroxides precipitates) were dissolved in 2.5 mol/L hydrochloric acid and the recovered concentration of metal ions was measured by ICP-OES. Finally, oxalic acid ($H_2C_2O_4$) was proposed to produce scandium oxide as solid powder and further purification. The preliminary precipitation experiments were performed with Sc model

solution under the following conditions: 0.5 and 1 mol/L $H_2C_2O_4$, 20 mL:20 mL, pH values of 0.7 and 1.8, and Sc concentration of 250 mg/L in the model solution.

2.4.2 Liquid-Liquid Extraction by TBP

Two proposed techniques were applied, the first one is to remove the Fe(III) content by diethyl ether from leachate solution before TBP solvent extraction (see section 2.3), and the second one is to remove the Fe(III) content after TBP solvent extraction. In this experiment, the red mud leachate was contacted with TBP organic phase for 5 min of shaking time and 1:1 volume ratio of organic to aqueous phase (10 mL:10 mL). The following parameters were found to be essential to the Sc recovery procedure: Aqueous to organic volume ratio A/O (1: 4), concentration of TBP (2-20 vol.%) in kerosene, concentration of acidic HCl solution (0-1 mol/L) as stripping agent. The obtained HCl leachate concentration was adjusted to (~6 mol/L) to form $HFeCl_4$ molecules prior to solvent extraction by diethyl ether. Also, 0.8 mL of H_2O_2 was added to the solution to improve the converting of iron content to trivalent iron. The Sc-loaded aqueous solution (6 mol/L of HCl) was treated with 99% of diethyl ether for two cycles with 1:1 A/O ratio.

2.4.3 Scandium Extraction and Separation Protocols

Five protocols (A, B, C, D and E) were investigated involving D2EHPA, TBP and TOPO organophosphorus compounds as extractants. In addition to extraction steps, the ion exchange separation was carried out in Protocol E.

2.4.3.1 Single Liquid- Liquid Extraction by DE2HPA (Protocol A)

The proposed **A** protocol based on one extraction stage:

The protocol steps were:

(1) The removal of iron content from Sc loaded acid solution by diethyl ether solvent extraction at the following conditions: 15 min shaking time, and 1:1 organic to aqueous phase ratio. The obtained Sc loaded aqueous solution was heated up to ~50 °C for 15 min to remove the remaining amount of diethyl ether. (2) The prepared red mud leachate (see section 2.2) was contacted with 0.05 mol/L DE2HPA organic phase in kerosene for 5 min of shaking time in order to extract target metal ions. The volume ratio of organic to

aqueous phase was 1:3.3 (15 mL: 50 mL). (3) The loaded DE2HPA organic phase was separated from raffinate aqueous phase prior to back extraction step. (4) The recovery of Sc content from the Sc-DE2HPA loaded organic phase was done by back extraction by using 2.5 mol/L of NaOH stripping agent. The obtained precipitated amount was dissolved with (3 mol/L) HCl before ICP-OES analysis.

2.4.3.2 Single Liquid- Liquid Extraction by TBP (Protocol B)

The proposed B protocol based on three extraction stages:

The protocol steps were:

(1) The prepared red mud leachate (see section 2.2) was contacted with 2 vol% TBP organic phase in kerosene for 5 min of shaking time in order to extract target metal ions. The volume ratio of organic to aqueous phase was 1:3.3 (30 mL:100 mL). (2) The loaded TPB organic phase was separated from raffinate aqueous phase prior to back extraction step. (3) The recovery of Sc content from the Sc-TBP loaded organic phase was done by back extraction by using 1 mol/L of HCl stripping agent. (4) Hydrochloric acidification the obtained Sc loaded aqueous solution (lowering the pH value) prior to iron removal. (5) The removal of iron content from Sc loaded acid solution by diethyl ether solvent extraction at the following conditions: 15 min shaking time, and 1:1 organic to aqueous phase ratio. The obtained Sc loaded aqueous solution was heated up to 50 °C for 15 min to remove remaining amount of diethyl ether before ICP-OES analysis.

2.4.3.3 Tripel Liquid-Liquid Extraction by TBP (Protocol C)

The proposed **C** protocol based on three extraction stages (Fig. 12):

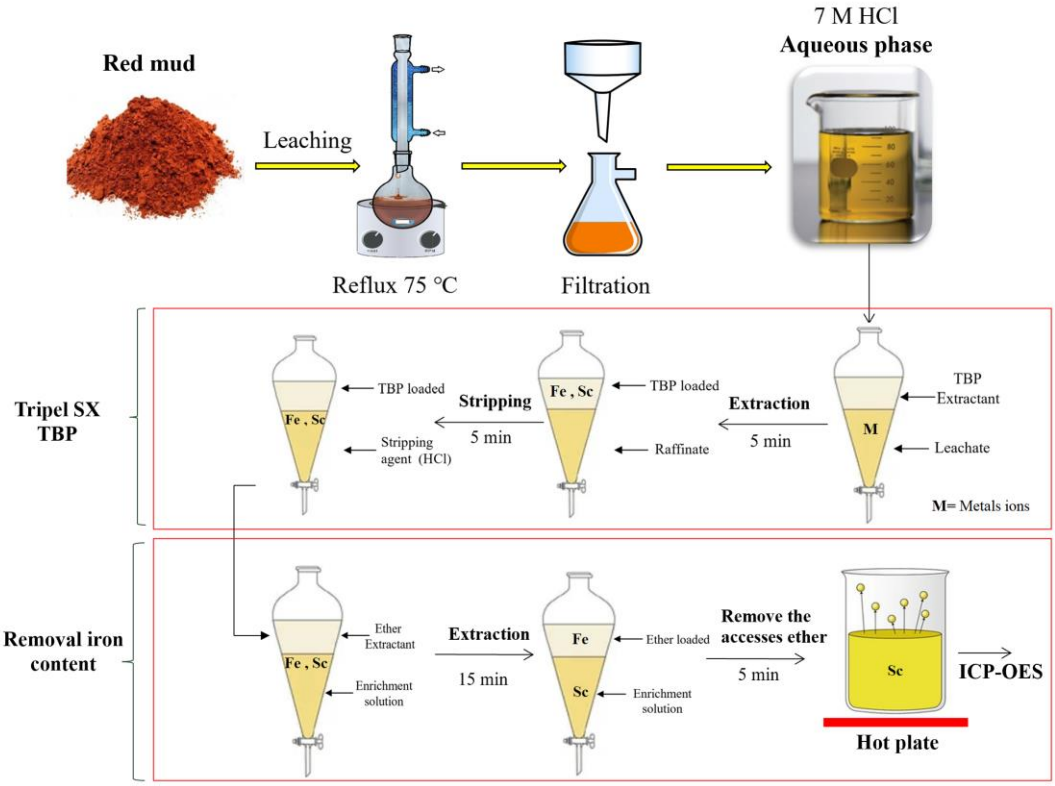

Fig. 12. Schematic presentation of Sc extraction from red mud and its purification applying TBP triple Liquid-Liquid extraction method (Protocol C)

The protocol steps were:

(1) The same as in Protocol **B** excepting the concentration of TBP was 10 vol.%, and the volume ratio of organic to aqueous phase was 1:2.7 (75 mL:200 mL).

(2) The same as step 2 in Protocol **B**.

(3) The same as step 3 in Protocol **B**.

(4) The same as step 4 in Protocol **B**.

The 1-4 steps were repeated three times, respectively.

(5) The same as step 5 in Protocol **B**.

2.4.3.4 Multiple Liquid-Liquid Extraction by TBP and TOPO (Protocol D)

The proposed **D** protocol based on four extraction stages (Fig. 13):

The protocol steps were:

(1) - (5) The same as in Protocol **C**.

(6) Sc loaded iron free aqueous solution was contacted with (0.05 mol/L) TOPO for 5 min shaking time in order to remove the co-extracted metal ions, such as Ti, Al, Na and REEs. The volume ratio of organic to aqueous phase was 1:2 (5 mL:10 mL);

(6) and (7) The same as step 3 and 5 in Protocol **C**. The concentrations of metal ions were measured by ICP-OES.

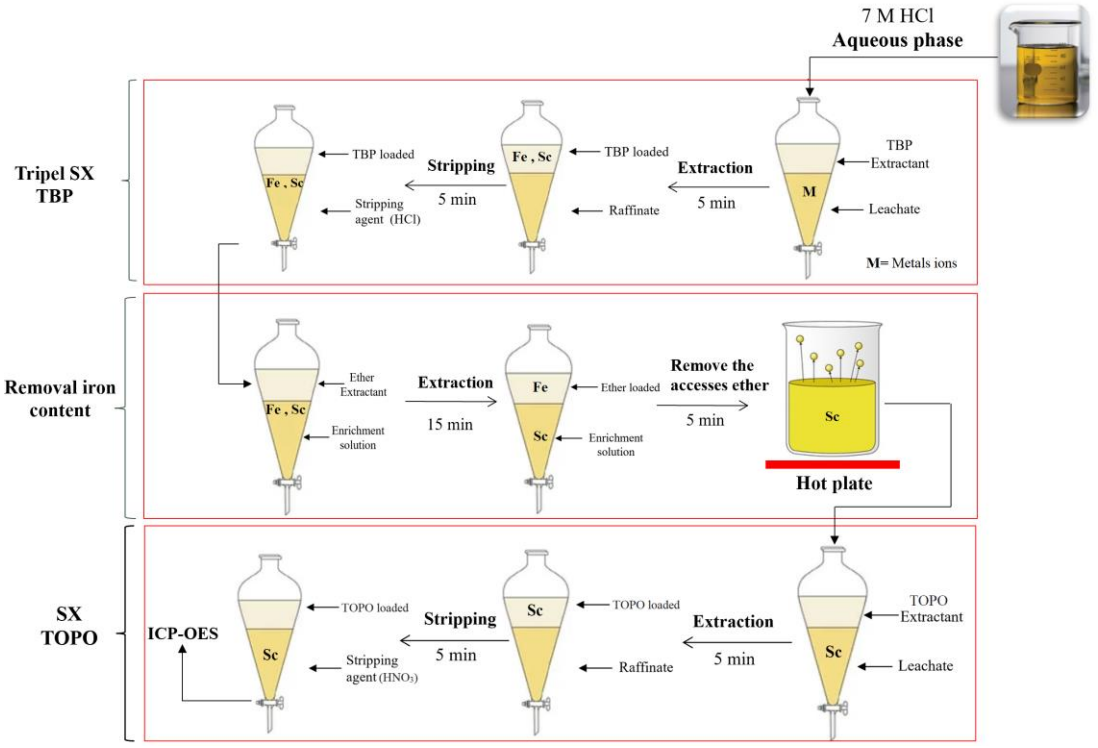

Fig. 13. Schematic presentation of Sc extraction from red mud and it purification applying TBP and TOPO double Liquid-Liquid extraction method (Protocol D)

2.4.3.5 Combination of Liquid-Liquid Extraction by TBP and Ion Exchange Method (Protocol E)

The protocol steps were:

(1) The same as in Protocol **B** excepting the concentration of TBP was 5 vol%, and the volume ratio of organic to aqueous phase was 1:1 (10 mL:10 mL);

(2) - (5) The same as in Protocol **B**;

(6) Sc loaded acid solution was purified applying ion exchange technique. Before pouring Sc loaded solution onto the ion exchange column containing 100 g of Amber Chrom

50Wx8 100-200 (H) type resin, the pH value was adjusted to a pH equivalent to (0.5 mol/L) HCl using 25% NH_4OH solution. The pH adjustment was done for the selective separation of Sc from the solution. At this pH value, scandium trivalent cations are easily replaced by three protons getting out of the resin. The resin was washed with (0.5 mol/L) HCl before the ion-exchange experiment. Samples were poured into the ion-exchange column in 20 or 40 mL parts. 2 mL/min flow rate of the elution was set by a valve at the bottom of glassware. The elution was done with different acids and their concentrations (0.5 mol/L HCl, 1.75 mol/L HCl, 8 mol/L HCl, and 6 mol/L HNO_3). The eluted fractions were collected separately in plastic flacon tubes and sealed with caps. Samples were measured with ICP-OES for different elements. Before each measurement, the samples were diluted with milliQ water 5 or 10 times.

2.5 Liquid-Liquid Extraction by Macrocyclic Compounds

Extraction and stripping experiments were carried out for Sc model solution at 25 °C with three types of macrocyclic compounds, DC18C6, K 2.2.2 and C 2.2 which their structures are illustrated in Fig. 14.

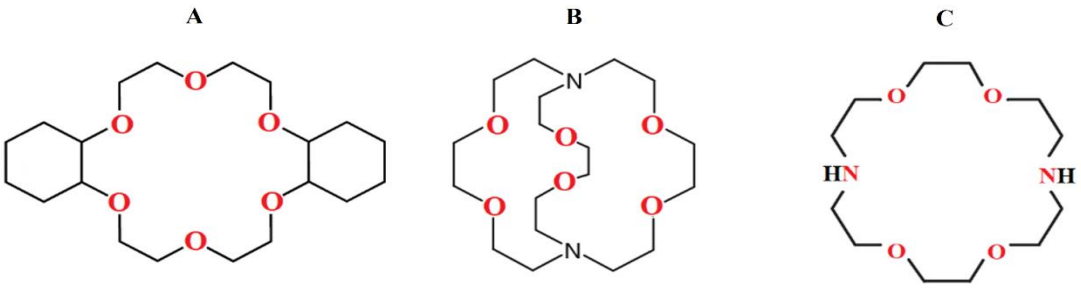

Fig.14. Chemical structures of macrocyclic extractants compounds: (A) DC18C6, (B) K 2.2.2 and (C) C 2.2

The impact of the all possible variables, which effect on the Sc extraction process, such as the concentration of macrocyclic compounds (0.002, 0.004, 0.006, 0.008 and 0.01 mol/L), pH (1, 2, 3, 4 and 5), time (3, 6, 9, 12 and 15 min), solvent type, and the model solution concentration of Sc (25, 50, 75, 100 and 125 mg/L), was investigated in order to determine the most influencing extraction process variables. The equal volumes (10 mL) of 1,2 dichloroethane organic phase and aqueous Sc model solutions were contacted and

mixed in a separation funnel. It is preferable to mix the organic phase with distilled water at the beginning of extraction to ensure the saturation with the aqueous phase. After the phases stabilized, the aqueous phase and organic phase were separated, and the aqueous phase was analyzed by ICP-OES to check the Sc concentration. The organic phase separated contained the Sc ions (complex) and in the next step, the recovery of Sc was aimed at. Back extraction (stripping) experiments were conducted by contacting 10 mL of Sc-loaded organic phase with 10 mL of the 0.1 mol/L of HCl solution (stripping reagents) for 15 min in a separation funnel. After separating the aqueous phase, the concentration of metal in the aqueous phase (stripping acid) was determined using an ICP-OES instrument. The Sc-complex concentration in the organic phases can be calculated from the mass balance. The distribution ratio (D) of metal ion between aqueous and organic phases, extraction (E) and stripping (S) efficiencies were calculated by the following Eqs. 2-4:

$$D = \frac{C_i - C_f}{C_f} \quad (2)$$

where C_i and C_f represent the initial and final concentration of a metal in aqueous phase (ppm).

$$E(\%) = \frac{C_i - C_f}{C_i} \times 100 \quad (3)$$

$$S(\%) = \frac{C_{aq}}{C_{org}} \times 100 \quad (4)$$

where C_{aq} is the equilibrium concentration of a metal in stripping aqueous solution, and C_{org} which is the initial concentration of a metal in the metal loaded organic phase (ppm, mg/L).

2.5.1 Optimization of Liquid-Liquid Extraction by Macrocyclic Compounds

In order to properly analyze any process, it is necessary to first identify and evaluate the parameters that have a direct influence on the actions of system behavior, as well as the variables that influence the system goal function. As a result, a series of studies must be conducted to account for the influence of each parameter, as well as the correlations between them if they are not independent. "Experimental Design" is a methodical strategy that covers the above function with the minimum number of experiments possible. A

statistical method was employed to extract the information from the pre-existing data in order to explain the results in a systematic way with the minimum number of experiments possible, using the experimental design. The validity of the second-order polynomial model has been demonstrated through STATSTICA software-based analysis of variance (ANOVA). ANOVA is an analysis tool used in statistics that splits an observed aggregate variability found inside a data set into two parts: systematic factors and random factors [113]. The block diagram shown in Fig. 15 explains the solution procedures starting from finding the coefficients of polynomial and model equations using STATISTICA software. Then, the model equations, which describe the extraction process, were optimized by using WinQSB software to maximize the extraction efficiency or the objective functions.

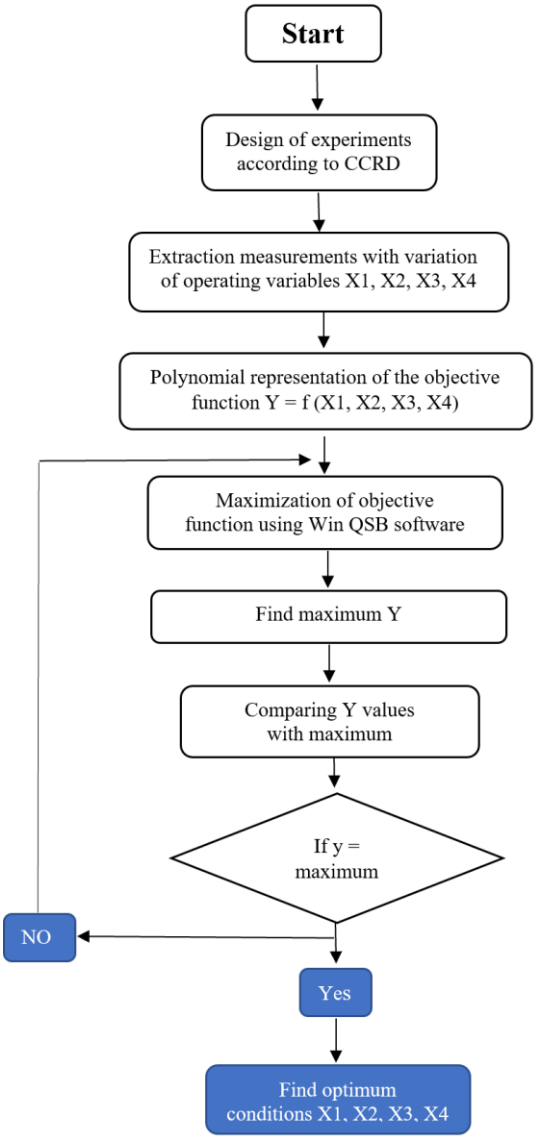

Fig. 15. Block diagram of optimization procedures

The first component of the experimental design approach is to design the experiments according to a predetermined plan, taking into account the description of the variable values in the plan using a coded form. The second section entails performing the regression analysis for the specific set of runs in the plan, taking into account the coded form of the variables as well as the results of the objective function for every trial in the set. The central composite rotatable design technique is the most effective of the various experimental design strategies available [114, 115].

The central composite rotatable design (CCRD) technique [116] was applied in the optimization process to evaluate the interaction of independent operating variables. The independent operating variables chosen for this study were the extractant solution concentration of macrocyclic compounds (A: 0.002–0.01 mol/L), pH (B: 1-5), time (C: 3-15 min), and the concentration of Sc (D: 25-125 mg/L) that were correlated in a non-linear second order model, equation Eq. 6, for extraction efficiency (E%) which represents the objective function (Y) to be maximized.

$$Y = \beta_0 + \beta_1 A + \beta_2 B + \beta_3 C + \beta_4 D + \beta_{11} A^2 + \beta_{22} B^2 + \beta_{33} C^2 + \beta_{44} D^2 + \beta_{12} AB + \beta_{13} AC + \beta_{14} AD + \beta_{23} BC + \beta_{24} BD + \beta_{34} CD \quad (5)$$

where,

β_0 is the intercept;

β_1, β_2, β_3, β_4 is the linear coefficients;

β_{11}, β_{22}, β_{33}, β_{44} is the squared coefficients;

β_{12}, β_{13}, β_{14}, β_{23}, β_{24}, β_{34} is the interaction coefficients;

A, B, C, D, A^2, B^2, C^2, D^2, AB, AC, AD, BC, BD, CD is the levels of independent variables.

As shown in Table 4, each independent operating variable in the CCRD was investigated at five levels (-α, -1, 0, +1, +α). Six center points were used in the design, with an α value of ±2 [114, 117]. The total number of experiments in the current experimental design is 2k + 2k + n, where k is the number of independent variables, and n is the number of times the experiments are repeated at the central stage. The aim of this design was to optimize the selected variables and maximize the Sc extraction efficiency by running 30 experiments with four variables.

Table 4. Experimental range, level and code of independent variables for CCRD design

Variables	Code	Range and levels				
		-2	**-1**	**0**	**+1**	**+2**
MC concentration (mol/L)	A, X1	0.002	0.004	0.006	0.008	0.01
pH	B, X2	1	2	3	4	5
Time (min)	C, X3	3	6	9	12	15
Sc concentration (mg/L)	D, X4	25	50	75	100	125

2.6 Preparation of Solid Phase for Solid-Liquid Extraction

2.6.1. Preparation of Iron Oxide Magnetic Nanoparticles

The co-precipitation technique was employed to produce iron oxide nanoparticles (Fig. 16A) [118, 119]. To achieve that, 4.4 g of $FeCl_3 \cdot 6H_2O$ and 1.98 g of $FeCl_2 \cdot 4H_2O$ were dissolved successively in 60 mL of de-aerated water by nitrogen gas. However, the solution was purged with nitrogen for 30 min to avoid the oxidation of Fe(II) ions. The co-precipitation process was carried out at two pH values pH 10 and pH 11 in order to prepare the optimum morphology and the nanoscale dimensions of iron oxide nanoparticles. Under continuous stirring at 25 °C of the ferric and ferrous iron mixture, 140 mL of the 0.8 mol/L of NH_4OH were added to the solution, and the pH was adjusted with (0.1 mol/L) HCl. During the addition of NH_4OH solution, it was observed that there is a color variation and after 5 min, the color has been changed from brown to black totally. The produced iron oxide nanoparticles were collected by external magnetic field. This characteristic is very advantageous for particle separation from the sample solutions. The sample is abbreviated as Fe_3O_4.

2.6.2. Preparation of Fe_3O_4/SiO_2/OPCs by Sol-Gel Method

It was proposed to immobilize the OPCs molecules over a solid support to prepare efficient solid–phase extraction (SPE) system. The incorporation of OPCs molecules, such as D2EHPA, TBP and TOPO was carried out by the entrapment technique of sol–gel method [120, 121].

The first step was the hydrolysis of tetraethyl orthosilicate (TEOS) which used as precursor for synthesis of siloxanes groups (Fig. 16B). 3 mL of TEOS were mixed with 1 mL of water and 0.1 mL of 1 mol/L HCl at room temperature at vigorous stirring for an hour to complete the hydrolysis of TEOS. Then 1 mL of D2EHPA or TBP, or 350 mg of TOPO dissolved in 3mL tetrahydrofuran (THF) was then added separately to the solution. After 10 min of stirring, 10 wt% of Fe_3O_4 were added to the mixture and sonicated for 5 min, followed by stirring at 72 h at the room temperature in order to complete the condensation. Finally, the obtained product was washed with distilled water and dried at 75 °C for 12 h and ground into powder using mortar and pestle. The preparation steps of F_3O_4/SiO_2/OPCs nanocomposite samples are presented in Fig. 16. The prepared samples are abbreviated in the text as Fe_3O_4/SiO_2/D2EHPA, Fe_3O_4/SiO_2/TBP and Fe_3O_4/SiO_2/TOPO.

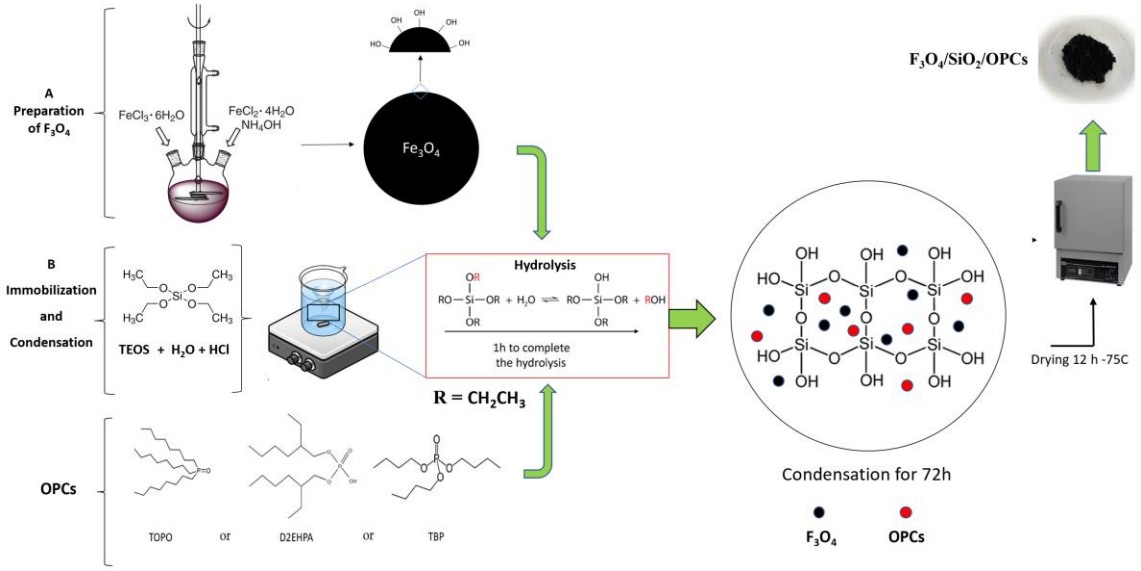

Fig. 16. Schematic illustration of the preparation of (A) Preparation of Fe_3O_4 and (B) hydrolysis of TEOS and condensation by sol–gel method

Figure 17 reveals the proposed mechanism for the immobilization of OPCs molecules into Fe_3O_4/SiO_2 nanocomposites materials. The pH of the reaction mixture has a strong influence on the structure and porosity of the formed solid phase [122]. In a sol-gel process, long siloxane chains formed on the Fe_3O_4 surface at pH < 7 (Fig. 17A and B/red chains). In this case, the siloxane group is less tightly packed giving the structure of 'crosslinked spaghetti', having a long and narrow pore. When the pH is above 7, siloxane chains with a lot of branches can form clusters with cylindrical pores (Fig. 17A/blue clusters) [122]. In this work, the chains structure is expected.

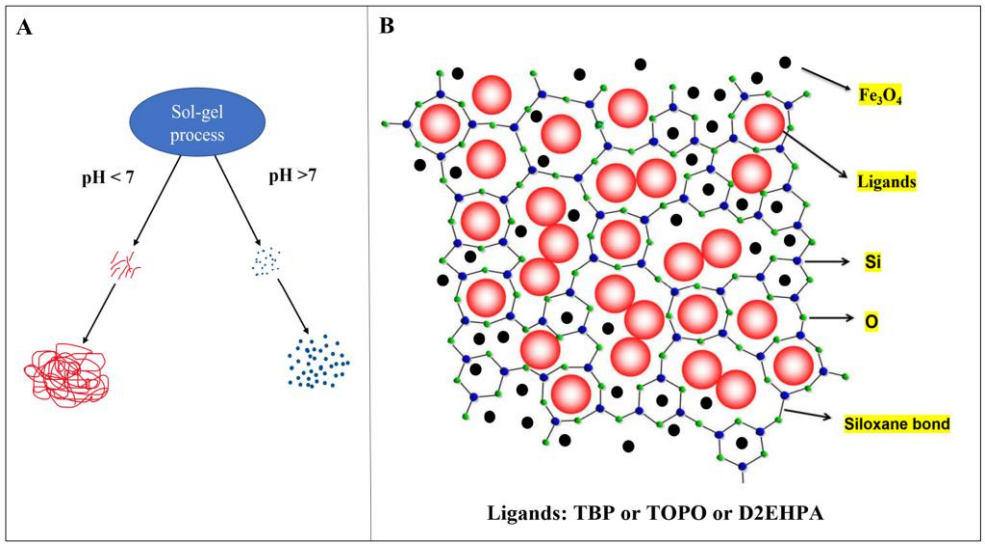

Fig. 17. Schematic illustration of the incorporation of OPCs to Fe_3O_4/SiO_2 by sol–gel method

2.6.3 Solid-Liquid Extraction Experiments

The prepared OPCs solid phase was tested by flow column method. The method was performed using 5 mL column (internal diameter of 6 mm) containing different weights of solid phase (0.1, 0.3, 0.5 g). The SP-loaded column was first wetted with 5 mL of deionized water, and then the real red mud leachate solution (5 mL, 7 mol/L HCl) was passed through the column at 5 mL/min flow rate. After the extraction, the ions were stripped from the solid phase with 10 mL of 1 mol/L HCl and analyzed by ICP-OES.

2.7 Characterization and Analytical Methods

The physico-chemical properties of the solid phase extraction and red mud were examined using several characterization techniques to obtain information about the structural, chemical and surface properties of the prepared solid phase.

2.7.1 X-ray Fluorescence Measurements

X-ray fluorescence (XRF) was used to determine the elemental compositions of the solid red mud. The major (Fe, Al, Si, K, Ca, Ti, and Na) and minor (Sc, Y, La, and Ce) elements of red mud were analyzed by Bruker S8-TIGER type XRF equipment. The RM samples were dried at 105 °C until a constant weight was obtained and sieved through a 200-mesh sieve after ultrafine grinding before analysis. The detection limit of equipment is 0.005 wt% (50 ppm).

2.7.2 Low Temperature Nitrogen Adsorption

The specific surface area, pore volume and pore size distribution in the 1.7-100 nm diameter ranges were determined from the N_2 adsorption−desorption isotherms at -196 °C. The samples (weight ≈ 0.2-0.7 g) were first degassed using a micromeritics flow prep 060-type at 100 °C (or 160 °C) for 2 h at static condition overnight before transferring to the micromeritics 3Flex 3500-type instrument, USA and then continued under vacuum at 100 °C (or 160 °C) for a further 4 h. The Brunauer-Emmett-Teller (BET) method within a relative pressure range of 0.05-0.3 was used to calculate the specific area (S_{BET}), while the pore volume (V) was calculated from the max N_2 adsorption uptake at a relative pressure (p/p_0) of 0.990. The micropore surface area (S_{micro}) and micropore volume (V_{micro}) data were reported by t-plot methods. The mesopore size distributions were calculated from the nitrogen desorption isotherms using the Barrett−Joyner−Halenda (BJH) model.

2.7.3 Fourier Transform Infrared Spectrometric Measurements

Fourier-transform infrared (FTIR) spectroscopic measurements were carried out by using a BRUKER Vertex 70 type spectrometer with a Bruker Platinum ATR adapter on the ground samples without additional sample manipulation. The spectra were recorded in the

range between 400^{-1} and 4000 cm^{-1} at a resolution of 2 cm^{-1} at the room temperature with a DTGS detector by averaging 512 scans.

2.7.4 Scanning Electron Microscopy and Energy Dispersive X-ray Measurements

The surface morphology and chemical composition of the prepared solid phase samples were investigated by Philips XL 30 ESEM scanning electron microscope combined with Energy Dispersive X-ray (EDX) analyzer. An accelerating voltage of 20 kV was used for the analyses. The magnifications of 100X and 300X allow obtaining the images in a 100 μm and 200 μm scale, respectively.

2.7.5 Inductively Coupled Plasma Optical Emission Spectrometric Method

Elemental analysis was performed using inductively coupled plasma optical emission spectrometry (ICP-OES) with Avio 550 Max instrument (Perkin Elmer Inc., USA). The ICP-OES was calibrated with using standards for 28 major and rare earth metals. The wavelengths of the element identification lines are summarized in Table 5.

Table 5. ICP-OES wavelengths of investigated elements.

Elements		Wavelength (nm)
Major elements	Fe	238.204
	Ti	368.519
	Al	396.153
	Ba	233.527
	Ca	317.933
	Co	230.786
	Cr	267.716
	K	766.490
	Mg	279.077
	Mn	257.610
	Na	589.592
	Si	251.611
	Sr	407.771
	Th	401.913
	Zr	343.823
REEs	Sc	361.383
	La	408.672
	Y	360.073
	Yb	369.419
	Tb	350.917
	Sm	442.434
	Nd	401.225
	Pr	390.844
	Dy	353.170
	Er	337.271
	Eu	381.967
	Gd	342.247
	Ce	418.660

3. RESULTS AND DISCUSSION

3.1 Composition of Red Mud

The chemical composition of Hungarian red mud measured by XRF analyzer is summarized in Table 6. It can be seen that the main components of red mud are Fe_2O_3, Al_2O_3, SiO_2, CaO, Na_2O, and TiO_2. Furthermore, the XRF study identified the minor Sr and Ni elements, as well as the trace elements, such as As, Cu, and REEs (Ce, Gd, Y, and Sc).

Table 6. The chemical composition of red mud measured by XRF analyzer.

Major oxides (wt%)		**Rare earth elements (ppm)**	
Fe_2O_3	38.9	Ce	690
Al_2O_3	11.1	Gd	290
SiO_2	9.1	Y	230
CaO	9.0	Sc	100
TiO_2	4.2	La	220
MnO	0.3	**Trace elements (ppm)**	
SO_3	0.3	Sr	1300
P_2O_5	0.3	Ni	370
K_2O	0.1	As	170
ZrO_2	0.1	Cu	150
Gd_2O_3	0.1		

3.2 Red Mud Digestion

The results indicate that the scandium leaching efficiency in (7 mol/L) HCl reached an optimum value of (79%) after 5 h. Only the partial dissolution was achieved. The elements composition in the obtained leachate was compared with those elements which were analyzed by XRF in red mud (Table 6). Due to the fact that scandium is commonly associated in hematite and goethite mineral phases, the leaching of the element was linked to the dissolution of iron [123]. The dissolution of titanium and other undesirable metals is also affected by the conditions under which they are leached [124]. The formation of

silica gel, which increases acid consumption, decreases scandium extraction, and complicates solid–liquid separation, is a major issue in the direct leaching of RM [90].

The current investigation found that the maximum concentration of Sc ranged 72-93 mg/kg depending on the RM batch, temperature 75-85 °C under reflux conditions, and its concentration 7-8 mol/L HCl as well as red mud (S)/acid solution (L) 1/30 ratio all contributed to optimize the leaching efficiency of the RM components.

Consequently, 7 mol/L of HCl, a S/L ratio of 1/30, and 5 h of leaching time 75 °C reflex temperature were found to be the most favorable conditions for scandium leaching from RM. Table 7 illustrates the chemical composition of the leachate solution. The major impurities are Ti, Al, Si and Fe, while the most valuable element is Sc which accounts for more than 95% of the economic value among REEs [125]. As a result, the current investigation concentrated on the extraction of scandium.

Table 7. Chemical composition of the red mud acid leachate used in this work (digestion acid 7 and 8 mol/L HCl).

Elements	Fe	Al	Ti	Sc	La	Y
XRF (mg/kg)	351700	53600	27300	100	220	260
Leachate (mg/L) * 7 mol/L HCl,3h	5045	2195	431.95	2.42	5.15	3.46
Leachate (mg/kg) 7 mol/L HCl,3h	151350	65850	12958.5	72.6	154.5	103.8
Leachate (mg/L) * 7 mol/L HCl,5h	4899	2533	714.2	3.1	5.16	3.63
Leachate (mg/kg) 7 mol/L HCl,5h	146970	75990	21426	93	154.8	108.9
Leachate (mg/L) * 7 mol/L HCl,5h	4634	2376	699.6	2.65	5.17	3.38
Leachate (mg/kg) 7 mol/L HCl,5h	139020	71280	20988	79.5	155.1	101.4
Leachate (mg/L) * 8 mol/L HCl,3h	5791.6	3265	897	2.88	6.98	3.24
Leachate (mg/kg) 8 mol/L HCl,3h	173748	97950	26910	86.4	209.4	97.2

* value for 1 g of red mud sample

3.3 Removal Iron Content from Leachate Solution

In the preliminary experiment to remove Fe(III) by tri-n-octylamine (N235), the extractant different volume percentages of N235 ranging from 5% to 30% in kerosene were investigated with two cycles and volume ratio O/A of 1:1. The results indicated that as the volume percentage of N235 was increased, the extraction efficiency of Fe(III) increased progressively. However, it had a little influence on the Sc(III), with an extraction efficiency no more than 2 vol.%, as shown in Fig. 18. Furthermore, the organic phase became turbid when the volume percentage of N235 exceeded 20 vol.%. As a consequence, the phase separation of organic and aqueous layers was difficult due to the formation of a third phase at the interface zone. A 2-octanol was utilized as modifier, where a 15 vol.% of 2-octanol was introduced to the organic phase to alleviate the third phase problem. The volume percentage 2-octanol was determined based on the investigation ranging from 0 to 20 vol%. The results manifested that under the following conditions: 20 vol.% N235, 15 vol.% 2-octanol, 65 vol.% kerosene, 25 °C, volume ratio O/A of 1:1, and one cycle, 99% of Fe(III) is extracted into the organic phase, whilst the 3% of scandium is co-extracted.

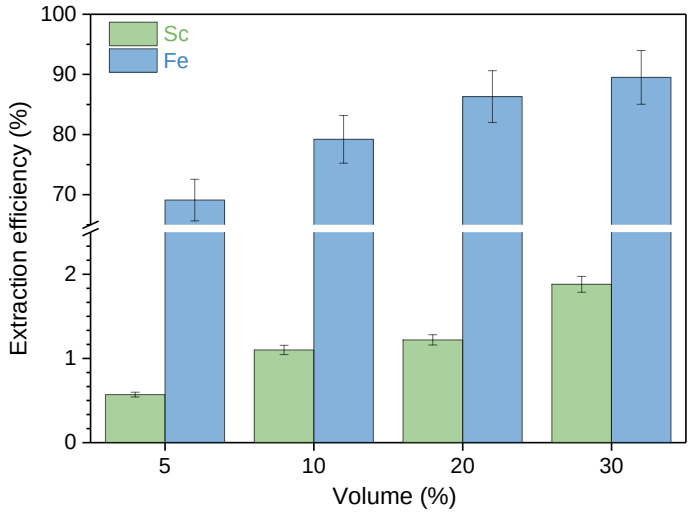

Fig. 18. Effect of N_{235} volume percentage on extraction efficiency (conditions: 20 vol% N_{235}, 15 vol% 2-octanol, 65 vol% kerosene, 25 °C, volume ratio O/A of 1:1)

Different cycles were studied during the Fe(III) removal by diethyl ether experiments in order to enhance the extraction process. The results revealed that after one cycle of SX by diethyl ether, the extraction efficiency of Fe(III) was 70%, whereas the extraction efficiency of Sc(III) was ~ 0%. The extraction efficiency of Fe(III) increased to 99% after two cycles of SX, whereas the extraction efficiency of Sc(III) was 0.3%. In third cycle, the extraction efficiency of Fe(III) increased just 0.3%, and the losses of Sc were 1.0%, as shown in Fig. 19. Based on the performance results, diethyl ether was selected for iron separation experiments.

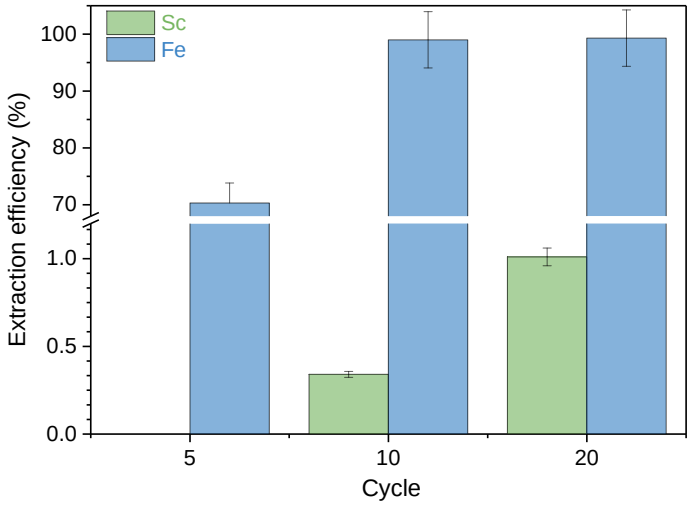

Fig. 19. Effect of number of cycles of diethyl ether on extraction efficiency (conditions: volume ratio O/A of 1:1, 25 ˚C)

3.3.1 Mechanism of Removal Iron Content by Diethyl Ether

To recover the scandium from red mud and eliminate the Fe(III) content from leachate, hydrochloric acid was chosen as the leaching agent, as shown in Sections 3.1 and 3.2. To achieve a high iron removal efficiency, trivalent iron should exist in its chloride form, as its primary form of $FeCl_4^-$ is the most common form. Because there are many H^+ in the leach liquid, diethyl ether will extract Fe(III) in the form of $HFeCl_4$, as shown in Equations 6, 7, 8, 9 and 10.

$$Fe^{3+} + Cl^{-} \leftrightarrow FeCl^{2+} \quad (6)$$

$$FeCl^{2+} + Cl^{-} \leftrightarrow FeCl_2^{+} \quad (7)$$

$$FeCl_2^{+} + Cl^{-} \leftrightarrow FeCl_3 \quad (8)$$

$$FeCl_3 + Cl^{-} \leftrightarrow FeCl_4^{-} \quad (9)$$

$$Fe^{3+}_{(aq)} + 4Cl^{-}_{(aq)} + H^{+}_{(aq)} + nEther_{(Org)} \leftrightarrow nEther_{(Org)} \cdot HFeCl_4 \quad (10)$$

where, the subscript *aq* and *org* represent the water phase and organic phase respectively; *n* is the stoichiometry coefficient of extraction. The concentration of Cl^{-} in the solution had a significant impact on the Fe(III) extraction efficiency. The Fe(III) content was extracted in the form of $HFeCl_4$, and the complex formed in the extraction process was $nC_4H_{10}O{\cdot}HFeCl_4$. When the Cl^{-} content reached a suitable concentration, the majority of the Fe(III) was converted to the form of $HFeCl_4$, and the extraction efficiency increased substantially. According to theoretical studies, the ferric species exists mostly as $FeCl_3$ or $FeCl_4^{-}$ at chloride concentrations more than 6.65 mol/L. In hydrochloric acid, Fe(III) readily forms a series of Fe-Cl complexes, and $FeCl_4^{-}$ anion is formed when the chloride concentration in the solution is high enough [126]. Although scandium can also form $ScCl^{2+}$ complex but to a lesser extent, therefore the ether solvent extraction can be used for the selective separation iron from scandium. As a result, an anion can selectively extract iron while retaining scandium. As a consequence, the goal of this step is to develop a better method for selectively removing iron from the chloride system while preserving scandium.

3.4 Liquid-Liquid Extraction

3.4.1 Liquid-liquid extraction by organophosphorus compounds

3.4.1.1 Liquid-liquid extraction by D2EHPA

3.4.1.1.1 Effect of aqueous to D2EHPA phase ratio on extraction efficiency of metal ions

From the economic point view, it is very important to check the loading capacity and reduce the consumption of the D2EHPA extractant as well as improve the extraction process (enrichment). The effect of the aqueous to organic phase (A/O) ratio on the effectiveness of the extraction of investigated metal ions has been studied, and the findings are presented in Fig. 20. The results showed that the effect of phase ratio was clear on the extraction efficiency of Sc and Ti more than Al, Y, and La. When the A/O ratio was increased from 3 to 4, the extraction efficiency of Sc dropped from 97% to 90%, and the Ti extraction efficiency dropped from 50% to 42%. Whilst, when the A/O ratio was increased from 4 to 5, the extraction efficiency of Sc decreased from 90% to 85%, and the titanium extraction efficiency dropped from 42% to 35%. Likewise, the yttrium and aluminum extraction efficiency were quite low. Finally, the best ratio A/O was determined to be 3.

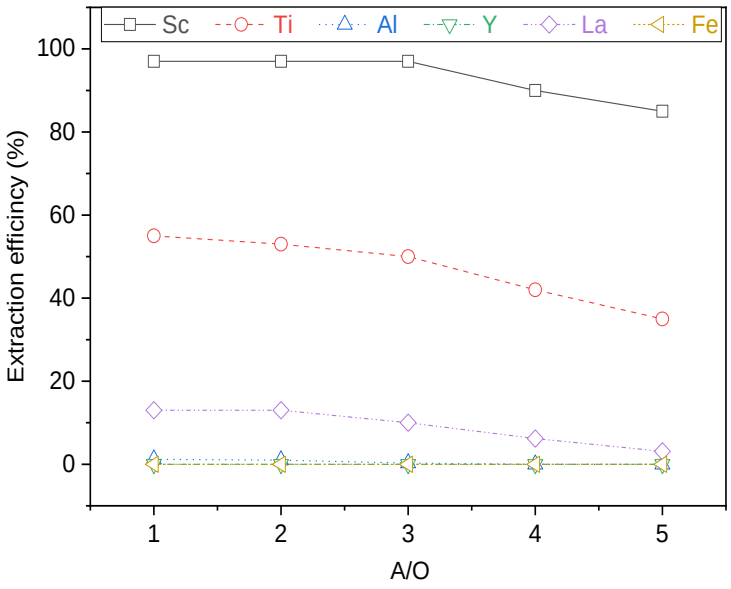

Fig. 20. Effect of A/O phase ratio on the extraction efficiency on metal ions (organic phase: 0.05 mol/L D2EHPA, temperature: 25 ℃, time: 10 min, aqueous phase: 10-50 mL)

3.4.1.1.2 Effect of pH Solution on Extraction Efficiency in D2EHPA System

Under the conditions of 0.05 mol/L of D2EHPA concentration, A/O of 3 (15 mL:5mL), the temperature of 25 °C, and shaking time of 10 min, the influence of pH solution on the extraction behavior was examined in a pH value range of 0–1. The findings in Fig. 21 indicated that the scandium extraction efficiency decreased slightly from 97% to 95% when the initial pH range was increased from 0 to 0.6, but it then stayed constant as the pH value was increased to 1. On the other hand, the titanium extraction efficiency increased from 55% to 67.1% when the pH was settled from 0 to 1. The extraction performance of yttrium and lanthanum was similar to some extent, and there is no noticeable increase with pH value increased. Based on the above results, the appropriate pH value for the selective extraction of scandium in the hydrochloric acid medium was therefore recommended as 0–1.

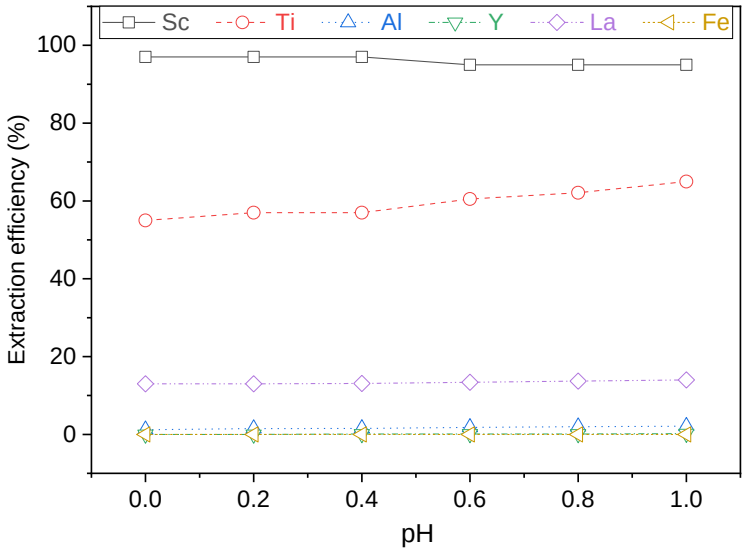

Fig. 21. Effect of pH on extraction efficiency on metal ions (organic phase: 0.05 mol/L D2EHPA, A/O: 15 mL: 5 mL=3, shaking time: 10 min, temperature**:** 25 °C).

3.4.1.1.3 Effect of Shaking Time on Extraction Efficiency

The rapid extraction kinetics has a great advantage in the industrial production. The impact of shaking time on the extraction efficiency of investigated metals was investigated, and the findings are given in Fig. 22. Where, the results showed that the extraction efficiency

of Sc jumped from 60% to 97% as the time was increased from 5 to 10 min, and thereafter it remained stable. On the other hand, the extraction efficiency of Ti increased from 41% to 55% as the time was increased from 5 to 10 min, after that the increase of extraction efficiency became limited. The extraction efficiency of the other metal ions, on the other hand, has steadily grown throughout the time. Consequently, the results showed that the metal ion extraction rates rise with the time and tend to be steady at 10 min.

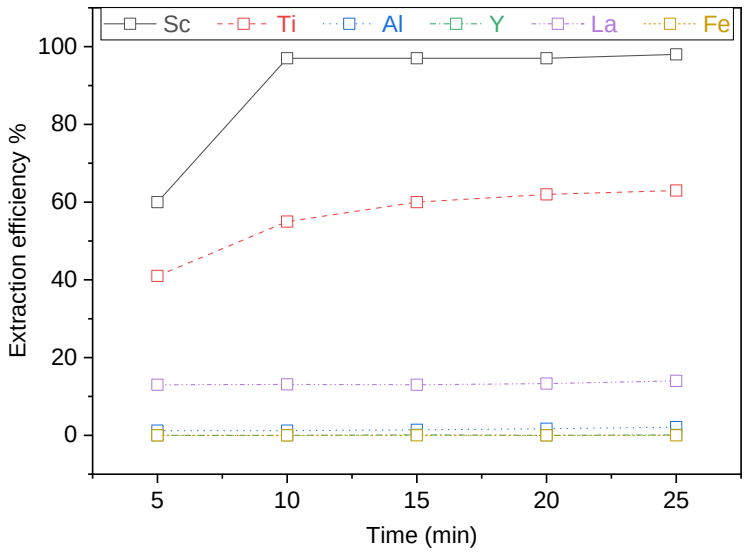

Fig. 22. Effect of shaking time on the extraction efficiency (organic phase: 0.05 mol/L D2EHPA, A/O: 15 mL:5mL =3, temperature: 25 ℃)

3.4.1.1.4 Effect of NaOH concentration and temperature on stripping efficiency of metal ions from D2EHPA organic phase

Some unwanted metals, such as aluminum, calcium, magnesium, silicon and rare earths were co-extracted with the scandium during the extraction process**.** However, the aforementioned scandium extraction chemistry suggests that stripping the scandium from the D2EHPA loaded organic phase, even with a strong acid solution is difficult. The loaded organic phase, on the other hand, can be scrubbed off most of the co-extracted impurities using an acid solution [127]. The loaded extractants is usually stripped by mixing it with mineral acids. Efforts have been made to recover the scandium from the D2EHPA loaded organic phase using different chemical reagents, such as mineral acids (e.g., hydrochloric, sulfuric, and nitric acids), organic acids (e.g., citric and oxalic acids),

or a combination of both [88, 128-131]. Because the scandium ion can form a very strong complex with D2EHPA, it was difficult to entirely remove the scandium from the loaded organic phase with these acids. The extracted scandium in the extractant (organic phase) should be recovered to allow it to provide more processing and reuse [128]. In this work, the alkaline solution was used as the stripping agent, as reported in the literature [132]. NaOH solution was selected as stripping agent to back extract the scandium from the Sc-loaded phase that $Sc(OH)_3$ would form as a kind of precipitation according to the following Eq. 11:

$$Sc^{3+}_{(O)} + 3OH^{-}_{(a)} = Sc(OH)_{3\,(S)} \downarrow \qquad (11)$$

It is worth noting that the chemical species of scandium hydroxide, whether it is solid or soluble, depends on the concentration of the alkaline solution. Scandium stripping efficiency as a function of NaOH concentration (0.5 - 3 mol/L) is shown in Fig. 23.

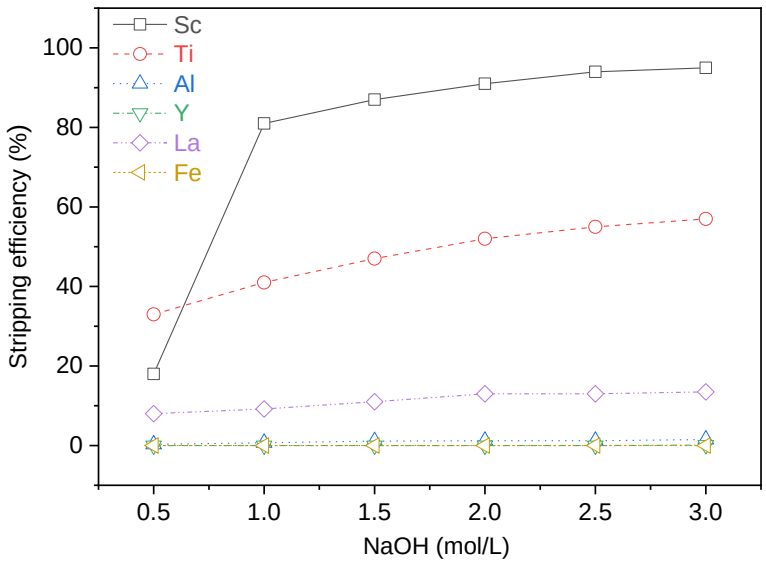

Fig. 23. Effect of the NaOH concentration on the stripping efficiency (organic phase: 0.05 mol/L D2EHPA, A/O: 5mL:5 mL=1, shaking time: 15 min, temperature**:** 25 ℃).

Where, the stripping results in figure showed that from 0.5 mol/L to 1 mol/L, the scandium's stripping efficiency rose dramatically, but there was no a noticeable rise above 2.5 mol/L NaOH. Moreover, at 2.5 mol/L concentration of NaOH, 95% of scandium was

back extracted. This is a result of the extracted scandium in the D2EHPA phase has stronger affinity to the hydroxyl ions in the alkaline solution [128, 132]. It was observed that if the NaOH concentration is high (more than 2.5 mol/L), a white precipitate at the interface between the two phases appears that is disadvantageous for phase separation and leaves a small amount of precipitation in the organic phase leading to the decrease of scandium stripping efficiency. The temperature impact on the back extraction of investigated metals is elucidated in Fig. 24.

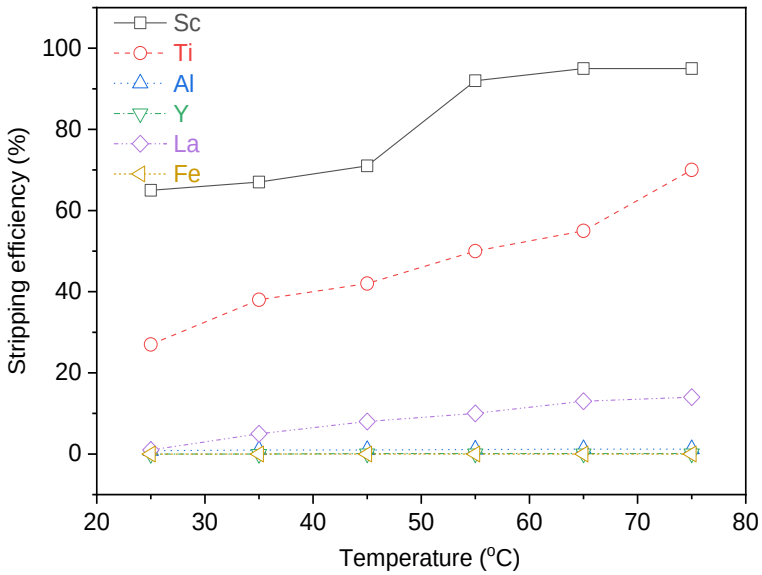

Fig. 24. Effect of temperature on stripping efficiency (organic phase: 0.05 mol/L D2EHPA, 2.5 mol/L NaOH, A/O: 5mL: 5mL=1, shaking time: 15 min).

Where, the results showed that the scandium's stripping efficiency improved with temperature, reaching 95% at temperatures above 65 °C. Moreover, the temperature-dependent stripping efficiency of titanium is identical to that of scandium. In addition, no aluminum or yttrium is detected in the back-extraction stage. Furthermore, because the phase separation is simple and easy at higher temperatures, 65 °C is an excellent choice for back extraction.

Based on these results, a 2.5 mol/L of NaOH solution was recommended for the following stripping process. During the stripping process, hydroxyl ions precipitated the extracted metal ions with the assistance of heat. The white precipitate was then centrifuged and

dissolved into HCl to form the pre-enrichment liquor. Moreover, titanium was also co-extracted, and its concentration was remained high when the extraction process was completed. As a result, scandium separation from titanium was still not ideal and depended on the efficiency of washing step. The result indicates that the two stripping stages are enough to nearly completely strip scandium from the D2EHPA loaded organic phase [129, 130]. During further purification, the precipitation with oxalic acid can eliminate the remaining impurities of components in the trace amount, and the final product might be produced in a very pure manner.

3.4.1.2 Liquid-liquid extraction by TBP

3.4.1.2.1 Effect of TBP concentration on extraction efficiency of metal ions from RM leachate

The organic extractants that were investigated were TBP in kerosene at different volume concentrations. The influence of organic extractant concentration within the range 2 to 20 vol.% was investigated at an A/O ratio of 1 (5 mL:5 mL) for 15 min shaking time at 25 °C. The results are illustrated in Fig. 25.

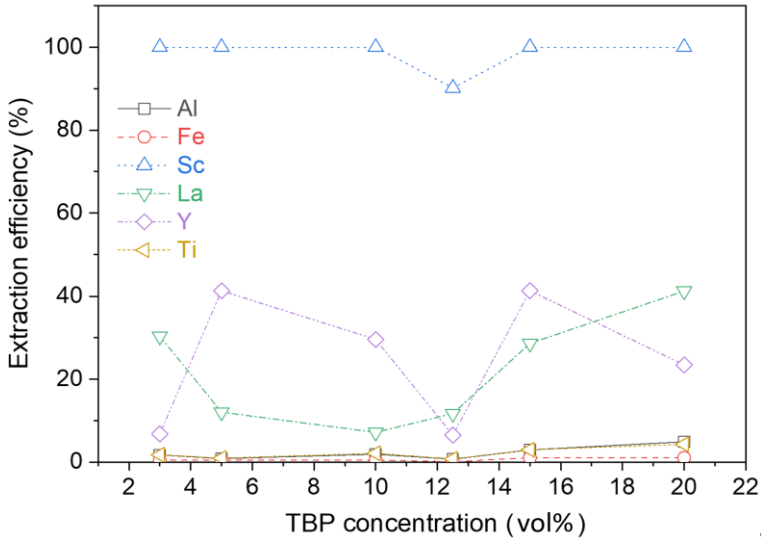

Fig.25. Effect of TBP concentration on extraction of metals from RM based on leachate solution (organic phase: TBP, A/O: 5 mL:5mL, shaking time: 15 min, temperature: 25 ℃).

The results showed that there was no statistically significant fluctuation in the extraction of scandium during the time intervals tested. As the TBP concentration was increased, the extraction efficiency for aluminum and titanium reached 4.9% and 4.3%, respectively. With a rise in the TBP concentration, the extraction efficiency of lanthanum and yttrium fluctuated, where the yttrium increased in extraction efficiency from 6.8% to 41.3% as the TBP concentration increased from 3 to 5 vol.%. In contrast, the extraction efficiency of yttrium fell by 29.6% and 6.4% at 10% and 12.5 vol.% TBP, respectively. In the instance of lanthanum, the extraction efficiency declined as the TBP concentration increased until it reached 10 vol.%, after which it climbed to 41.3% at 20.0 vol.% TBP. However, even though all of the scandium was extracted, the organic phase may still present a challenge to the final solution in the recovery process. As a result, choosing the optimal conditions that prevent the extraction of unwanted elements is an important task. It can be concluded, compared to the data presented in Fig. 25, the scandium separation was more selective over titanium, aluminum, and other rare earth elements at 12.5 vol.% TBP.

3.4.1.2.2 Effect of aqueous to TBP phase ratio (A/O) on extraction efficiency of metal ions

The influence of the A/O ratio was investigated at 25 °C for 15 min with a TBP of 5 vol% in different A/O ratios from 1 to 4. The results are illustrated in Fig. 26. Using an A/O ratio of 1:1, the extraction of scandium was almost 100% effective and remained stable as the organic fraction increased.

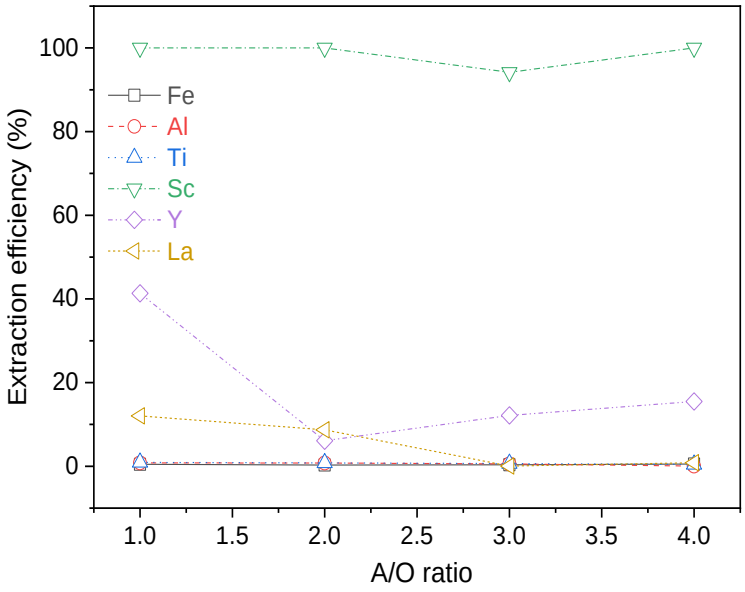

Fig.26. Effect of TBP phase ratio on extraction efficiency based on leachate solution (organic phase: 5 vol% TBP, shaking time: 15 min, temperature: 25 ˚C, aqueous phase: 10 - 50 mL)

It was observed that the extraction of titanium was relatively steady and it declined as the phase ratio was increased. Between 1:1 and 2:1 of the A/O phase ratio, the extraction of yttrium was dropped from 41.3% to 6.1%, and then increased to 12.2% and 0.5% in A/O equals 3:1 and 4:1. Between 3:1 and 4:1, the extraction of lanthanum remained stable and subsequently increased to 12.0% and 8.7% in A/O equals 1:1 and 2:1, respectively. In all A/O ratios investigated, the extraction of iron (0.3-0.5%) and aluminum (0.03-0.8%) held steady in these ranges. Based on above investigation and considering the extraction efficiency of investigated elements, the best phase's ratio is 3.

3.4.1.2.3 Stripping from TBP organic phase by water and HCl

To recover the scandium content from the Sc-loaded TBP organic phase, the stripping experiments have been done with distilled water with 0 mol/L, 0.1 mol/L, 0.5 mol/L, and 1 mol/L of HCl. The stripping efficiency from TBP organic phase after one solvent extraction cycle is displayed in Fig. 27. The obtained results manifested that the stripping efficiency was sensitive to the pH of solution.

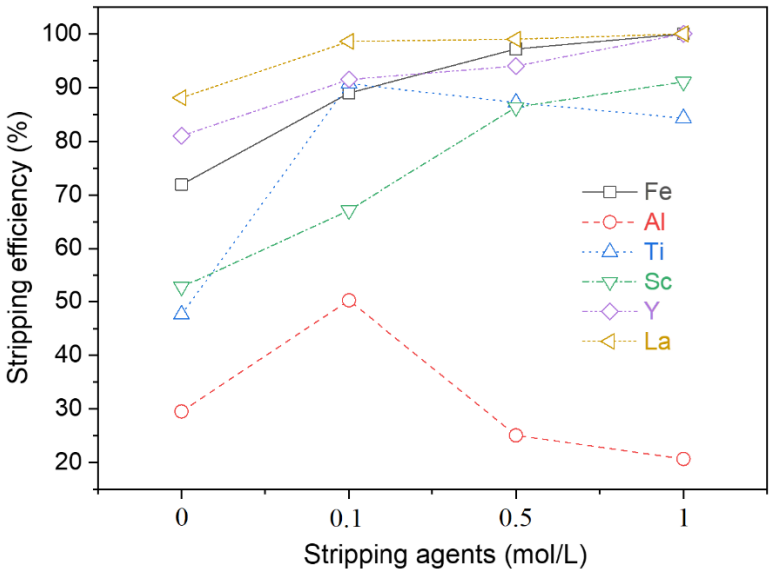

Fig.27. Effect of stripping agent on stripping efficiency of metal ions (organic phase: 5 vol% TPB, A/O: 5mL:5mL, shaking time: 15 min, temperature: 25 ˚C).

When the water was used as a stripping agent from the TBP organic phase, the results of back extraction were 71.9% Fe and 52.8% Sc compared with 81% Y, 88.1% La, 29.6 % Al and 47.6% Ti. The stripping efficiency of all investigated elements increased with 0.1 mol/L of HCl as follow: 67.1% Sc, 88.9% Fe, 91.5% Y, 98.6% La, 50.2% Al and 90.7% Ti. At (0.5 mol/L), the stripping efficiency of Fe, Sc, Y and La increased, whilst Al and Ti decreased. At 1 mol/L of HCl, the stripping efficiency of Sc, Fe, Y and La increased to 91%, 100%, 100% and 100%, respectively. Whilst the stripping efficiency of Al and Ti decreased to 20.7% and 84.31% compared with 0.5 mol/L of HCl (see Fig. 27). Based on above results, 1 mol/L of HCl seems to be the optimum stripping agent and it was chosen for the all recovery experiments from the TBP loaded organic phase for comparison. It was found that when the acid concentration is increased more than 1 mol/L, the stripping efficiency of Sc, Y, and La was relatively constant as 91.3%, 100%, 100%, respectively. Moreover, Al and Ti decreased to 1.9%, 4.2%, respectively, compared with their normal extraction efficiency. On the other hand, the trivalent iron content was removed in the final step of the recovery process by two cycles of solvent extraction with diethyl ether, where the extraction efficiency of Fe was 99%. It is noteworthy that the number of

extractions cycles depends on the amounts of accumulated elements after the stripping process, which should be removed from the organic phase for the recyclable process.

3.4.1.3 Mechanism of Extraction of Sc by Organophosphorus Extractants

The trivalent metals (e.g. Sc^{3+}, La^{3+}) generally exist in aqueous solution as hydrated ions ($[M(H_2O)_6]^{3+}$). Before the extraction of those metals into a nonpolar organic phase, the water molecules must be replaced and any ionic charge reduced or removed. This can be achieved in different ways by using three types of extractants: acidic, basic, and solvating (neutral). D2EHPA, TOPO and TBP organophosphorus extractants based on phosphoric acid, where the π bond is classified as a d-pπ bond [60]. The d-pπ bond is formed by a non-bonded p-electron pair in a 3d empty orbital on a phosphorus atom. Because the phosphorus atoms have high-energy d orbitals and a large effective atomic radius (0.106 nm), the phosphorus has a high degree of polarization and relatively low electronegativity. Consequently, the electronic impact is relatively strong when the phosphorus atom is directly coupled to the oxygen atom, and the polarity of the phosphoryl group (≡P = O) or the charge density of oxygen varies strongly. Because of the structural features of the phosphorus‑oxygen bond, these OPCs compounds have shown their resistance and high stability to strong oxidants such as HNO_3 acid [60]. Due to OPCs' high extraction performance, the solvent extraction might significantly boost the scandium concentration in the liquor organic phase during the pre-enrichment process.

3.4.1.3.1 Scandium ions extraction mechanism by acidic extractants

Acidic extractants including organophosphorus (D2EHPA), carboxylic and sulphonic acids with function group –POOH, –COOH and $–SO_3H$, respectively. In general, when the organic phase has a high metal loading of metal ions (M^{n+}), and the extraction of a metal cation (M^{n+}) by an acidic extractant (HA) occurs via a cation exchange mechanism, as illustrated in Eq. 12 [41, 70]:

$$M^{n+}_{(aq)} + nHA_{(org)} \leftrightarrow MA_{n(org)} + nH^{+}_{(aq)} \quad (12)$$

When there is a low metal loading in the organic phase, the extraction can be represented by Eq.13:

$$M_{(aq)}^{n+} + nHA_{2(org)} \leftrightarrow MA_{n(org)} + nH_{(aq)}^{+} \quad (13)$$

Eq.13 generalized the extraction mechanism of D2EHPA in an acidic environment.

The extent of extraction also depends on the magnitude of the metal-extractant formation constant (K_f) and the concentration of extractant (HA) [106]. These factors can be combined with the distribution coefficient (D) in the following equation derived from Eq. 14 and the law of mass action:

$$LogD = logK_f + nlog[HA] + n\,pH \quad (14)$$

Where, n is the stoichiometric moles of equation, and pH is the value of pH of aqueous solution.

This equation allows the stoichiometry of Eq. 14 to be confirmed by constructing the linear plots of logD versus pH and logD versus log(HA) [106]. Based on that, the extraction occurs by a change of the acidity in solution; thus, increasing the pH of solution increases the extraction, and decreasing the pH promotes the stripping or back-extraction. Therefore, by changing the acidity of the system, the metal can be cycled to and from the organic phase. The number of D2EHPA molecules needed for Sc extraction was calculated using the slope method, and its mechanisms were determined [133]. In this method (Fig. 27), different D2EHPA concentration and pH solution were correlated with varied distribution ratio based on Eq. 14. The straight line in Fig. 28A had a slope of 3.10, indicating that the value of n was close to 3. The straight line in Fig. 28B has a slope of 2.91, and the value of n was also close to 3. As a result, three molecules of D2EHPA are sufficient to form a stable complex for the extraction process.

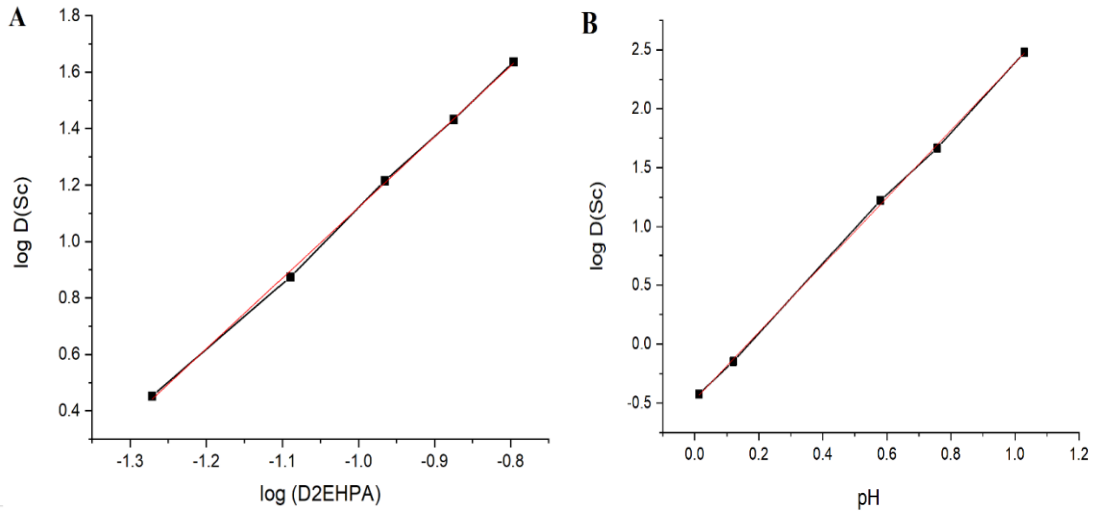

Fig. 28. Effect of D2EHPA concentration (A) and pH solution (B) on the distribution ratio value of Sc between organic and aqueous phases

The chemical interactions between the Sc ions of red mud leachate and the D2EHPA organic extractant as well as Sc-D2EHPA complex and NaOH solution are shown in Fig. 29A and Fig. 29B, respectively.

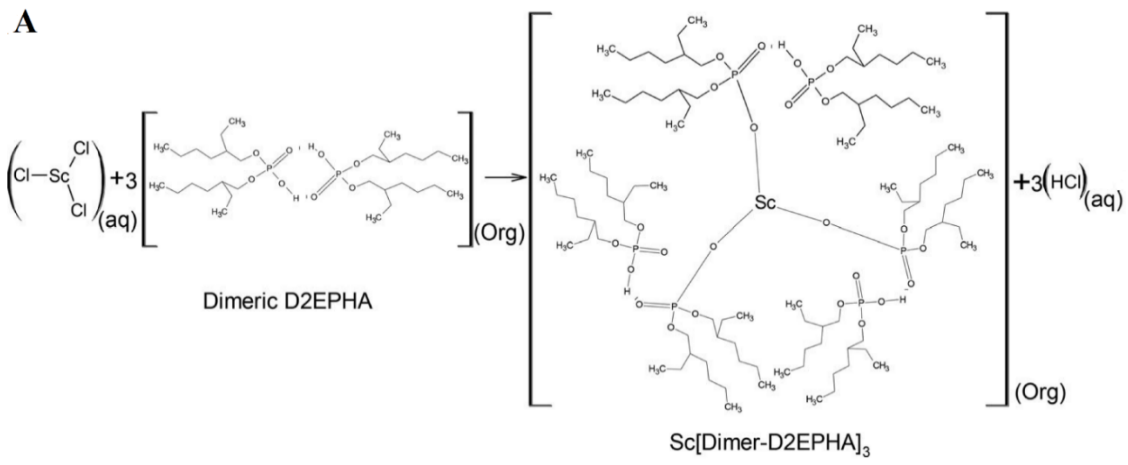

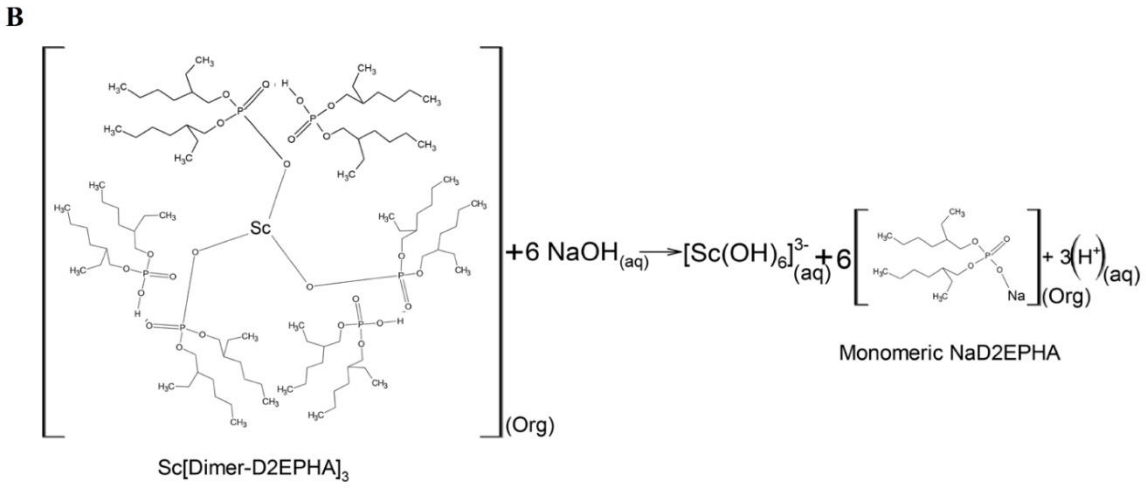

Fig. 29. Illustration of chemical interaction between D2EHPA extractant and Sc^{3+} during (A) solvent extraction and (B) stripping steps with NaOH

3.4.1.3.2 Scandium ions extraction mechanism by neutral extractants

Solvating extractants mainly include organic reagents containing C=O and P=O groups, such as ketones, ethers and phosphate. The most commonly used solvating extractants are neutral OPCs, such as TBP and TOPO.

Scandium exists mainly as $[Sc(H_2O)_6]^{3+}$ cation complex in nitric or hydrochloric solutions at pH <3 [105]. It is known that the TBP and TOPO are neutral extractants, for these types of extractants, and a hydration-solvation mechanism including the formation of complexes in organic phase that contain different numbers of acid and water molecules is postulated and described by Eq. 15 [106].

$$MX_{n(aq)} + mS_{(org)} \leftrightarrow MX_nS_{m(org)} + mH_2O_{aq} \quad (15)$$

Where, MX is a cation complex, S is the neutral OPCs (TBP or TOPO), and m & n are the stoichiometric moles organic and aqueous phases, respectively.

In case of HCl solution, the increase of hydrochloric acid concentration in the aqueous phase promotes the substitution of water molecules by Cl^- ions in $[Sc(H_2O)_6]^{3+}$ complex forming more extractable chloro-aqua complexes by Eq. 16 [105]:

$$[ScCl_3(H_2O)_3]_{aq} + 3S_{(org)} \leftrightarrow [ScCl_3(S)_3]_{(Org)} + 3H_2O_{(aq)} \quad (16)$$

The extraction of scandium by TBP, TOPO and iron from RM hydrochloric leachate can be represented, as shown in Fig. 30A, B and C respectively.

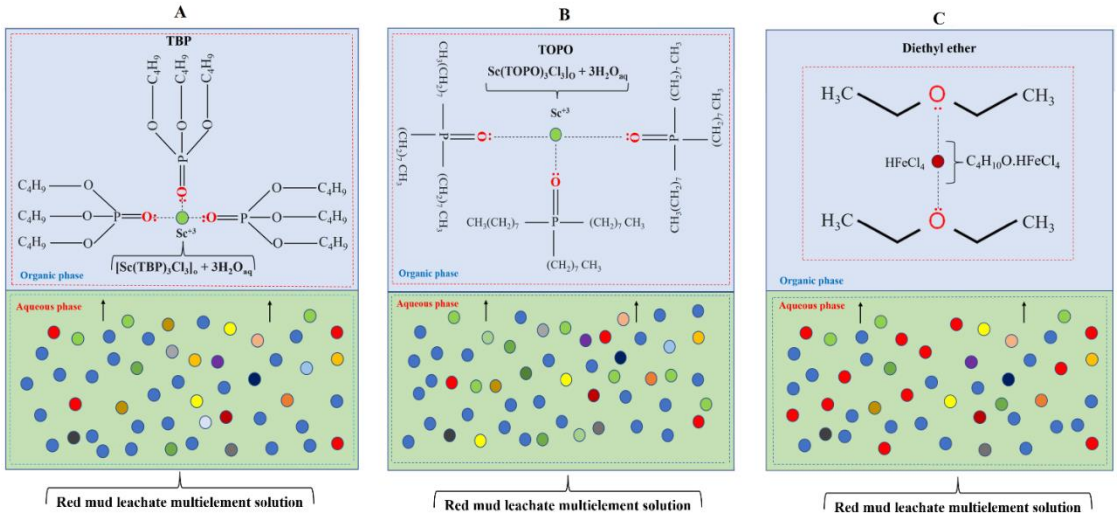

Fig. 30. Illustration of chemical interaction between (A) TBP extractant and Sc^{3+} ions, (B) TOPO extractant and Sc^{3+} ions (C) diethyl ether extractant and Fe^{3+} ions

3.4.1.4 Proposed Protocols and their Flowsheets for Sc Recovery from Red Mud

Based on the above findings (see section 3.4.1), five integrated protocols for Liquid-Liquid extraction and purification of scandium and iron from the red mud leachate solution were proposed, as shown in Figs. 32-36. Sections 3.3.1.1 and 3.3.1.2 summarize the most important parameters which have a direct effect on the Sc recovery process from the red mud leachate, such as the concentration of extractant, A/O phase ratio, the concentration of stripping solution, and pH value. This section represents and reflects the vision of the researcher based on the analysis of the results of the above investigation, considering the economic aspects of the extraction process, such as A/O phase ratio and the concentration of extractant in process design. For all proposed protocols, the leaching efficiency of Sc was monitored by ICP-OES and it is important to be not less than 70 mg/kg.

3.4.1.4.1 Single liquid-liquid extraction by DE2HPA (Protocol A)

In the D2EHPA Protocol **A** (Fig. 31), the first step in extraction process was iron removal by diethyl ether prior to the scandium separation. According to the above investigation (see section 3.4.1.1), the following conditions have been identified for best extraction: A/O=50:15, the 0.05 mol/L of D2EHPA, pH < 0, 5 min extraction time, and 2.5 mol/L of NaOH as stripping agent.

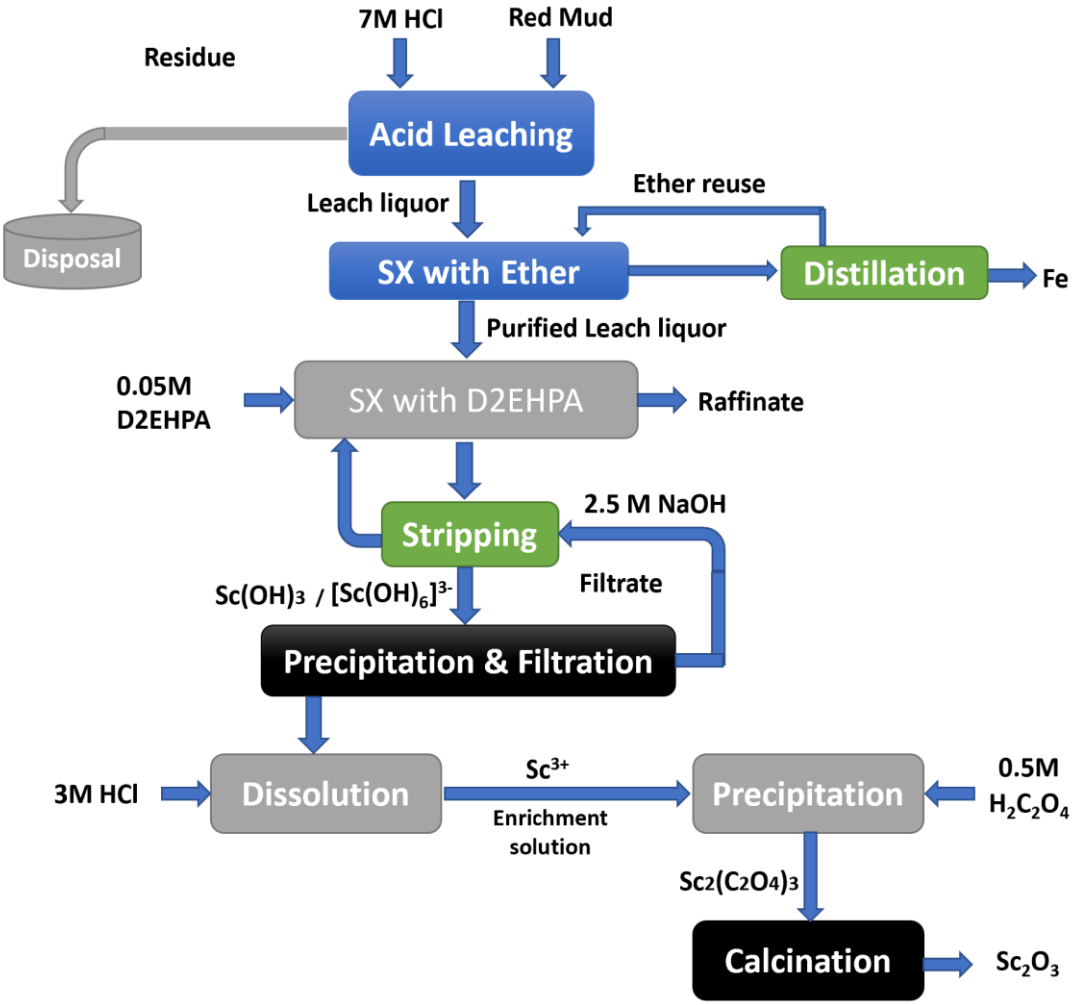

Fig. 31. Proposed flow sheet for the recovery of Sc from RM leachate step applying liquid-liquid extraction by DE2HPA (Protocol A)

As seen in the Table 8, the increase in concentration of Sc (86 to 402 ppm) after one cycle SX with 0.05 mol/L D2EHPA extractant was observed in comparison with the other elements. The D2EHPA was also selective towards Fe and Ti removal from the aqueous

solution. Table 8 shows a numerical comparison between the leachate solution and the final enrichment solution, obtaining an aqueous phase after the NaOH stripping step. The problem with this protocol is that the co-extracted elements, such as titanium, get trapped in the extractant or concentrate in the stripping solution. For that, an additional purification steps have been proposed, as shown in next protocols **(B, C, D** and **E).**

Table 8. Comparison between the leachate solution and final solution after SX (Protocol A)

	Elements	**Fe**	**Al**	**Ti**	**Sc**	**La**	**Y**
Protocol (A)	**Leachate (mg/L)* 8 mol/L HCl,3h**	5791.6	3154	897	2.88	6.98	3.46
	Leachate (mg/kg) 8 mol/L HCl,3h	173748	97950	26910	86.4	209.4	97.2
	SX (Extraction conditions: A/O=50:15 , 0.05M D2EHPA, extraction time 5 min)						
	Enrichment solution (mg/L)*	2.4	3.8	767.6	13.4	0.46	0.22
	Enrichment solution (mg/kg)	72	114	23028	402	13.8	6.6
	Recovery efficiency from leachate, R%	0.008	0.02	17.1	93.5	2.7	6.6

* value for 1 g of red mud sample

Finally, oxalic acid ($H_2C_2O_4$) was proposed to produce scandium oxide as a solid powder and further purification. It was observed that the precipitation step by oxalic acid was not applicable for low Sc concentration. The evaluation of the ability of oxalic acid as precipitation agent was done with the model solution to estimate the best conditions. The precipitation of Sc was achieved 90.8% (227 mg/L) at the following conditions: 1 mol/L $H_2C_2O_4$, 20 mL, pH=1.8, C(Sc) =250 mg/L, and 20 mL model solution (Table 9). Figure 3.2 depicts the scandium oxalate precipitate after the centrifugation process.

Table 9. Results of Sc precipitation from model solution by oxalic acid

Oxalic acid concentration (mol/L)	Volume, mL	pH of solution	Model solution concentration (mg/L)		Precipitation, %
			Sc before precipitation	Sc after precipitation	
1	40	0.7	300	271.2	9.6
0.5	40	1.8	250	22.8	90.8

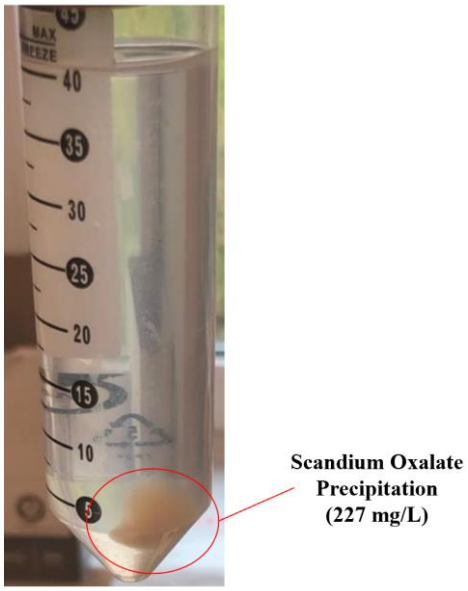

Fig. 32. Formation of $Sc_2(C_2O_4)_3$ solid particles during precipitation of Sc in model solution (250 mg/L) by oxalic acid

3.4.1.4.2 Single Liquid-Liquid Extraction by TBP (Protocol B)

In the TBP Protocol **B** (Fig. 33), a new technique was proposed and used for the first time, which included four main steps: Leaching, SX with 2 vol.% of TBP, stripping with 1 mol/L HCl, and SX with diethyl ether. In these experiments, the volumes of the aqueous and organic solutions were increased and maintained at the A/O phase ratio close to 3 based on the investigation (see section 3.4.1.2).

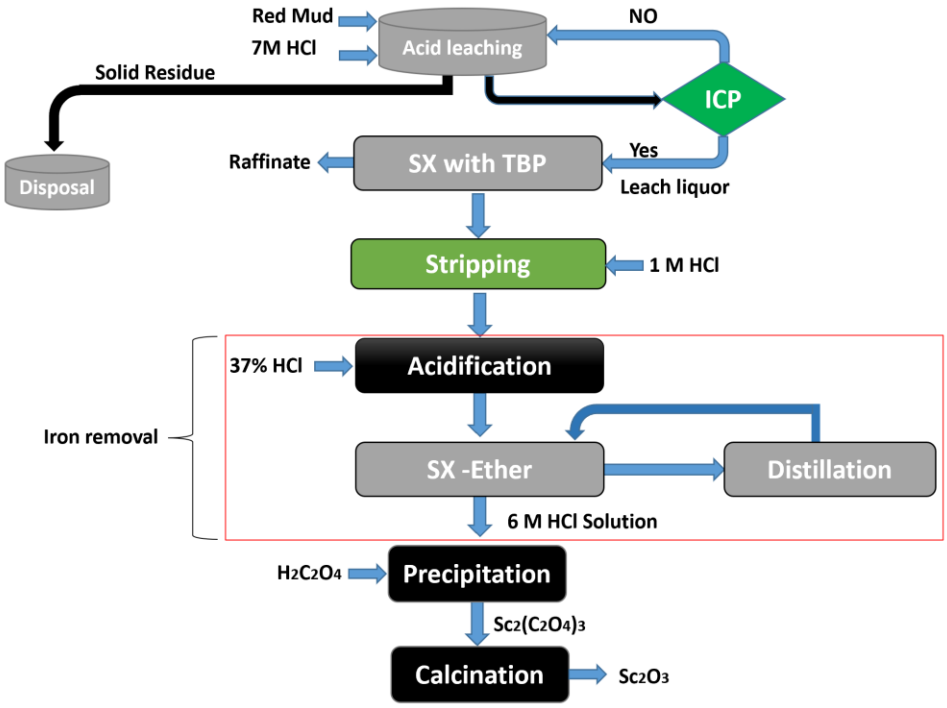

Fig. 33. Proposed flow sheet for the recovery of Sc from RM based on liquid-liquid extraction by TBP (Protocol B)

The analysis of previous results evinced that the iron concentration helps increase the extraction efficiency of scandium and at the same time reduces the consumption of used TBP extractant considering maintaining the A/O phase ratio not more than 4. The one SX cycle with TBP extractant has proven an exceptional effectiveness in the extraction in terms of selectivity Furthermore, the numerical values of initial solution, leachate and the final solution, and the enrichment solution obtained after the HCl stripping are compared in the Table 10. towards the iron and scandium compared with the D2EHPA extractant. The concentration of scandium increased from 93 to 769 ppm compared with the other elements, and this is due to the high selectivity of TBP towards the Sc ion extraction. The main advantages of this protocol are faster, the Sc recovery is more efficient, and the A/O phase separation is easier in comparison to the D2EHPA Protocol A. In addition, it is not necessary to use the NaOH solution for the stripping step.

Table 10. Comparison between the leachate solution and final solution after SX (Protocol B)

	Elements	Fe	Al	Ti	Sc	La	Y
Protocol (B)	**Leachate (mg/L)* 7 mol/L HCl,5h**	4899	2533	714.2	3.1	5.1	3.6
	Leachate (mg/L)* 7 mol/L HCl,5h	146970	75990	21426	93	155	108
	SX by TBP (Extraction conditions: A/O=100:30, 2 vol% TBP, extraction time 5 min)						
	SX by diethyl ether (Extraction conditions: A/O=20:10, 100% diethyl ether, 2 cycles, extraction time 15 min)						
	Enrichment solution (mg/L)*	5	67.1	32.2	25.6	0.1	0.1
	Enrichment solution (mg/kg)	150	2012	965	769	3.6	3
	Recovery efficiency from leachate, R%	0.1	0.3	0.4	80.6	2.3	2.7

* value for 1 g of red mud sample

Despite the good performance of the previous protocols (A and B), and some unwanted elements, such as Ti, Al, and REEs remain in the final solution. For this reason, further multiple solvent extraction using neutral extractants (TBP and TOPO) and ion exchange (IX) techniques were proposed.

3.4.1.4.3 Triple Liquid-Liquid Extraction by TBP (Protocol C)

Triple solvent extraction by TBP and purification cycles with diethyl ether were employed in this protocol. Moreover, the volume of the aqueous solution was increased for the purpose of increasing the final concentration of scandium with maintaining the A/O volume ratio close to 3. Bearing in mind the following important points: (1) increase the concentration of TBP extractant to 10 vol.% in order to avoid any loss of scandium due to the coextraction of high iron amount at the first SX1 extraction stage; and (2) decrease

the A/O volume ratio in the SX2 and SX3 to 3 and 2 due to the decrease in the iron content in the aqueous solution entering to the SX2 and SX3 stages (iron remaining in the organic phase after stripping). Table 11 reveals a numerical comparison between the leachate solution and the last enrichment solution, after triple TBP solvent and diethyl ether extraction. As a result, this protocol showed the exceptional separation and purification efficiency of leachate: Sc content increased from 79 to 869 ppm, Fe and Ti amount decreased drastically, and Al, La and Y were absent in last solution. The change in concentration of all 28 elements investigated in the red mud leachate during the Protocol **C** steps is shown in the Table S2 of supplementary section.

Table 11. Comparison between the leachate solution and final solution after multi SX (Protocol C)

	Elements	**Fe**	**Al**	**Ti**	**Sc**	**La**	**Y**
Protocol (C)	**Leachate (mg/L)* 7 mol/L HCl**	4634	2376	699.6	2.65	5.17	3.38
	Leachate (mg/kg) 7 mol/L HCl	139020	71280	20988	79.5	155.1	101.4
	SX 1 (Extraction conditions: A/O=200:75, 10 vol% TBP, and extraction time 5 min)						
	SX 2 (Extraction conditions: A/O=150:50, 10 vol% TBP, and extraction time 5 min)						
	SX 3 (Extraction conditions: A/O=60:30, 10 vol% TBP, and extraction time 5 min)						
	SX by diethyl ether (Extraction conditions: A/O=1, 100% diethyl ether, 2 cycles and extraction time 15 min)						
	Last enrichment solution* (mg/L)	5	0	0.05	28.9	0	0
	Last enrichment solution (mg/kg)	150	0	1.5	869.1	0	0
	Recovery efficiency from leachate, R%	0.008	0	0.005	81.1	0	0

* value for 1 g of red mud sample

The proposed flowsheet in Fig. 34 shows all the technological steps of protocol **C**.

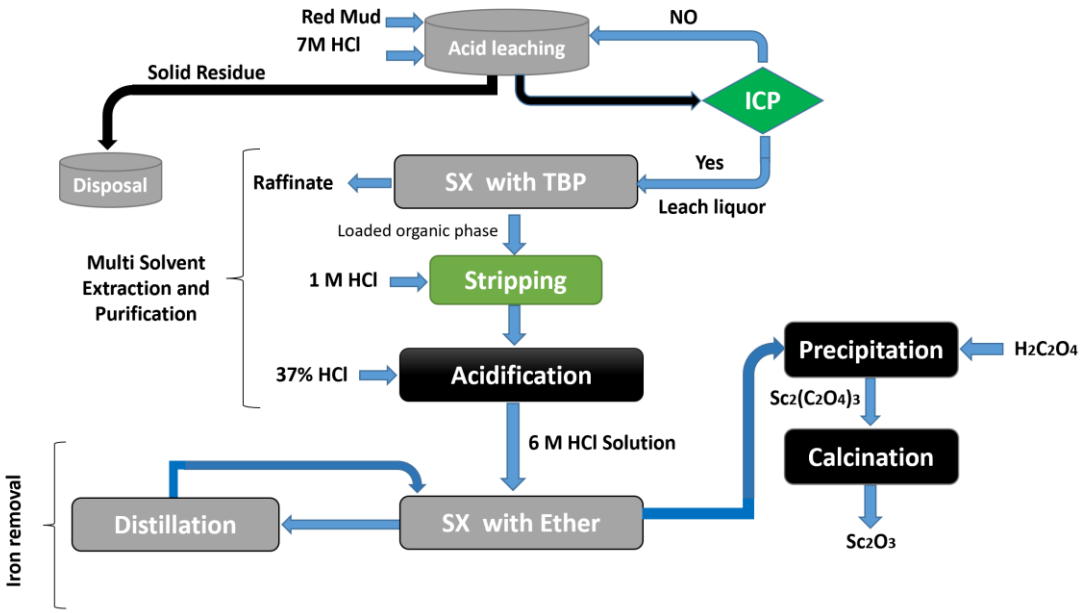

Fig. 34. Proposed flowsheet of Sc recovery from red mud leachate based on triple liquid-liquid extraction by TBP (Protocol C)

3.4.1.4.4 Multiple Liquid-Liquid Extraction by TBP and TOPO (Protocol D)

The Protocol **D** (Fig. 35) included the following steps: RM leaching, triple SX with 10 vol.% of TBP, stripping by 1 mol/L of HCl, SX with diethyl ether to remove the iron content prior to the proposed purification step by SX with TOPO extractant. The A/O volume ratio (40 mL: 10 mL) in the first SX stage was increased to 4 for better Sc extraction.

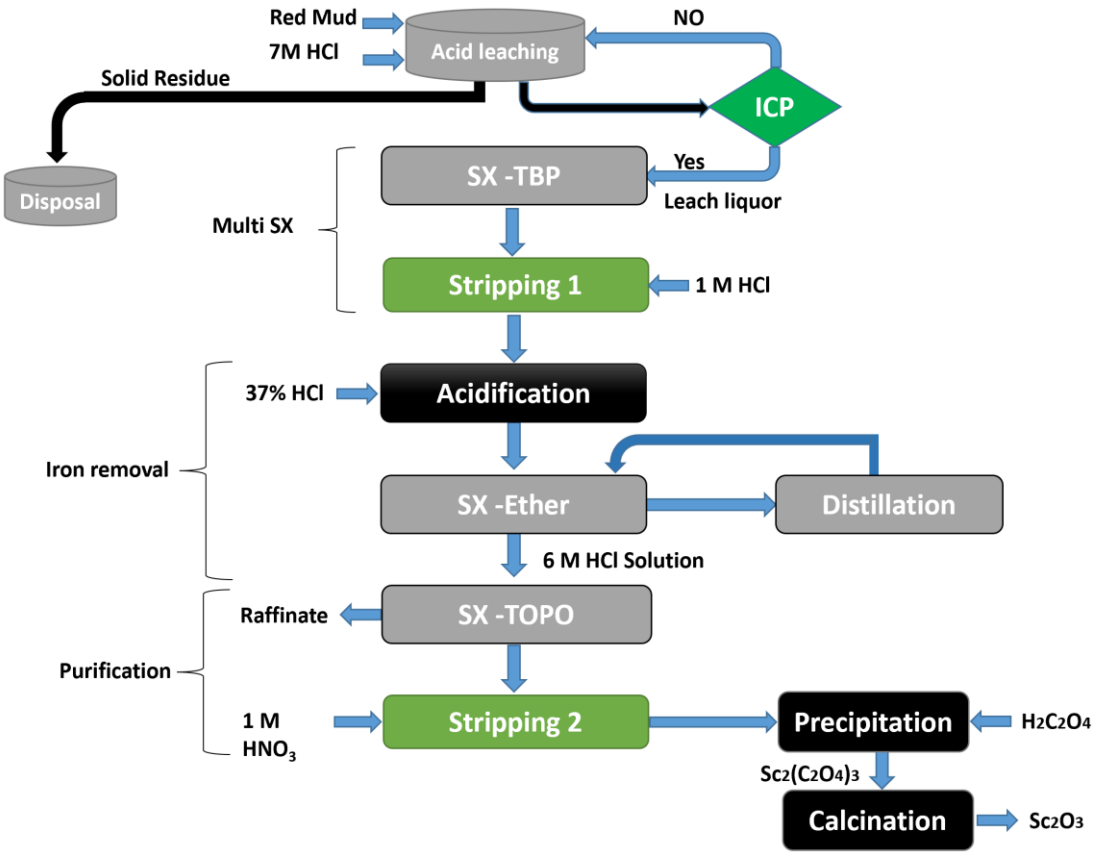

Fig. 35. Proposed flowsheet of Sc recovery from red mud leachate based on multi liquid-liquid extraction by TBP and TOPO (Protocol D)

In the purification step, the SX with (0.05 mol/L) of TOPO and the stripping by 1 mol/L of HNO_3 were applied. The purpose of this step is to maximize the purity of the final solution before the oxalic precipitation step. Table 12 shows a numerical comparison between the leachate solution and the final solution after multiple SX steps. The results showed that increasing the number of SX stages up to 4 for the purpose of purification leads to a gradual loss in Sc content during the extraction and stripping steps. This in turn leads to a decrease in the Sc recovery efficiency from the leachate. All these aspects must be considered in the technological process design.

Table 12. Comparison between the leachate solution and final solution after multi SX (Protocol D)

	Elements	Fe	Al	Ti	Sc	La	Y
Protocol (D)	**Leachate (mg/L)* 7 mol/L HCl, 5h**	4587	2262	658.5	2.74	4.7	3.23
	Leachate (mg/L)* 7 mol/L HCl,5 h	137610	67860	19755	82.2	141	97
	SX 1 (Extraction conditions: A/O=40:10, 10 vol% TBP, extraction time 5 min)						
	SX 2 (Extraction conditions: A/O=20:10, 10 vol% TBP, extraction time 5 min)						
	SX 3 (Extraction conditions: A/O=20:10, 10 vol% TBP, extraction time 5 min)						
	SX by diethyl ether (Extraction conditions: A/O=10/10, 100% diethyl ether, 2 cycles, extraction time 15 min)						
	SX4 (Extraction conditions: A/O=20:10, 0.05M TOPO, extraction time 3 min)						
	SX 4 solution (mg/L) *	5	0.1	0.22	7.0	0	0
	SX 4 solution (mg/kg)	150	3	6.6	210	0	0
	Recovery efficiency from leachate, R%	0.02	0.01	0.08	64.2	0	0

* value for 1 g of red mud sample

3.4.1.4.5 Liquid-Liquid Extraction by TBP and Ion Exchange (Protocol E)

The purpose of this protocol was to replace the SX2 and SX3 purification steps of Protocols **C** and **D** by ion exchange step. It leads to reduce the consumption of organic solvents and at the same time increase the amount of acid solutions used. In the protocol **E** (Fig. 36), the proposed procedures included five main steps: RM leaching, one SX stage with 5 vol.% TBP, stripping by 1 mol/L of HCl and SX with diethyl ether, and the ion exchange IX was used for the purification step of Sc solution from the others extracted

metals. Similar results to other protocols were achieved by SX steps. There is an effectiveness of ion exchange in terms of purification towards two elements, titanium and aluminum. The analysis of data (Table 13) showed that the solvent extraction stages cannot be reduced and replaced completely by ion exchange technique.

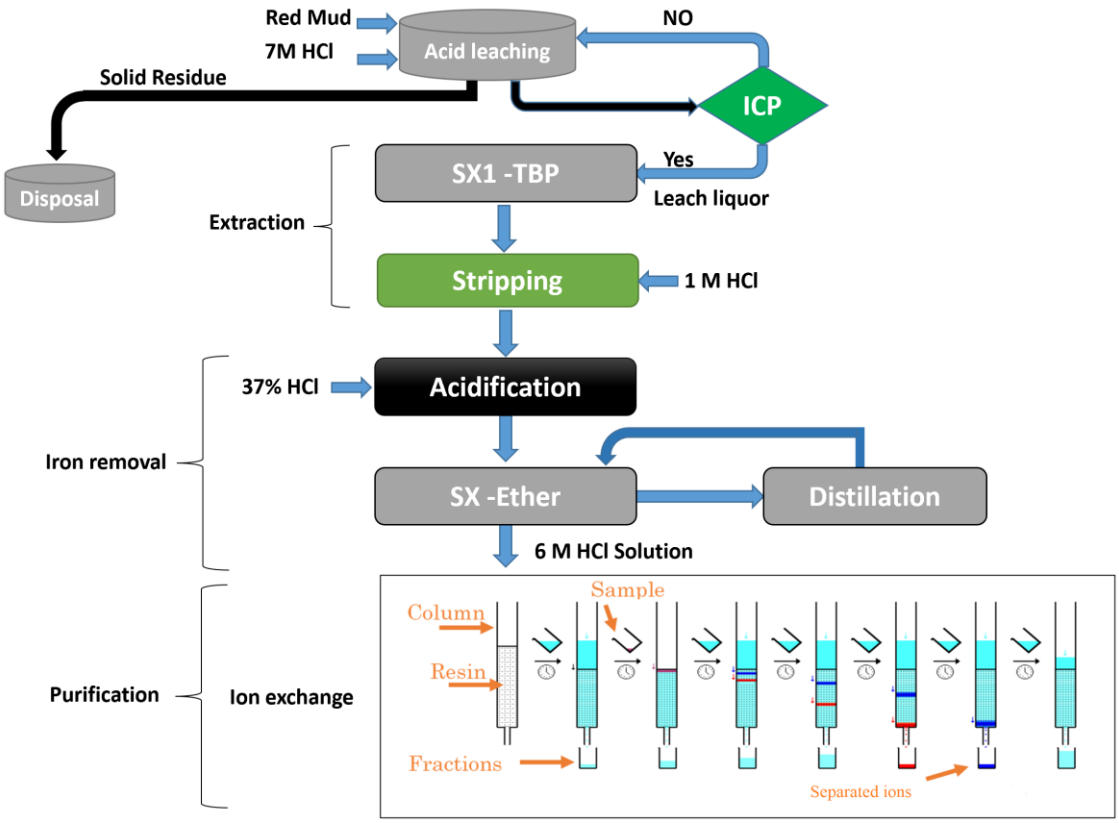

Fig. 36. Proposed flowsheet based on TBP extraction and ion exchange for the recovery of scandium from red mud leachate (protocol E)

Tables 13 shows a numerical comparison between the leachate solution and final solution after SX-IX processes.

Table13. Comparison between the leachate solution and final solution after SX (Protocol E)

	Elements	Fe	Al	Ti	Sc	La	Y
Protocol (E)	**Leachate (mg/L) * 7 mol/L HCl**	5045	2195	431.95	2.42	5.15	3.46
	Leachate (mg/kg) 7 mol/L HCl	151350	65850	12958.5	72.6	154.5	103.8
	SX (Extraction conditions: A/O=1, 5 vol% TBP, extraction time 5 min)						
	Enrichment solution (mg/L)*	3650	41.2	13.5	2.5	0.08	0.04
	Recovery efficiency from leachate, R%	72.3	1.8	3.1	99.9	1.5	1.1
	SX by diethyl ether (Extraction conditions: A/O=10:10, 100% diethyl ether, 2 cycles, extraction time 15 min)						
	Enrichment solution before IX (mg/L)*	12.7	20.6	6.77	1.63	0.04	0.02
	Enrichment solution (mg/kg)	381	618	203.1	48.9	1.2	0.6
	Ion exchange						
	Solution after IX (mg/L)*	11.6	2.6	0.47	1.56	0.04	0
	Solution after IX (mg/kg)	345	78	14.1	46.8	1.2	0
	Recovery efficiency from enrichment solution before IX, R%	91.1	12.6	6.9	95.7	100	0
	Recovery efficiency from leachate, R%	0.2	0.11	0.1	64.4	0.7	0

* value for 1 g of red mud sample

3.4.1.4.6 Comparison between A, B, C, D and E Protocols

Figure 37 illustrates a comparison between the proposed protocols based on the metal ions recovery efficiency from the red mud leachate solution. According to this comparison,

protocols **C** achieved the highest Sc recovery and the lowest impurities (Table S2) and to be recommended to use at industrial scale.

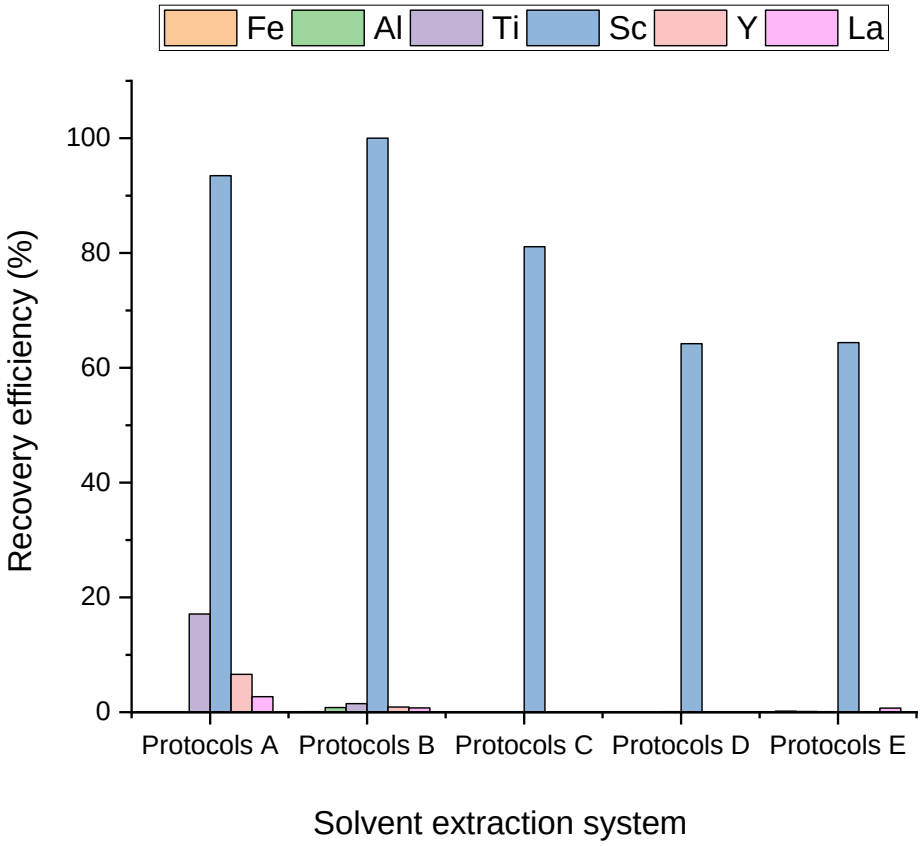

Fig. 37. Metal ions recovery efficiencies achieved by applying different extractans at different protocols

The summary of advantages, disadvantages, and comparison between the D2EHPA and TBP extraction system is shown in Table 14. As a consequence of this, the TBP extractant is the best in all respects.

Table 14. Summary of advantages and disadvantages of D2EHPA and TBP extraction system

D2EHPA	TBP
Strong bonding with heavy REEs, particularly Sc ions, makes it hard to strip them from the loaded organic phase.	Weak bonding with heavy REEs
High loading capacity	Moderate loading capacity
Selectivity towards of Sc, Fe, Ti	Selectivity towards of Sc, Fe
The number of required steps is more than for TBP; Little bit difficult to process and take time	The number of required steps is less Easy to process
95% recovery efficiency by precipitation with 2.5M NaOH	100% recovery efficiency by 1M HCl
The acidic solution concentration influences the formation of the third phase (interlayer between organic and aqueous)	There is no third phase
It works with different concentrations of HCl	The selective extraction can only be carried out in a high concentration of chloride system (>6M HCl)
The stripping process to recover of Sc from organic phase is possible just by alkaline solution	The stripping process is possible by an acidic solution
Difficult phase separation then third phase is formed	Easy phase separation
More expensive chemical	Cheaper chemical

To clarify the new findings of this study compared to previous studies, it is necessary to highlight the challenges facing the extracting scandium from RM. The greatest challenges associated with the scandium extraction process from red mud is the co-extracted metals ions, such as iron, titanium, zirconium, aluminum, silicon, and lanthanides which have the same oxidation state. Prior to that, the leaching process directly controls the dissolution of the major and minor constituents in the leachate solution, as well as the overall process efficiency. The red mud leachate solution is very complex and contains many metals ions.

Many researchers have worked on this topic and put in a significant effort to achieve the selective separation of Sc from red mud. All the previous reports used the synergism extraction system (a mixture of two or more extractants), a comparison is made between several previously published reports and the current study (Table 15). Subsequently, this is not economically viable. Moreover, their experiments included a complicated and multiple extraction process which increase the operating extraction cost such as multiple scrubbing steps by H_2O_2-minreal acids for loaded organic phase to remove the Fe, Ti, and Zr content. The disadvantage of this step is that it reduces the recovery efficiency in addition to being expensive. While in this study, the scandium as a main product and the iron content as a byproduct are recovered.

Table 15. Comparison of solvent extraction techniques and their extraction and stripping efficiencies for Sc recovery

Extraction step		**Stripping step**		**Extracted element**	**Year [Reference]**
Extractant combination	**E(%)**	**Stripping agent**	**S(%)**		
15 vol% D2EHPA 5 vol % TBP	99	2 M NaOH	95.4	Sc	2017 [58]
8 vol % D2EHPA 2% TBP	99.7	2 M NaOH + 1M NaCl	85	Sc	2018 [134]
16 vol % D2EHPA 4 vol % TBP	99	2 M NaOH	96	Sc	2019 [128]
60 vol % Cyanex272 40 vol % Cyanex923	98	10% $H_2C_2O_4$	98.8	Sc	2020 [68]
15 vol % D2EHPA 15 vol % N1923	99	5 M HNO_3	89.3	Sc	2020 [57]
10 vol % D2EHPA 5 vol % TBP	99	5 M NaOH	99.61	Sc	2021 [129]
10 vol % D2EHPA 5 vol % TBP	99	3 M NaOH	99	Sc	2021 [130]
10 vol % Cyanex 923 10 vol % Alamine336	92	5M H_3PO_4	100	Sc, Zr	2021 [90]
0.05M D2EHPA	97	2.5 M NaOH	95	Sc, Fe	This work
10 vol% TBP	99	1M HCl	99	Sc, Fe	

The most significant characteristics of the suggested process are a high-quality and cost-effective extraction technique that targets two elements at the same time, scandium and iron, as well as it is a time-effective compared with previous reports. The optimized conditions, which are applied in leaching and SX steps, maintained on the titanium, zirconium, aluminum, silicon and lanthanides in the raffinate, in the leachate solution after extraction. This was achieved by the integration of the processes of effective reflex leaching system and efficient solvent extraction. Future research may look into how to get the rest of the REEs out of the process. It is worth noting that the number of studies that dealt with the extraction of scandium from real RM leachate is few and limited. In this context, Zhu et al. recovered Sc from the red mud hydrochloric leachate solution by 15 vol.% P507 and 5 vol.% TBP, and the pure Sc reached 99.2%. However, four scrubbing stages were necessary, which took a substantial cost of the entire process [58]. Zou et al. utilized 15 vol% D2EHPA and 15 vol.% N1923 mixed extractants to extract Sc from a sulfuric acid solution of titanium dioxide, which should keep the extraction system's acidity below 0.5 mol/L sulfuric acids, and the three scrubbing stages were required [57]. Zhang et al.[134] observed that the 8 vol% D2EHPA and 2 vol.% TBP mixture extracted up to 95% of the Sc. However, increasing the TBP concentration decreased the Sc separation and slightly increased the Fe extraction. As a result, the impact of D2EHPA in the organic phase reduced, and the Sc extraction efficiency reduced too. Zhang et al.[135] investigated the preparation of ultrahigh purity Sc_2O_3 (99.9% purity). The procedures included two solvent extraction circuits, the first of which was used to remove the zirconium from 6 mol/L perchloric acid ($HClO_4$) using 100 vol.% TBP. The second extraction circuit separates the Sc from a 5.8 mol/L HCl solution that also contains impurities, like Ca, Al, Mn, Ti, Y, and La, with a 40 vol.% solution of di(l-methyl heptyl) methyl phosphate (P_{350}) in kerosene.

3.4.2 Liquid-Liquid Extraction by Macrocyclic Compounds and their Mechanism

Macrocyclic compounds are known to form stable complexes with metal ions [136, 137] . Depending on the number of oxygen and nitrogen donor atoms being in the macrocyclic ring, it has the size selectively matching to metal ions. Oxygen donor groups have an affinity for lanthanides ions. Nitrogen and sulfur donor groups are considered soft bases

and therefore prefer the transition metal ions (e.g., nickel, copper, iron) and heavy metal ions (e.g., silver, lead, mercury), which are classified as soft acids [138]. The selection of the macrocyclic compounds depends on different aspects, such as the proper spatial orientation of the macrocyclic compounds, oxygen dipole in the direction of metal ions, solvation of the cations, size of metal ions, etc. During the cation-macrocyclic compound interaction, the cation is transferred from the aqueous phase and is captured in the cavity of the macrocyclic compound with a weak coordinate covalent bond. In Fig. 38, an illustration of the Sc complexion process with macrocyclic compounds selected is shown.

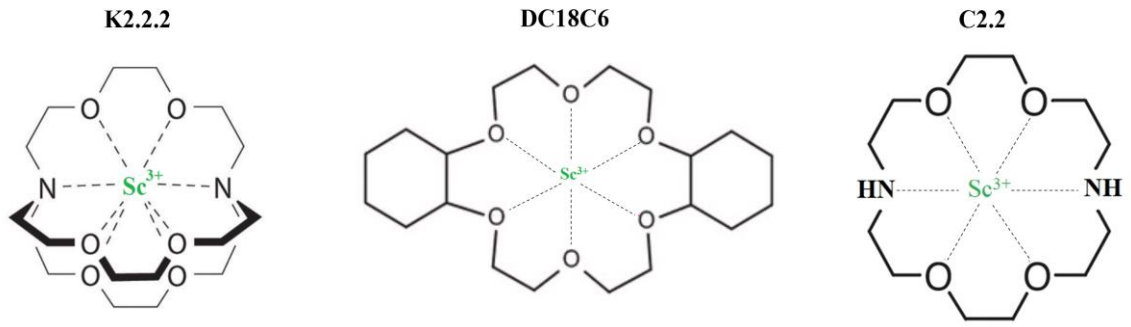

Fig. 38. Representation of complexation process of Sc and the selected macrocyclic compounds

3.4.2.1 Optimization of Liquid-Liquid Extraction by Macrocyclic Compounds

The experimental results of extraction efficiency measurements according to CCRD are presented in Table S1. The summary of the polynomial coefficients of the second order model equation obtained using STATSTICA software for Sc extraction efficiency by macrocyclic compounds is illustrated in Table 16.

Table 16. Polynomial coefficient results

K 2.2.2														
β_0	β_1	β_2	β_3	β_4	β_{11}	β_{22}	β_{33}	β_{44}	β_{12}	β_{13}	β_{14}	β_{23}	β_{24}	β_{34}
40.1	1869.9	-26.1	6.4	-0.9	4400.7	-489.3	-24.7	1.1	0.1	0.0	362484.8	-1.2	-0.5	0.0
DC18C6														
β_0	β_1	β_2	β_3	β_4	β_{11}	β_{22}	β_{33}	β_{44}	β_{12}	β_{13}	β_{14}	β_{23}	β_{24}	β_{34}
3.2	360.1	1.3	1.9	-0.3	153.8	-134.6	3.1	0.0	0.0	0.0	104110.9	-0.4	-0.1	0.0
C2.2														
β_0	β_1	β_2	β_3	β_4	β_{11}	β_{22}	β_{33}	β_{44}	β_{12}	β_{13}	β_{14}	β_{23}	β_{24}	β_{34}
-0.9	4080.2	-13.3	7.7	-0.7	4190.5	-544.6	-69.6	0.1	0.1	0.0	517072.6	-1.6	-0.2	0.0

The confidence of the second-order polynomial model has been proved by ANOVA analysis obtained using STATSTICA software, and the results are presented in Tables 17, 18 and 19. This analysis includes important parameters indicating the model performance such as correlation coefficient R2, where the coefficient value of R2 defines how well the model fits the data [139]. The ANOVA results manifested that the coefficient R2 value is closer to 1 signifying better correlation between the practical (observed) extraction efficiency values which obtained from the experiments and the predicted extraction efficiency values which obtained from the software and indicated the accuracy of the model with better response.

In case of K 2.2.2, DC18C6 and C2.2, the model resulted in R2=0.96, 0.90 and 0.95, respectively. The other important indicators in this analysis are the P-values which in turn reflects the quality of model [114, 139]. The models having P-value < 0.05 were considered significant. In case of K 2.2.2, DC18C6 and C2.2, the model has 0.000017, 0.000577 and 0.000249, respectively. All these indicators support the confidence in the thoroughness of the model.

Table 17. ANOVA analysis for extraction efficiency by K 2.2.2 as a function of independent variables

Source of variance	Sum of squares	df	Mean square	F- Value	P-Value	R^2
Regression model SS_R	64379.54	15	4291.970	17.03054	0.000017	0.96000
Error (residual) SS_E	2772.18	11	252.016			
Total SS_T	67151.72	26				
Corrected Total	25439.64	25				
Regression vs. Corrected Total	64379.54	15	4291.970	4.21780	0.000756	

Table 18. ANOVA analysis for extraction efficiency by DC18C6 as a function of independent variables

Source of variance	Sum of squares	df	Mean square	F- Value	P-Value	R^2
Regression model SS_R	494.7220	15	32.98147	9.247829	0.000577	0.90000
Error (residual) SS_E	35.6640	10	3.56640			
Total SS_T	530.3860	25				
Corrected Total	222.4467	24				
Regression vs. Corrected Total	494.7220	15	32.98147	3.558404	0.002789	

Table 19. ANOVA analysis for extraction efficiency by C 2.2 as a function of independent variables

Source of variance	Sum of squares	df	Mean square	F- Value	P-Value	R^2
Regression model SS_R	52978.61	17	3116 389	15.62262	0.000249	0.95000
Error (residual) SS_E	1595.83	8	199.479			
Total SS_T	54574.44	25				
Corrected Total	20482.51	24				
Regression vs. Corrected Total	52978 61	17	3116.389	3 65157	0.001942	

The distribution of practical values obtained from the experimental results and predicted values obtained from the software for Sc extraction is shown Fig. 39, where the data points are converging near to the diagonal line, suggesting that the model is accurate and satisfactory. Moreover, Fig. 39 reveals and estimates the precision of a regression model by comparing the practical versus predicted extraction efficiency values. On other hand, the plot identifies the relationship between the model predictions and practical data, and that way indicates how well the model fits the data.

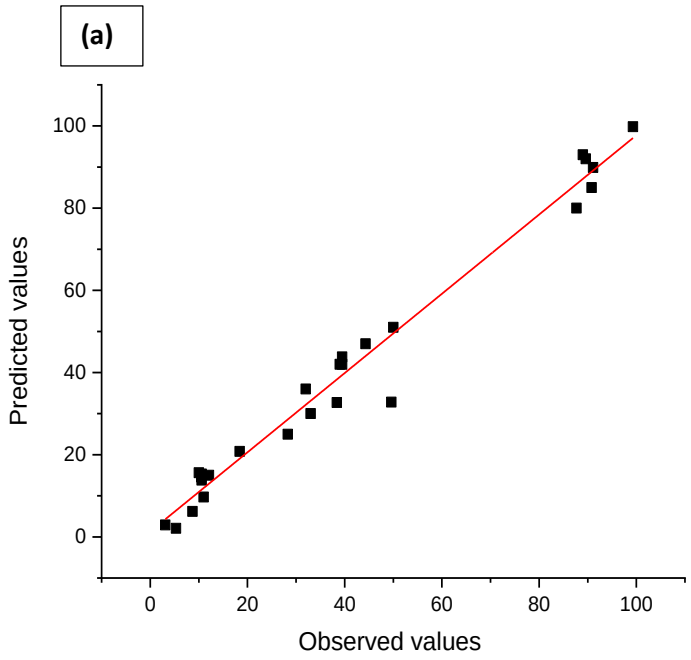
(a)
Predicted values
Observed values
0
20
40
60
80
100

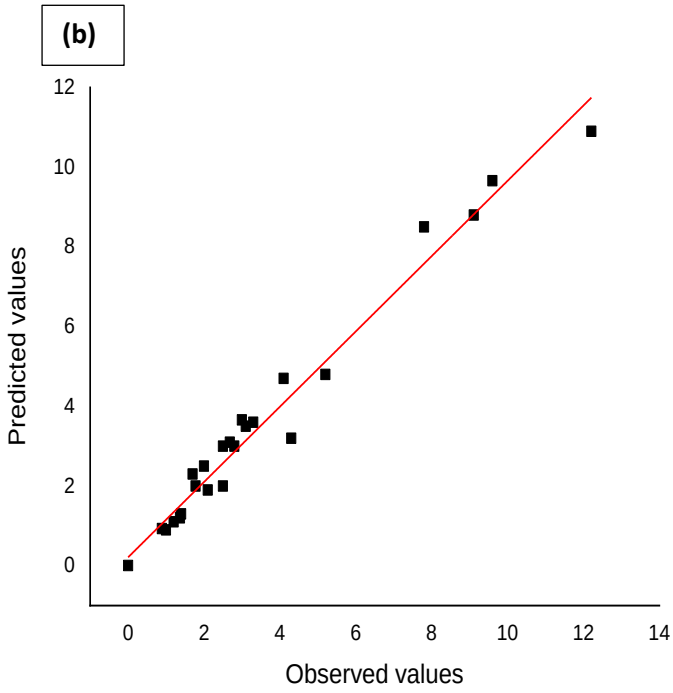
(b)
Predicted values
Observed values
0
2
4
6
8
10
12
14

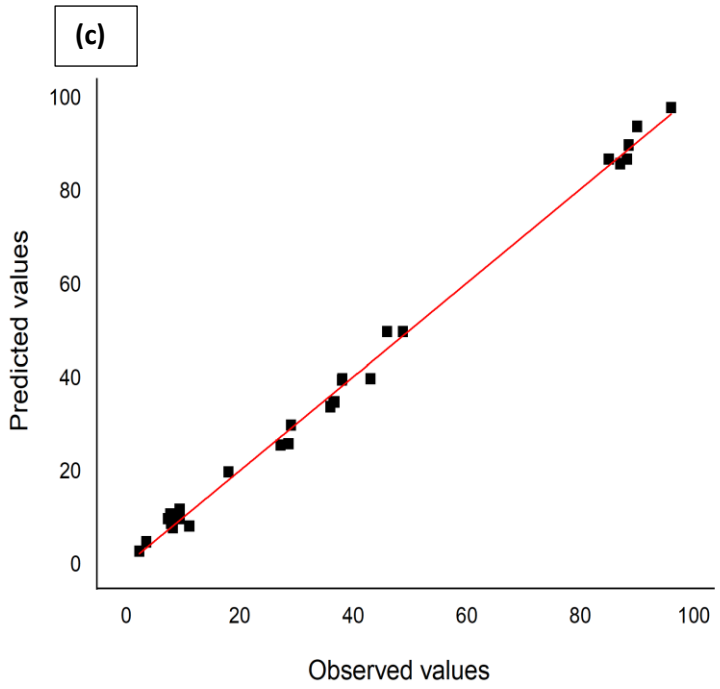

Fig. 39. Observed values vs predicted values for Sc extraction efficiency by (a) K 2.2.2 and (b) DC18C6 (c) C 2.2

The statistical analysis displays the correlation strength between the independent operating variables X1, X2, X3 and X4 (concentration of macrocyclic compounds, pH, time and concentration of Sc ions) and the dependent variable Y (extraction efficiency) through the 3D-response surface and contour plot in Figs. S1, S2, and S3 in the supplementary section. For example, Fig. 40 illustrates the response surface and contour plot which describes the two variables of interaction (concentration of K 2.2.2 and pH), where one variable affects the response of another variable. Furthermore, the color scale indicates the interaction strength and the visualization of optimum levels. The level of extraction efficiency can be seen from the contour plot, where the red color indicates the region of optimal extraction efficiency, yellow indicates the medium efficiency, and green indicates the low efficiency. Moreover, it can be concluded easily from the color scale that the change effect of the concentration of K 2.2.2 and pH together is on the extraction efficiency as response, e.g., to get the higher extraction ~ 99%, the following adjustment can be done at pH ~ 2.5 and concentration of K 2.2.2 ~ 0.01 mol/L, or at pH ~ 3 and

concentration of K 2.2.2 ~ 0.008 mol/L, or at pH ~ 4 and concentration of K 2.2.2 ~ 0.007 mol/L.

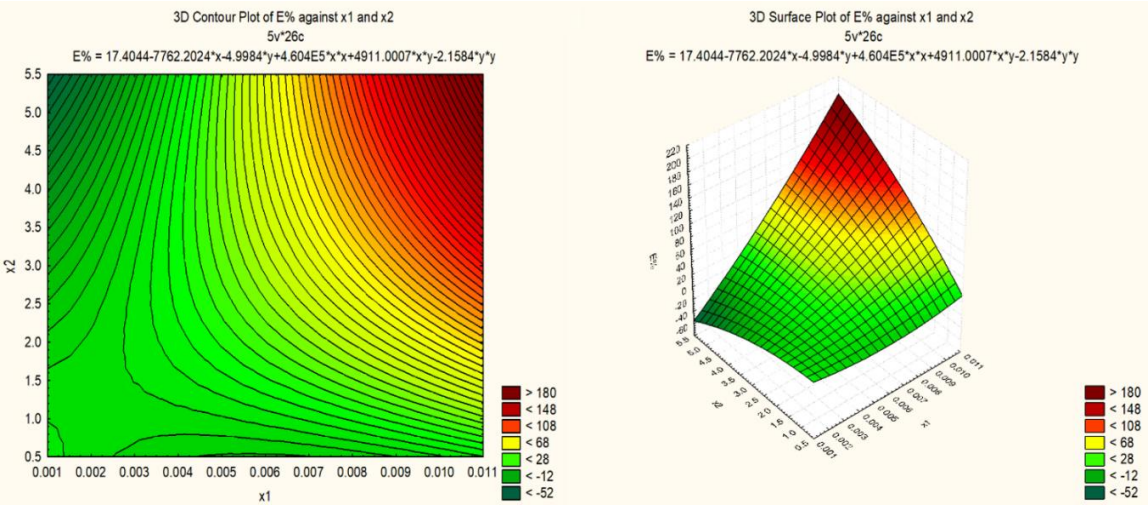

Fig. 40. 3D-response surface and contour plot showing the interaction between tow variables of extraction by K 2.2.2 (X1= concentration of K 2.2.2 and X2= pH)

The response surface and contour plot, which describes the two variables interaction (concentration of DC18C6 and pH) in Fig. 41a, showed another observation, where it can be seen from the color scale that the level of extraction efficiency has not too much effected with changing the concentration of DC18C6 and pH. Moreover, the higher Sc extraction ~ 15% can be achieved at the following parameters combination: At pH ~ 2 and concentration of DC18C6 ~ 0.009 mol/L, at pH~3 and concentration of DC18C6 ~ 0.008 mol/L, and at pH ~ 4 and concentration of DC18C6 ~ 0.007 mol/L. The optimum conditions which are shown in Table 20 have been obtained using WinQSB software. It can be concluded that at the optimum condition, the value of extraction efficiency is maximum within the range of input operating variables. Where, K 2.2.2 achieved the highest extraction efficiency (99.7%) at the following conditions: 0.006 mol/L K 2.2.2 concentration, 4 pH value, 11 min extraction time, and 75 mg/L Sc concentration.

There is also an important factor which plays an important role in the extraction process, such as the size of the cavity or the ring diameter of the macrocyclic compounds, and the pH of solution. The ionic diameter of Sc ~ 1.4 Å is compatible with the diameter of K 2.2.2 (1.4 Å) and C 2.2 (1.8 Å) and depends on the pH value of acid solution due to the

nitrogen atoms in their structure but not compatible with the ionic diameter of DC18C6 (2.6–3.2 Å) [136, 137]. The initial pH solution value impacts the selectivity of K 2.2.2 and C 2.2 towards Sc. Furthermore, because K 2.2.2 and C2.2 are diprotic bases, their ability to form complex with ions in aqueous solutions is highly influenced by the pH value of 3.

Table 20. The optimum operating variables values for extraction of Sc by K 2.2.2, C 2.2 and DC18C6

Macrocyclic compounds	Concentration (mol/L) X1	pH of Sc solution X2	Time (min) X3	Sc (mg/L) X4	E (%) Y
K 2.2.2	0.006	4	11	75	99.7
C 2.2	0.01	3.7	6	75	97.3
DC18C6	0.006	4	11	75	15.2

The working concept of the software is that seeking for the maximum value of the objective function (extraction Sc efficiency), while it has been subjected to a maximization function. This software worked with thirty constraints suggested by CCRD to be solved using non-linear programming technique in order to find the optimum variables within the experimental range.

3.5 Characterization of Solid Phases for Solid-Liquid Extraction

3.5.1 FTIR results

Figure 41 demonstrates the FTIR spectra of OPCs modified solid phase samples which includes three modified nanocomposites (Fe_3O_4/SiO_2/OPCs). Three characteristic peaks of organic phosphate phases (TOPO, TBP and D2EHPA) were seen in all OPCs modified solid phase samples (Fig. 41C, D and E).

The sharp peaks to be attributed to C–H stretching modes were seen around 3000 cm^{-1}. Other peaks which correspond to P–O-alkyl stretching mode (~1050 cm^{-1}) and P=O stretching mode (~1400 cm^{-1}), respectively were found although the clarity was inferior to that of C–H stretching mode due to the overlap of the absorbance band by the silica matrix [121, 140]. Table 21 summarizes the IR wavenumbers assignment of the

characterize peaks of sample compounds. These results are in good agreement with the results obtained by [121, 141]. It can be concluded that the immobilization of TOPO, TBP and D2EHPA onto Fe_3O_4/SiO_2 surface was successfully achieved during the preparation step.

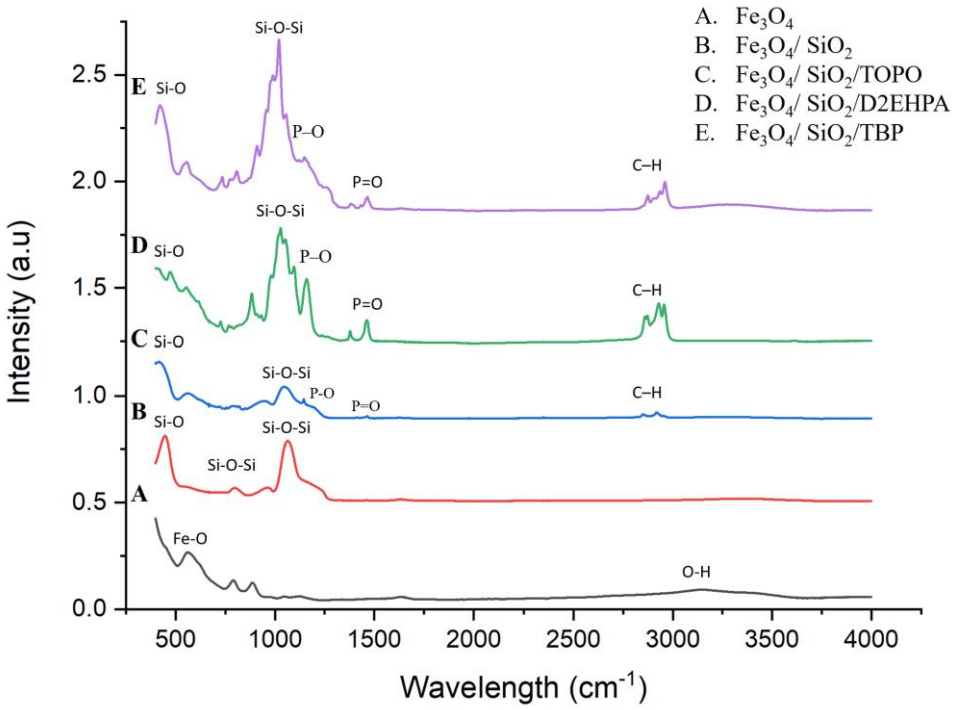

Fig. 41. FTIR spectra of SiO_2, Fe_3O_4/SiO_2 and OPCs modified solid phase

Table 21. Wavenumber assignment of FTIR [121, 141]

Wavenumber, cm^{-1}	Assignment
455	Si-O
577	Fe-O
794	Si-O-Si
1050	P–O
1082	Si-O-Si
1400	P=O
3000	C–H
3146	O-H

3.5.2 SEM-EDX Results

The SEM images of organophosphorus compounds modified Fe_3O_4/SiO_2 are given in Figs. 42-44 and illustrate the morphology, size and composition of the OPCs modified solid phase samples. It can be seen that the particles have agglomerate structure with different sizes (20-500 nm) formed during the sol-gel preparation. The elemental analysis obtained from the EDX spectra showed a presence of phosphorous in the all OPCs modified solid phase samples which confirmed that the OPCs were successfully incorporated into the sol–gel composites. The EDX analysis results of the prepared SPE are summarized in Table 22. Where, Table 22 depicts a comparison between the experimental and theoretical percentage of elements, such as O, C, P, Si, and Fe. The results elucidated that there is a difference between the measured/experimental and the theoretical data. Moreover, the main compound is SiO_2 which produced from the hydrolysis of tetraethylorthosilicate. The diverse distribution of Fe_3O_4 support material in the composite matrix is caused by the magnetic field from the magnetic stirrer during the 72-h condensation period. As a result, this is the reason for the irregularity of the components inside the structure of the resulting material.

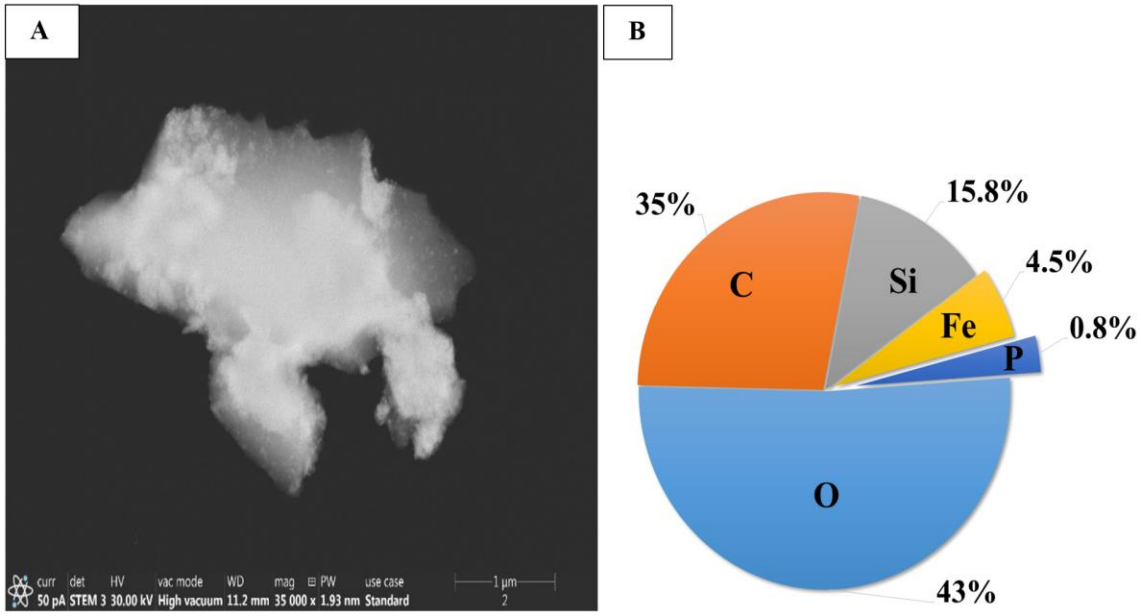

Fig. 42. SEM image (A) and elemetnal composion (B) Fe_3O_4/SiO_2/TOPO

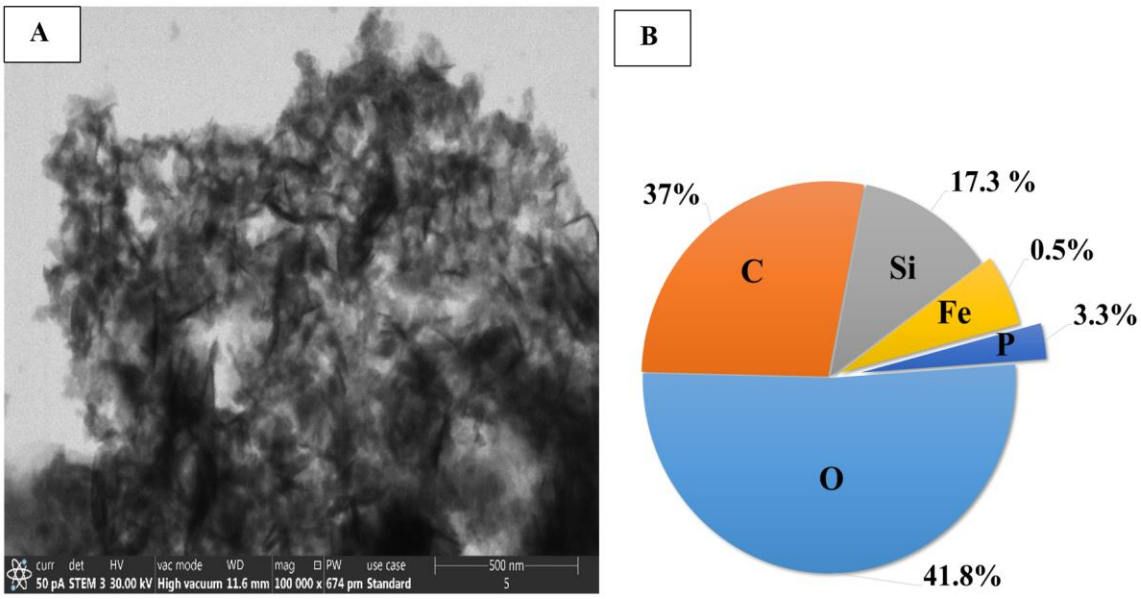

Fig. 43. SEM image (A) and elemetnal composion (B) of Fe_3O_4/SiO_2/TBP

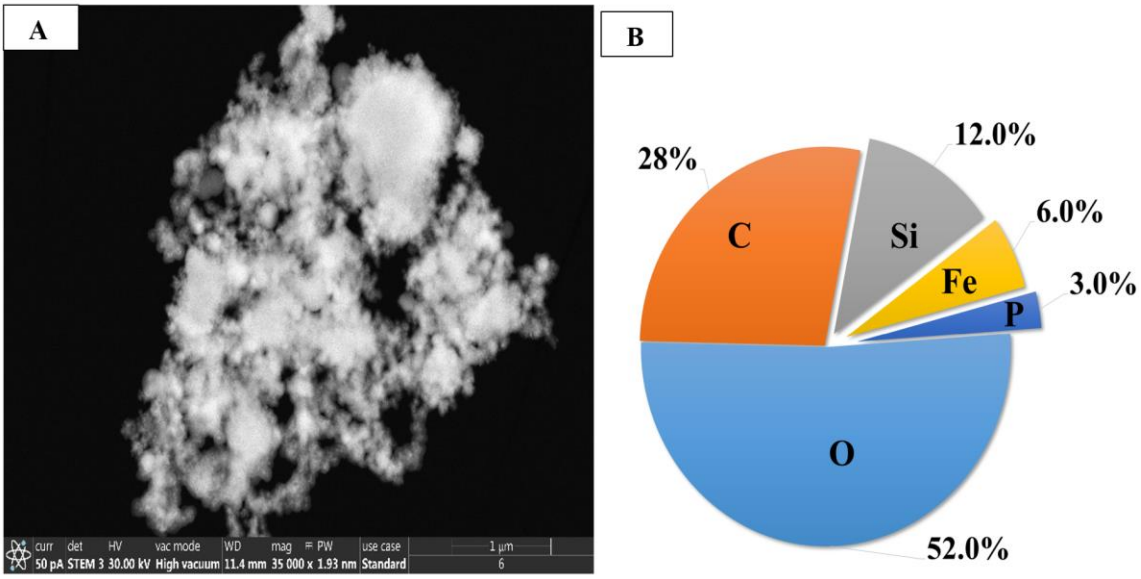

Fig. 44. SEM image (A) and elemetnal composion (B) of Fe_3O_4/SiO_2/D2EHPA

Table 22. EDX results of Solid Phase OPCs materials

Element wt%	Theoretical, calculatied based on amount chemical used			Experimental, measured by EDX		
	Fe_3O_4/ SiO_2/ TBP	**Fe_3O_4/ SiO_2/ TOPO**	**Fe_3O_4/ SiO_2/ D2EHPA**	**Fe_3O_4/ SiO_2/ TBP**	**Fe_3O_4/ SiO_2/ TOPO**	**Fe_3O_4/ SiO_2/ D2EHPA**
O	28.2	26.9	26.9	41.8	43.3	52.1
C*	46.5	47	47.8	37.1	35.4	28.3
Si	9.2	11	9.2	17.3	15.8	12.6
Fe	1.8	2.2	1.8	0.5	4.5	6.7
P	2.72	0.85	2.3	3.3	0.8	0.3

∗C experimental values are not reliable and having only informative feature since EDX sample holder contains carbon

3.5.3 Low Temperature Nitrogen Adsorption Result

The total surface area, S_{BET}, volume of pores between 1.7 and 100 nm diameter, V1.7–100 nm and average pore size, and the Dav values of prepared solid phases are presented in Table 23. The obtained results portrayed that the iron oxide solid supports used for the preparation of samples have the highest specific surface areas S_{BET} =135 m^2/g amount investigated sample. It was observed that after the immobilization process of the organophosphorus molecules for both sol–gel the surface areas decreased in higher extent, on 99%, for Fe_3O_4/SiO_2/TBP, Fe_3O_4/SiO_2/TOPO and in less extent, as well as on 79% for Fe_3O_4/SiO_2/D2EHPA samples. The explanation of this drop in the surface areas is that the molecules of organophosphorus occupied and covered all or most of the surface of support, thus blocking the micro- and mesopores. Moreover, as a result of the surface modification, the pore volume of the modified samples decreased, and the pore average diameters increased.

Table 23. The surface area, pore volume, pore size of the prepared Fe_3O_4/SiO_2/OPCs samples

Sample	S_{BET}, m^2/g	$V_{1.7–300\ nm}$, cm^3/g	D_{av}, nm
Fe_3O_4	135.00	0.3058	9.0
Fe_3O_4/SiO_2/TOPO	0.12	0.0077	140.2
Fe_3O_4/SiO_2/TBP	0.07	n.d*	n.d*
Fe_3O_4/SiO_2/ D2EHPA	15.30	0.0807	17.0

n.d*: not determined

3.6 Solid – Liquid Extraction Results

One of the important factors affecting the solid – liquid extraction process is the weight of the solid (Fe_3O_4/SiO_2/OPCs). Therefore, based on the amount of Fe_3O_4/SiO_2/OPCs used, some conclusions in terms of selectivity towards Sc can be drawn.

For Fe_3O_4/SiO_2/TBP, the selectivity of Sc to other elements was found to decrease remarkably when the amount of Fe_3O_4/SiO_2/TBP increased from 0.3 to 0.5 g (Fig. 45).

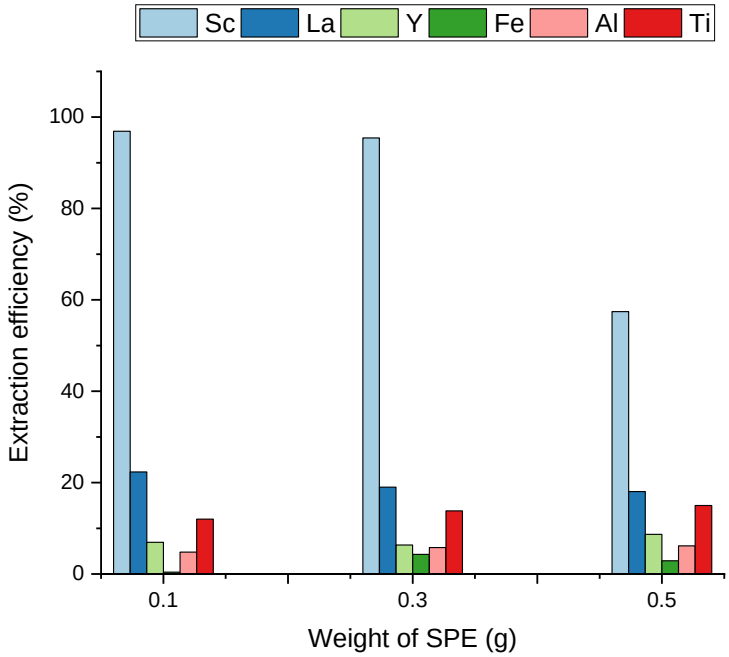

Fig. 45. Metal extraction efficiency of Fe_3O_4/SiO_2/TBP for different weights

Sc (III) adsorption by Fe_3O_4/SiO_2/TBP is always higher than for any other studied metal ions (Al, Fe, Ti, La, Y) when the pH of solution is < 1. Furthermore, these findings are in harmony with the results of solvent extraction system (see section 3.4.1.2). Under the optimized solvent extraction conditions (RM leachate solution 7M HCl; low TBP concentration 3-5vol.% and 5 min extraction time), among the investigated elements, Sc achieved the highest extraction efficiency. According to the SLE results, Fe(III) gives the highest interference in the extraction of Sc(III), while the other metal ions are not significantly extracted (E < 20%) due to the similarity of their chemical features.

In the recovery step of Fe_3O_4/SiO_2/TBP, it was observed that Sc(III) and Fe(III) achieved the highest efficiency for different weights compared with the other metal ions, as shown in Fig. 46.

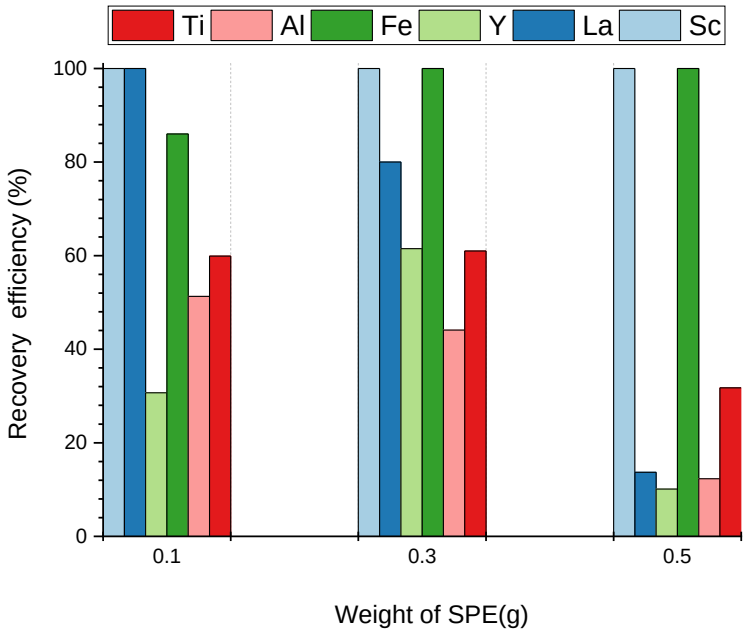

Fig. 46. Metals recovery efficiency of Fe_3O_4/SiO_2/TBP for different weights

Different results were obtained with Fe_3O_4/SiO_2/TOPO extraction. Where, the extraction efficiency towards the investigated elements was found to increase when the amount of Fe_3O_4/SiO_2/TOPO was increased (Fig. 47).

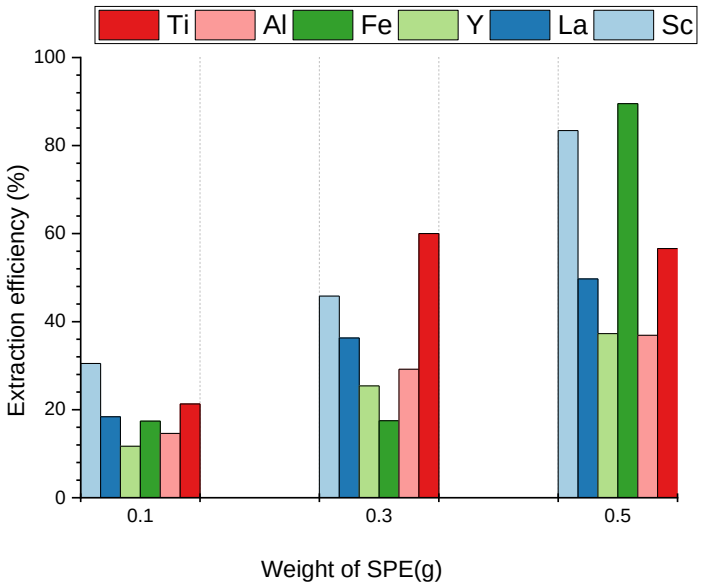

Fig. 47. Metal extraction efficiency of Fe_3O_4/SiO_2/TOPO for different weights

Moreover, Fe_3O_4/SiO_2/TOPO did not show selectivity there towards the Sc ions. Figure 48 displays the recovery efficiency of Fe_3O_4/SiO_2/TOPO. In this context, the recovery levels (0.1, 0.3 and 0.5 g) reflected the concentration of extracted metal ions in the extraction step. Where, there was a progressive increase approximately for the all investigated metal ions.

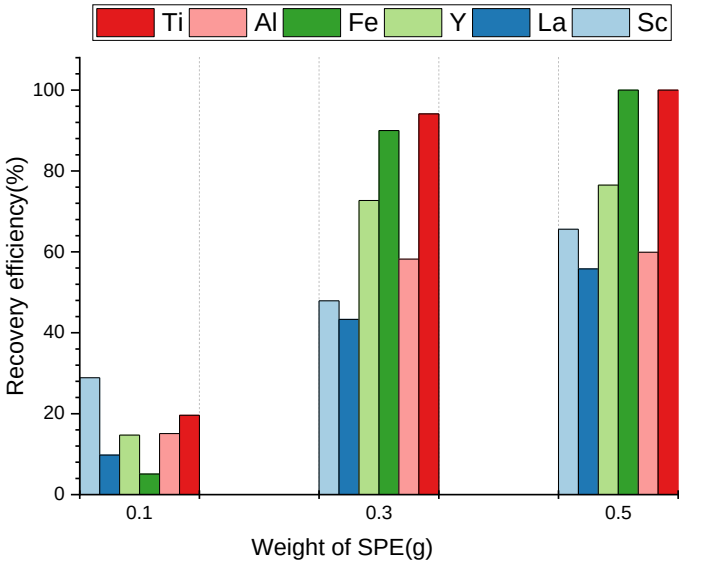

Fig. 48. Metal recovery efficiency of Fe_3O_4/SiO_2/TOPO for different weights

Figure 49 exhibits the extraction behavior of Fe_3O_4/SiO_2/D2EHPA. At 0.1 g, the extraction efficiency for Sc (III) , Fe(III) and Ti(III) was higher than of any other metal ions (E >50%). At 0.3 g, the extraction efficiency of Sc (III) and Fe(III) increased dramatically, whereas the extraction efficiency of other metal ions remained rather stable (E <50%). The extraction efficiency reached the values 94.2% for Sc (III) and 87.8% for Fe(III) at 0.5 g of SP.

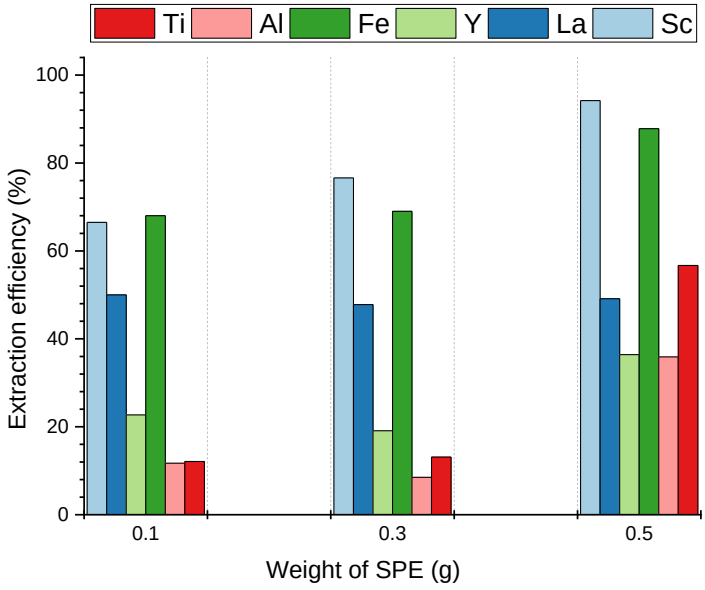

Fig. 49. Metal extraction efficiency of Fe_3O_4/SiO_2/ D2EHPA for different weight

It was difficult to carry out the recovery step and to strip the scandium from the loaded organic phase with acid, since the scandium ion produces with D2EHPA a very strong complex [132]. Based on the liquid-liquid extraction results (see 3.4.1.1 section), the aqueous 2.5 M NaOH solution was proposed as a stripping agent, which could completely remove the Sc from solution. But, unfortunately, the alkaline solution (2.5 M NaOH) destroys the Fe_3O_4/SiO_2/D2EHPA solid phase structure. In order to solve this problem, the polymer matrix, such as polystyrene rather than silica network for solid support can be suggested.

4. CONCLUSIONS

The main purpose of this dissertation work is the recovering of scandium from the red mud. The summary of the main outcomes including the drawbacks for the three techniques studied in this work is given below:

4.1. Recovery of Scandium from Red Mud Leachate by Organophosphorus Compounds Applying Liquid- Liquid Extraction Technique

Hydrometallurgy methods (leaching and solvent extraction) were applied in this study to recover the Sc from RM and remove the co-leached and co-extracted metal content, mainly Fe, Al, Ti, La, and Y. Metals' red mud content was partially dissolved with 7 M HCl at a S/L ratio of 1 g: 30 mL for 5 h at 75 °C from the red mud. These conditions were found optimum towards the selective dissolution of scandium from the RM. The leachate used in this study had the following average composition: Fe 14 wt.%, Al 7 wt.%, Ti 2.1 wt%, Sc 79 ppm, La 155 ppm, and Y 101 ppm. The efficient Fe(III) removal (99%) from the red mud leachate was achieved by diethyl ether extraction at A/O equals to one.

The influence of several parameters on the extraction system, such as the type, DEHPA and TBP concentration, pH, shaking time, temperature of solution and aqueous to organic phase ratio (A/O) was studied. The Sc extraction protocols were carried out based on the best conditions found. The separation of Sc from the others metal ions was carried out applying several protocols (**A, B, C, D,** and **E**). Those protocols included three main steps, namely leaching, organophosphorus compounds liquid-liquid extraction and Sc stripping with 2.5 mol/L sodium hydroxide agent (protocol **A**), and 1 mol/L hydrochloric acid agent (protocols **B, C, D** and **E**). In protocol **E**, additional ion exchange purification step was applied. OPCs (D2EHPA, TPB, TOPO) manifested different extraction abilities towards the metal ions: E% > 95% for Sc, E%=0-60% for Ti, E% ~ 1% for Al, E%=0-1% for La, and E%=0-2% for Y.

With Protocol **C**, applying triple liquid-liquid extraction by TBP, the best Sc recovery efficiency was achieved: 81% of Sc (869 ppm), 0.005% of Ti (1.5 ppm), 0.008% of Fe (150 ppm), and 0% of La, Y and Al under the following conditions: Triple SX step, 10 vol.% TBP in kerosene, A/O=200 mL:75 mL volume phase ratio, and 5 min extraction time.

4.2 Recovery of Scandium from Model Solution by Macrocyclic Compounds Applying Liquid- Liquid Extraction Technique

Response surface methodology employing a central composite rotatable design technique revealed to be a strong statistical tool to evaluate the interaction of the chosen operating variables and find the best conditions that improve the extraction efficiency of Sc. The extraction of Sc by K 2.2.2, C 2.2 and DC18C6 macrocyclic compounds from nitric and hydrochloric acid medium scandium model solution has been studied. The results of optimization obtained using ANOVA analysis, STATISTICA, and WinQSB software indicated that the maximum Sc extraction efficiency by K 2.2.2, C 2.2 and DC18C6 can be obtained under the following optimum experimental conditions: 0.006 mol/L concentration of K 2.2.2, C 2.2 and DC18C6, 11 min contact time, pH 4 of the aqueous solution, and 75 mg/L initial Sc concentration with 99%, 97% and 15%, respectively.

The experimental results were in very good correlation with the predicted results, demonstrating the model's validity. The results revealed that K2.2.2 and C2.2 have a greater affinity for Sc when compared to DC18C6 when evaluated under the same conditions. The extraction ability of K 2.2.2 and C 2.2 can be due to the good compatibility between them and the ionic radii of Sc diameter (~ 1.4 Å). Moreover, the K 2.2.2 (1.4 Å) and C 2.2 (1.8 Å) compounds have a unique feature and capable of encapsulating metal ions in their cage-like cavities to form stable complexes. This could be of a potential value in the separation and the purification of Sc in the REEs processing industry. The incorporated Sc metal ions can be efficiently recovered/stripped by 0.1, 0.5 and 1 mol/L HCl and HNO_3 solutions. The stripping ratios of scandium varied between 95 and 99%. However, it is to be noted that the Sc recovery experiments are to be continued with model solutions containing several metal ions and red mud leachate to formulate a solid view on the feasibility of this procedure.

4.3 Recovery of Scandium from Red Mud Leachate by OPCs Modified Solid Phases Applying Liquid-Solid Extraction Technique

This study elucidated the successful immobilization of OPCs (D2EHPA, TBP and TOPO) into the nanocomposites matrix (Fe_3O_4/SiO_2/OPCs) prepared through a sol–gel process to form eco-friendly new type SPE materials. The immobilization of organophosphorus molecules on the Fe_3O_4/SiO_2 solid surface was confirmed by FTIR, SEM-EDX and BET.

The solid−liquid extraction process has been found as an attractive alternative for Sc extraction due to the elimination of toxic, inflammable, and expensive organic liquid extractants. Among the prepared solid phase samples, Fe_3O_4/SiO_2/TBP adsorbent showed superior extraction selectivity (97%) toward Sc compared with other metal ions (5% Al, 0.4% Fe, 12% Ti, 22% La and 7% Y). Sc 100% efficiency is achieved during recovery scandium from solid phase by stripping with acid solution. Fe_3O_4/SiO_2/D2EHPA showed high extraction efficiency not only for Sc but for Fe as well, main component of red mud. Moreover, recovery of Sc from mentioned before SP has not been achieved and requires further study. Fe_3O_4/SiO_2/TOPO did not show selectivity towards Sc ions.

5. NEW SCIENTIFIC RESULTS: THESIS

One of the main goals of this PhD thesis was to develop new techniques for the recovery of scandium from the acidic leachates of red mud bauxite residue. The recovery of scandium from the acidic solutions was studied by different separation technologies: Solvent extraction (organophosphorus or macrocyclic liquids), ion exchange, and solid phase extraction (organophosphorus compounds modified solid support).

5.1 Recovery of Scandium from Real Red Mud Leachate by Solvent Extraction with Organophosphorus compounds

5.1.1. I set and optimize the experimental parameters for effective and selective dissolution of scandium from red mud. 80% of Sc (79 ppm) dissolution was achieved under the following conditions: 7 mol/L HCl at a S/L ratio of 1:30 for 5 h at 75 ℃ reflex system. This leachate was further purified by liquid-liquid extraction method in order to remove other dissolved elements such as Fe 14wt%, Al 7wt%, Ti 2.1wt%, La 155 ppm, Y 101 ppm. The iron content was mainly removed by diethyl ether and remaining metals ions with organophosphorus extractants [76, 142, 143].

5.1.2. I recommend the Protocol C of ***triple liquid-liquid extraction for*** the efficient recovery of scandium from the red mud leachate at industrial scale. At Protocol C the highest Sc recovery 81% (869 ppm) from 7 mol/L HCl leachate solution was achieved after triple extraction with 10 vol% TBP, A/O = 3:1 and 5 min extraction time. The iron (150ppm) and titanium (1.5 ppm) content was lower and Al, La and Y were not observed in final recovered solution [76, 142, 143] .

5.2 Recovery of Scandium from Model Solution by Solvent Extraction with Macrocyclic Compounds

The main aim of this part was to figure out how well DC18C6, K 2.2.2 and C 2.2 macrocyclic compounds work as novel extractants for Sc (III) by using a central composite rotatable design technique. The following points are determined:

5.2.1. The experimental results obtained were in very good correlation with the predicted STATISTZICA and WinQSB softtwares ones, demonstrating the model's validity and its application for Sc recovery from real leachate of 75 mg/L initial concertation. The results showed that 0.006 mol/L K 2.2.2 and C 2.2 in 1,2 dichloroethane have a greater Sc capturing affinity compared to DC18C6 under the same experimental conditions: A/O ratio1, pH of solution 4, 11 min contact time. Therefore extraction efficiency was higher 99 and 97 % for K 2.2.2 and C 2.2 respectively in comparison with DC18C6 (E 15%) macrocyclic extractant [115].

5.2.2. I concluded that the incorporation of scandium into the macrocyclic compounds was feasible. The change in Sc concentration was monitored by AAS technique. K 2.2.2 and C 2.2 compounds has unique features and capable of encapsulating metal ions in their cage-like cavities to form stable complexes. This could be of potential value in the separation and purification of Sc in REEs processing [115, 144, 145].

5.3 Recovery of Scandium from Real Red Mud Leachate by SPE With Organophosphorus Compounds

The knowledge gained in the field of REE extraction with organophosphorus compounds (OPCs) has been implemented to develop a new type of solid phases for solid-liquid techniques. The following points are determined:

5.3.1. The FTIR, BET and EDX-SEM results confirmed that OPCs (D2EHPA, TBP and TOPO) were successfully incorporated to Fe_3O_4/SiO_2 solid phase/support by entrapment sol–gel preparation technique with formation of particles between 20 to 500 nm in size. Moreover, the formation of the P=O, P-O- functional (active) group for Sc binding was confirmed by FTIR analysis [146].

5.3.2. Among of solid samples the highest 97% Sc removal efficiency from 79 ppm Sc containing red mud leachate was achieved over Fe_3O_4/SiO_2/TBP solid phase (adsorbent). I recommend this solid phase for testing in the recovery of scandium from the red mud at pilot-plant scale.

BIBLIOGRAPHY

[1] L. Wang, N. Sun, H. Tang, and W. Sun, "A Review on Comprehensive Utilization of Red Mud and Prospect Analysis," *Minerals*, vol. 9, no. 6, p. 362, 2019. [Online]. Available: https://www.mdpi.com/2075-163X/9/6/362.

[2] R. Marin Rivera, "Innovative Technologies for Rare Earth Element Recovery from Bauxite Residue," 2019.

[3] A. W. Bray *et al.*, "Sustained bauxite residue rehabilitation with gypsum and organic matter 16 years after initial treatment," *Environmental science & technology*, vol. 52, no. 1, pp. 152-161, 2018.

[4] H. Agurto-Detzel *et al.*, "The tailings dam failure of 5 November 2015 in SE Brazil and its preceding seismic sequence," *Geophysical Research Letters*, vol. 43, no. 10, pp. 4929-4936, 2016.

[5] K. Evans, "The History, Challenges, and New Developments in the Management and Use of Bauxite Residue," *Journal of Sustainable Metallurgy*, vol. 2, no. 4, pp. 316-331, 2016/12/01 2016, doi: 10.1007/s40831-016-0060-x.

[6] W. M. Mayes *et al.*, "Advances in Understanding Environmental Risks of Red Mud After the Ajka Spill, Hungary," *Journal of Sustainable Metallurgy*, vol. 2, no. 4, pp. 332-343, 2016/12/01 2016, doi: 10.1007/s40831-016-0050-z.

[7] C. R. Borra, J. Mermans, B. Blanpain, Y. Pontikes, K. Binnemans, and T. Van Gerven, "Selective recovery of rare earths from bauxite residue by combination of sulfation, roasting and leaching," *Minerals Engineering*, vol. 92, pp. 151-159, 2016/06/01/ 2016, doi: https://doi.org/10.1016/j.mineng.2016.03.002.

[8] D. Avdibegović, M. Regadío, and K. Binnemans, "Efficient separation of rare earths recovered by a supported ionic liquid from bauxite residue leachate," *RSC advances*, vol. 8, no. 22, pp. 11886-11893, 2018.

[9] B. Onghena, C. R. Borra, T. Van Gerven, and K. Binnemans, "Recovery of scandium from sulfation-roasted leachates of bauxite residue by solvent extraction with the ionic liquid betainium bis(trifluoromethylsulfonyl)imide," *Separation and Purification Technology*, vol. 176, pp. 208-219, 2017/04/04/ 2017, doi: https://doi.org/10.1016/j.seppur.2016.12.009.

[10] G. Charalampides, K. I. Vatalis, B. Apostoplos, and B. Ploutarch-Nikolas, "Rare earth elements: industrial applications and economic dependency of Europe," *Procedia Economics and Finance*, vol. 24, pp. 126-135, 2015.

[11] C. R. Borra, B. Blanpain, Y. Pontikes, K. Binnemans, and T. Van Gerven, "Recovery of rare earths and other valuable metals from bauxite residue (red mud): a review," *Journal of Sustainable Metallurgy*, vol. 2, no. 4, pp. 365-386, 2016.

[12] V. Balaram, "Rare earth elements: A review of applications, occurrence, exploration, analysis, recycling, and environmental impact," *Geoscience Frontiers,* vol. 10, no. 4, pp. 1285-1303, 2019/07/01/ 2019, doi: https://doi.org/10.1016/j.gsf.2018.12.005.

[13] C. Borra, B. Blanpain, Y. Pontikes, K. Binnemans, and T. Van Gerven, "Recovery of Rare Earths from Bauxite Residue (Red Mud)," 2019, pp. 343-356.

[14] X. Liu, Y. Han, F. He, P. Gao, and S. Yuan, "Characteristic, hazard and iron recovery technology of red mud - A critical review," *Journal of Hazardous Materials,* vol. 420, p. 126542, 2021/10/15/ 2021, doi: https://doi.org/10.1016/j.jhazmat.2021.126542.

[15] S. M. A. Qaidi, B. A. Tayeh, H. F. Isleem, A. R. G. de Azevedo, H. U. Ahmed, and W. Emad, "Sustainable utilization of red mud waste (bauxite residue) and slag for the production of geopolymer composites: A review," *Case Studies in Construction Materials,* vol. 16, p. e00994, 2022/06/01/ 2022, doi: https://doi.org/10.1016/j.cscm.2022.e00994.

[16] A. Pyasi, "Value added metal extraction from red mud," 2014.

[17] É. Ujaczki, Y.-S. Zimmermann, V. Feigl, and M. Lenz, *Recovery Of Rare Earth Elements From Hungarian Red Mud With Combined Acid Leaching And Liqiud-Liquid Extraction*. 2015.

[18] C. Klauber, M. Gräfe, and G. Power, "Bauxite residue issues: II. options for residue utilization," *Hydrometallurgy,* vol. 108, no. 1, pp. 11-32, 2011/06/01/ 2011, doi: https://doi.org/10.1016/j.hydromet.2011.02.007.

[19] E. Balomenos *et al.*, "Efficient and complete exploitation of the bauxite residue (red mud) produced in the Bayer process," in *Proceedings of EMC*, 2011, vol. 3, pp. 745-758.

[20] R. Marin Rivera, B. Ulenaers, G. Ounoughene, K. Binnemans, and T. Van Gerven, "Behaviour of silica during metal recovery from bauxite residue by acidic leaching," in *Travaux 46, Proceedings of 35th International ICSOBA Conference, Hamburg, Germany, 2–5 October, 2017.*, 2017, pp. 547-556.

[21] C. R. Borra, Y. Pontikes, K. Binnemans, and T. J. M. E. Van Gerven, "Leaching of rare earths from bauxite residue (red mud)," vol. 76, pp. 20-27, 2015.

[22] R. M. Rivera, B. Ulenaers, G. Ounoughene, K. Binnemans, and T. Van Gerven, "Extraction of rare earths from bauxite residue (red mud) by dry digestion followed by water leaching," *Minerals Engineering,* vol. 119, pp. 82-92, 2018/04/01/ 2018, doi: https://doi.org/10.1016/j.mineng.2018.01.023.

[23] G. Li *et al.*, "Extraction of scandium from scandium-rich material derived from bauxite ore residues," *Hydrometallurgy,* vol. 176, pp. 62-68, 2018.

[24] A. B. Botelho Junior, D. C. R. Espinosa, J. Vaughan, and J. A. S. Tenório, "Recovery of scandium from various sources: A critical review of the state of the art and future prospects," *Minerals Engineering,* vol. 172, p. 107148, 2021/10/01/ 2021, doi: https://doi.org/10.1016/j.mineng.2021.107148.

[25] Xue L, and Li D. Extraction Of Scandium (III), Yttrium (III), Lanthanide (III) And Iron (III) From Hydrochloric Acid Solutions With Di-(2-Ethylhexyl) Phosphinic Acid. Chinese Journal of Applied Chemistry. 1992 Aug 10(4):21.

[26] J. Anawati and G. Azimi, "Recovery of scandium from Canadian bauxite residue utilizing acid baking followed by water leaching," *Waste Management*, vol. 95, pp. 549-559, 2019.

[27] A. Akcil, N. Akhmadiyeva, R. Abdulvaliyev, Abhilash, and P. Meshram, "Overview on extraction and separation of rare earth elements from red mud: Focus on scandium," *Mineral Processing and Extractive metallurgy review*, vol. 39, no. 3, pp. 145-151, 2018.

[28] S. Agrawal and N. Dhawan, "Evaluation of red mud as a polymetallic source – A review," *Minerals Engineering*, vol. 171, p. 107084, 2021/09/01/ 2021, doi: https://doi.org/10.1016/j.mineng.2021.107084.

[29] E. Scerri, *The periodic table: its story and its significance*. Oxford University Press, 2019.

[30] W. H. Wells and V. L. Wells, "The Lanthanides, Rare Earth Elements," in *Patty's Toxicology*, pp. 817-840.

[31] "1 - Origin of the Elements. Isotopes and Atomic Weights," in *Chemistry of the Elements (Second Edition)*, N. N. Greenwood and A. Earnshaw Eds. Oxford: Butterworth-Heinemann, 1997, pp. 1-19.

[32] C. K. Gupta and N. Krishnamurthy, "Extractive metallurgy of rare earths," *International materials reviews*, vol. 37, no. 1, pp. 197-248, 1992.

[33] J. R. Haas, E. L. Shock, and D. C. Sassani, "Rare earth elements in hydrothermal systems: Estimates of standard partial molal thermodynamic properties of aqueous complexes of the rare earth elements at high pressures and temperatures," *Geochimica et Cosmochimica Acta*, vol. 59, no. 21, pp. 4329-4350, 1995/11/01/ 1995, doi: https://doi.org/10.1016/0016-7037(95)00314-P.

[34] B. Mwewa, M. Tadie, S. Ndlovu, G. S. Simate, and E. Matinde, "Recovery of Rare Earth Elements from Acid Mine Drainage: A Review of the Extraction Methods," *Journal of Environmental Chemical Engineering*, p. 107704, 2022.

[35] N. N. Greenwood and A. Earnshaw, *Chemistry of the Elements*. Elsevier, 2012.

[36] M. Alemrajabi, "Recovery of Rare Earth Elements from an Apatite Concentrate," KTH Royal Institute of Technology, 2018.

[37] E. Polido Legaria, *Hybrid nanoadsorbents for extraction and separation of rare earth elements in solution*. 2016.

[38] G. Kostikova, N. Danilov, Y. S. Krylov, G. Korpusov, and E. Sal'nikova, "Extraction of scandium from various media with triisoamyl phosphate. Communication 1. extraction of Sc and impurity metals from

aqueous nitric acid solutions; Ehkstraktsiya Sc triizoamilfosfatom iz razlichnykh sred. 1. Ehkstraktsiya Sc iz azotnokislykh rastvorov," *Radiokhimiya,* vol. 47, 2005.

[39] L. Jiang, H. Yang, and Y. Sun, "Solvent extraction of scandium from chlorination system with EHPAEH," *MATEC Web Conf.,* vol. 277, p. 01002, 2019. [Online]. Available: https://doi.org/10.1051/matecconf/201927701002.

[40] S. Das *et al.*, "Extraction of scandium(III) from acidic solutions using organo-phosphoric acid reagents: A comparative study," *Separation and Purification Technology,* vol. 202, pp. 248-258, 2018/08/31/ 2018, doi: https://doi.org/10.1016/j.seppur.2018.03.023.

[41] W. Wang and C. Y. Cheng, "Separation and purification of scandium by solvent extraction and related technologies: a review," *Journal of Chemical Technology & Biotechnology,* vol. 86, no. 10, pp. 1237-1246, 2011.

[42] W. Wang, Y. Pranolo, and C. Y. Cheng, "Metallurgical processes for scandium recovery from various resources: A review," *Hydrometallurgy,* vol. 108, no. 1, pp. 100-108, 2011/06/01/ 2011, doi: https://doi.org/10.1016/j.hydromet.2011.03.001.

[43] A. Ditze and K. Kongolo, "Recovery of scandium from magnesium, aluminium and iron scrap," *Hydrometallurgy,* vol. 44, no. 1, pp. 179-184, 1997/01/01/ 1997, doi: https://doi.org/10.1016/S0304-386X(96)00041-2.

[44] E. Elbashier, A. Mussa, M. Hafiz, and A. H. Hawari, "Recovery of rare earth elements from waste streams using membrane processes: An overview," *Hydrometallurgy,* vol. 204, p. 105706, 2021.

[45] Y. Zhang, F. Gu, Z. Su, S. Liu, C. Anderson, and T. Jiang, "Hydrometallurgical recovery of rare earth elements from NdFeB permanent magnet scrap: A review," *Metals,* vol. 10, no. 6, p. 841, 2020.

[46] A. Yuksekdag, B. Kose-Mutlu, A. F. Siddiqui, M. R. Wiesner, and I. Koyuncu, "A holistic approach for the recovery of rare earth elements and scandium from secondary sources under a circular economy framework – A review," *Chemosphere,* vol. 293, p. 133620, 2022/04/01/ 2022, doi: https://doi.org/10.1016/j.chemosphere.2022.133620.

[47] S. R. Izatt, J. S. McKenzie, N. E. Izatt, R. L. Bruening, K. E. Krakowiak, and R. M. Izatt, "Molecular recognition technology: a green chemistry process for separation of individual rare earth metals," *White Paper on Separation of Rare Earth Elements,* pp. 1-13, 2016.

[48] Nasrollahzadeh M. Biopolymer-Based Metal Nanoparticle Chemistry for Sustainable Applications: Volume 2: Applications. Elsevier; 2021 Mar 5.

[49] K. Wang *et al.*, "Recovery of rare earth elements with ionic liquids," *Green Chemistry,* vol. 19, no. 19, pp. 4469-4493, 2017.

[50] N. V. Plechkova and K. R. Seddon, "Applications of ionic liquids in the chemical industry," *Chemical Society Reviews*, vol. 37, no. 1, pp. 123-150, 2008.

[51] R. Izatt, S. Izatt, N. Izatt, R. Bruening, L. Navarro, and K. Krakowiak, "Industrial Applications Of Molecular Recognition Technology to Separations of Platinum Group Metals and Selective Removal of Metal Impurities from Process Streams," *Green Chem.*, vol. 17, 02/13 2015, doi: 10.1039/C4GC02188F.

[52] S. Andronati, A. Mazurov, and T. Korotenko, "Application of Crown Ethers in Peptide Synthesis," in *Vol. 3 Proceedings of the Fifth USSR-FRG Symposium on Chemistry of Peptides and Proteins, Odessa, USSR, May 16–20, 1985*, 2019: de Gruyter, pp. 37-42.

[53] B. Çiçek and A. Yıldız, "Synthesis, Metal Ion Complexation and Computational Studies of Thio Oxocrown Ethers," *Molecules*, vol. 16, no. 10, pp. 8670-8683, 2011. [Online]. Available: https://www.mdpi.com/1420-3049/16/10/8670.

[54] K. Fujinaga *et al.*, "Separation of Sc(III) from ZrO(II) by solvent extraction using oxidized Phoslex DT-8," *Hydrometallurgy*, vol. 133, pp. 33-36, 2013/02/01/ 2013, doi: https://doi.org/10.1016/j.hydromet.2012.11.014.

[55] R. K. Singh and P. M. J. B. C. T. M. Dhadke, "Extraction and separation of scandium (III) from perchlorate media, by D2EHPA and PC-88A," vol. 22, pp. 1-11, 2003.

[56] V. Shalomeev, N. Lysenko, E. Tsivirko, V. Lukinov, V. J. M. S. Klochikhin, and H. Treatment, "Structure and properties of magnesium alloys with scandium," vol. 50, no. 1, pp. 34-37, 2008.

[57] D. Zou, H. Li, J. Chen, and D. Li, "Recovery of scandium from spent sulfuric acid solution in titanium dioxide production using synergistic solvent extraction with D2EHPA and primary amine N1923," *Hydrometallurgy*, vol. 197, p. 105463, 2020.

[58] X. Zhu, W. Li, S. Tang, M. Zeng, P. Bai, and L. Chen, "Selective recovery of vanadium and scandium by ion exchange with D201 and solvent extraction using P507 from hydrochloric acid leaching solution of red mud," *Chemosphere*, vol. 175, pp. 365-372, 2017.

[59] R. Cattrall and S. J. I. C. Slater, "Extraction of scandium from aqueous sulfate solutions by bis (3, 5, 5-trimethylhexyl) ammonium sulfate," vol. 9, no. 3, pp. 598-602, 1970.

[60] Y. Liu *et al.*, "New process consisting of oxidative stripping of vanadium from loaded D2EHPA organic solution with H2O2 and direct precipitation with sulfuric acid," *Hydrometallurgy*, vol. 203, p. 105611, 2021/08/01/ 2021, doi: https://doi.org/10.1016/j.hydromet.2021.105611.

[61] Y. Baba, A. Fukami, F. Kubota, N. Kamiya, and M. Goto, "Selective extraction of scandium from yttrium and lanthanides with amic acid-type extractant containing alkylamide and glycine moieties," *RSC Advances*, 10.1039/C4RA08897B vol. 4, no. 92, pp. 50726-50730, 2014, doi: 10.1039/C4RA08897B.

[62] N. Ismail, A. Hisyam, M. A. Abd Aziz, and M. Y. Mohd Yunus, "Selection of Extractant in Rare Earth Solvent Extraction System: A Review," vol. 8, pp. 728-743, 05/30 2019.

[63] C. Wang and D. Li, "Extraction mechanism of Sc(III) and separation from Th(IV), Fe(III) and Lu(III) with bis(2,4,4-trimethylpentyl)phosphinic acid in n-hexane from sulphuric acid solutions," (in English), vol. 12:3, 1994-06-01 1994, doi: 10.1080/07366299408918228

[64] Y. Chen, H. Wang, Y. Pei, and J. Wang, "Selective separation of scandium (III) from rare earth metals by carboxyl-functionalized ionic liquids," *Separation and Purification Technology*, vol. 178, pp. 261-268, 2017.

[65] M. Karve and B. Vaidya, "Selective Separation of Scandium(III) and Yttrium(III) from other Rare Earth Elements using Cyanex302 as an Extractant," *Separation Science and Technology*, vol. 43, no. 5, pp. 1111-1123, 2008/03/01 2008, doi: 10.1080/01496390801887435.

[66] Zhen, Peng, Li Qing-gang, Li Zhao-yang, Zhang Gui-qing, Cao Zuo-ying, and Guan Wen-juan, "Removal of impurities from scandium solutions by ion exchange," *Journal of Central South University*, vol. 25, no. 12, pp. 2953-2961, 2018.

[67] G. Alkan *et al.*, "Selective silica gel free scandium extraction from Iron-depleted red mud slags by dry digestion," *Hydrometallurgy*, vol. 185, 03/01 2019, doi: 10.1016/j.hydromet.2019.03.008.

[68] J. Hu, D. Zou, J. Chen, and D. Li, "A novel synergistic extraction system for the recovery of scandium (III) by Cyanex272 and Cyanex923 in sulfuric acid medium," *Separation and Purification Technology*, vol. 233, p. 115977, 2020/02/15/ 2020, doi: https://doi.org/10.1016/j.seppur.2019.115977.

[69] S. Reid, J. Tam, M. Yang, and G. Azimi, "Technospheric Mining of Rare Earth Elements from Bauxite Residue (Red Mud): Process Optimization, Kinetic Investigation, and Microwave Pretreatment," *Scientific Reports*, vol. 7, no. 1, p. 15252, 2017/11/10 2017, doi: 10.1038/s41598-017-15457-8.

[70] A. D. Salman *et al.*, "Scandium Recovery Methods from Mining, Metallurgical Extractive Industries, and Industrial Wastes," *Materials*, vol. 15, no. 7, p. 2376, 2022. [Online]. Available: https://www.mdpi.com/1996-1944/15/7/2376.

[71] M. Ochsenkühn-Petropulu, T. Lyberopulu, K. Ochsenkühn, and G. J. A. C. A. Parissakis, "Recovery of lanthanides and yttrium from red mud by selective leaching," vol. 319, no. 1-2, pp. 249-254, 1996.

[72] M. Ochsenkühn-Petropoulou, K. Hatzilyberis, L. Mendrinos, and C. Salmas, "Pilot-Plant Investigation of the Leaching Process for the Recovery of Scandium from Red Mud," *Industrial & Engineering Chemistry Research - IND ENG CHEM RES*, vol. 41, 10/10 2002, doi: 10.1021/ie011047b.

[73] Xue, An, Xiao-hu Chen, and Xiao-ning Tang, "The technological study and leaching kinetics of scandium from red mud," vol. 2, pp. 51-53, 2010.

[74] Zhang J, Deng Z, and Xu T, "Experimental investigation on leaching metals from red mud," vol. 2, pp. 13-15, 2005.

[75] C. R. Borra, Y. Pontikes, K. Binnemans, and T. Van Gerven, "Leaching of rare earths from bauxite residue (red mud)," *Minerals engineering*, vol. 76, pp. 20-27, 2015.

[76] A. D. Salman *et al.*, "Enhancing the Recovery of Rare Earth Elements from Red Mud," *Chemical Engineering & Technology*, vol. 44, no. 10, pp. 1768-1774, 2021, doi: https://doi.org/10.1002/ceat.202100223.

[77] K. Wang, Y. Yu, H. Wang, and J. J. C. R. E. Chen, "Experimental investigation on leaching scandium from red mud by hydrochloric acid," vol. 1, pp. 95-98, 2010.

[78] L. Xu, G. Shi, Y. Li, Q. Zhong, Y. Luo, and P. J. N. M. Yu, "Study of scandium pre-enrichment from red mud leached by hydrochloric acid," vol. 1, pp. 54-56, 2015.

[79] Tang XN, Chen XH, and Xue A, "Research on leaching kinetics of scandium from red mud," vol. 29, pp. 150-155, 2010.

[80] Z. Liu, Y. Zong, H. Li, and Z. Zhao, "Characterization of scandium and gallium in red mud with Time of Flight-Secondary Ion Mass Spectrometry (ToF-SIMS) and Electron Probe Micro-Analysis (EPMA)," *Minerals Engineering*, vol. 119, pp. 263-273, 2018/04/01/ 2018, doi: https://doi.org/10.1016/j.mineng.2018.01.038.

[81] J. Ross and J. Rosenbaum, *Reconnaissance of scandium sources and recovery of scandium from uranium mill solutions*. US Department of Interior, Bureau of Mines, 1962.

[82] V. L. Rayzman and I. K. J. J. Filipovich, "Integrating coal combustion and red mud sintering at an alumina refinery," vol. 51, no. 8, pp. 16-18, 1999.

[83] M. Ochsenkühn-Petropulu, T. Lyberopulu, K. M. Ochsenkühn, and G. Parissakis, "Recovery of lanthanides and yttrium from red mud by selective leaching," *Analytica Chimica Acta*, vol. 319, no. 1, pp. 249-254, 1996/01/30/ 1996, doi: https://doi.org/10.1016/0003-2670(95)00486-6.

[84] H. Kong, T. Zhou, X. Yang, Y. Gong, M. Zhang, and H. Yang, "Iron Recovery Technology of Red Mud—A review," *Energies*, vol. 15, no. 10, p. 3830, 2022.

[85] R. Khanna *et al.*, "Red Mud as a Secondary Resource of Low-Grade Iron: A Global Perspective," *Sustainability*, vol. 14, no. 3, p. 1258, 2022.

[86] S. Dashti, S. Shakibania, F. Rashchi, and A. Ghahreman, "Synergistic effects of Ionquest 801 and Cyanex 572 on the solvent extraction of rare earth elements (Pr, Nd, Sm, Eu, Tb, and Er) from a chloride medium," *Separation and Purification Technology*, vol. 279, p. 119797, 2021/12/15/ 2021, doi: https://doi.org/10.1016/j.seppur.2021.119797.

[87] Zhang JJ, Deng ZG, Xu TH, "Recovery scandium from leaching liquor of red mud," vol. 7, p. 16, 2006.

[88] Z. Liu, H. Li, Q. Jing, and M. Zhang, "Recovery of Scandium from Leachate of Sulfation-Roasted Bayer Red Mud by Liquid–Liquid Extraction," *JOM*, vol. 69, no. 11, pp. 2373-2378, 2017/11/01 2017, doi: 10.1007/s11837-017-2518-0.

[89] Z. Hualei, L. Dongyan, T. Yajun, and C. J. R. m. Yunfa, "Extraction of scandium from red mud by modified activated carbon and kinetics study," vol. 27, no. 3, pp. 223-227, 2008.

[90] A. B. Botelho Junior, D. C. R. Espinosa, and J. A. S. Tenório, "Selective separation of Sc(III) and Zr(IV) from the leaching of bauxite residue using trialkylphosphine acids, tertiary amine, tri-butyl phosphate and their mixtures," *Separation and Purification Technology*, vol. 279, p. 119798, 2021/12/15/ 2021, doi: https://doi.org/10.1016/j.seppur.2021.119798.

[91] W. Wang, Y. Pranolo, and C. Y. Cheng, "Recovery of scandium from synthetic red mud leach solutions by solvent extraction with D2EHPA," *Separation and purification technology*, vol. 108, pp. 96-102, 2013.

[92] M. Ochsenkühn-Petropulu, T. Lyberopulu, and G. J. A. C. A. Parissakis, "Selective separation and determination of scandium from yttrium and lanthanides in red mud by a combined ion exchange/solvent extraction method," vol. 315, no. 1-2, pp. 231-237, 1995.

[93] M. Hiraoka, *Crown ethers and analogous compounds*. Elsevier, 2016.

[94] G. V. Kostikova, O. G. Krasnova, A. Y. Tsivadze, and V. I. Zhilov, "Scandium Extraction with Benzo-15-crown-5 from Neutral Nitrate–Trichloroacetate Solutions," *Russian Journal of Inorganic Chemistry*, vol. 63, no. 4, pp. 555-560, 2018/04/01 2018, doi: 10.1134/S0036023618040125.

[95] Olszanski DJ, Melson GA. Coordination chemistry of scandium. X. Macrocyclic polyether complexes of scandium (III). Inorganica Chimica Acta. 1978 Jan 1;26:263-9, https://doi.org/10.1016/S0020-1693(00)87225-4.

[96] V. Lakshmanan and S. Vijayan, "A review on application of crown ethers in separation of rare earths and precious metals," in *Extraction 2018*: Springer, 2018, pp. 1913-1930.

[97] Tsay LM, Shih JS, Wu SC. Solvent extraction of rare earth metals with crown ethers. Analyst. 1983;108(1290):1108-13, https://doi.org/10.1039/AN9830801108.

[98] S. Demin, V. Zhilov, S. Nefedov, V. Baulin, and A. Y. Tsivadze, "Extraction of rare earth elements with 1-(diphenylphosphorylmethoxy)-2-diphenylphosphoryl-4-ethylbenzene with the use of 1, 1, 7-trihydrododecafluoroheptanol as a solvent," *Russian Journal of Inorganic Chemistry*, vol. 57, no. 6, pp. 897-902, 2012.

[99] S. Demin, V. Zhilov, A. Y. Tsivadze, V. Yakshin, and O. Vilkova, "Extraction of rare-earth elements by crown ethers from acid solutions into 1, 1, 7-trihydrododecafluoroheptanol," *Russian Journal of Inorganic Chemistry*, vol. 54, no. 3, pp. 385-388, 2009.

[100] X. Dai *et al.*, "Selective adsorption and recovery of scandium from red mud leachate by using phosphoric acid pre-treated pitaya peel biochar," *Separation and Purification Technology*, vol. 292, p. 121043, 2022.

[101] Z. Tu *et al.*, "Silica gel modified with 1-(2-aminoethyl)-3-phenylurea for selective solid-phase extraction and preconcentration of Sc (III) from environmental samples," *Talanta*, vol. 80, no. 3, pp. 1205-1209, 2010.

[102] A. Rahmani *et al.*, "Functionalized nanoporous silicon for extraction of Sc from a leach solution," *Hydrometallurgy*, vol. 211, p. 105866, 2022.

[103] J. Roosen, S. Van Roosendael, C. R. Borra, T. Van Gerven, S. Mullens, and K. Binnemans, "Recovery of scandium from leachates of Greek bauxite residue by adsorption on functionalized chitosan–silica hybrid materials," *Green chemistry*, vol. 18, no. 7, pp. 2005-2013, 2016.

[104] Q. Yu, S. Ning, W. Zhang, X. Wang, and Y. Wei, "Recovery of scandium from sulfuric acid solution with a macro porous TRPO/SiO2-P adsorbent," *Hydrometallurgy*, vol. 181, pp. 74-81, 2018.

[105] V. Korovin, Y. Shestak, and Y. Pogorelov, "Comparison of scandium recovery mechanisms by phoshporus-containing sorbents, solvent extractants and extractants supported on porous carrier," in *Scandium: Compounds, Productions and Applications*, 2011, pp. 77-100.

[106] M. Aguilar and J. L. Cortina, *Solvent extraction and liquid membranes: Fundamentals and applications in new materials*. CRC Press, 2008.

[107] V. Korovin and Y. Shestak, "Scandium extraction from hydrochloric acid media by Levextrel-type resins containing di-isooctyl methyl phosphonate," *Hydrometallurgy*, vol. 95, no. 3-4, pp. 346-349, 2009.

[108] V. Kuzmin and A. Kuzmina, "Obtaining Solid Extractants Based on Mixtures of Tributylphosphate and Molecular Iodine and Researching the Extraction of Scandium from Chloride Solutions," *Theoretical Foundations of Chemical Engineering*, vol. 55, no. 5, pp. 1073-1077, 2021.

[109] V. Korovin, Y. Shestak, and Y. Pogorelov, "Scandium extraction by neutral organo-phosphorus compounds supported on a porous carrier," *Hydrometallurgy*, vol. 52, no. 1, pp. 1-8, 1999.

[110] P. P. Aung, I. Troshkina, O. Veselova, Y. A. Davidovich, M. Tsyurupa, and V. Davankov, "Sorption of scandium by hypercrosslinked polystyrene impregnate containing organophosphorus acids," *Sorbtsionnye i khromatograficheskiye processy*, pp. 45-53, 2017.

[111] P. P. Aung, O. Veselova, and I. Troshkina, "Kinetics of scandium sorption by impregnate containing phosphinoxide," *Ivanovo State University of Chemistry and Technology*, vol. 60, no. 8, pp. 28-30, 2017.

[112] A. Shirikova, L. Pasechnik, and S. Yatsenko, "Prospects of application of microencapsulated extractants for extraction of scandium and rare-earth elements," *Non-Ferrous Metals*, no. 1, pp. 41-44, 2014.

[113] B. G. Tabachnick and L. S. Fidell, *Experimental designs using ANOVA*. Thomson/Brooks/Cole Belmont, CA, 2007.

[114] N. J. Saleh, R. I. Ibrahim, and A. D. Salman, "Characterization of nano-silica prepared from local silica sand and its application in cement mortar using optimization technique," *Advanced Powder Technology,* vol. 26, no. 4, pp. 1123-1133, 2015.

[115] A. Salman *et al.*, "Studying the extraction of scandium (III) by macrocyclic compounds from aqueous solution using optimization technique," *International Journal of Environmental Science and Technology,* pp. 1-18, 2022.

[116] A. Khusro, B. K. Kaliyan, N. A. Al-Dhabi, M. V. Arasu, and P. Agastian, "Statistical optimization of thermo-alkali stable xylanase production from Bacillus tequilensis strain ARMATI," *Electronic Journal of Biotechnology*, vol. 22, pp. 16-25, 2016/07/01/ 2016, doi: https://doi.org/10.1016/j.ejbt.2016.04.002.

[117] D. Marini and J. R. Corney, "Concurrent optimization of process parameters and product design variables for near net shape manufacturing processes," *Journal of Intelligent Manufacturing,* vol. 32, no. 2, pp. 611-631, 2021/02/01 2021, doi: 10.1007/s10845-020-01593-y.

[118] M. O. Besenhard *et al.*, "Co-precipitation synthesis of stable iron oxide nanoparticles with NaOH: New insights and continuous production via flow chemistry," *Chemical Engineering Journal,* vol. 399, p. 125740, 2020/11/01/ 2020, doi: https://doi.org/10.1016/j.cej.2020.125740.

[119] V. Chaudhary and R. Chaudhary, "Magnetic Nanoparticles: Synthesis, Functionalization, and Applications," 2018, pp. 153–183.

[120] B. Saad *et al.*, "Selective removal of heavy metal ions using sol–gel immobilized and SPE-coated thiacrown ethers," *Analytica chimica acta,* vol. 555, no. 1, pp. 146-156, 2006.

[121] F. Bari, N. Begum, S. B. Jamaludin, and K. Hussin, "Extraction and separation of Cu(II), Ni(II) and Zn(II) by sol–gel silica immobilized with Cyanex 272," *Hydrometallurgy*, vol. 96, no. 1, pp. 140-147, 2009/03/01/ 2009, doi: https://doi.org/10.1016/j.hydromet.2008.09.006.

[122] M. Zielecka, E. Bujnowska, K. Suwala, and M. Wenda, "Sol-Gel-Derived Silicon-Containing Hybrids," 2017.

[123] J. Vind *et al.*, "Modes of occurrences of scandium in Greek bauxite and bauxite residue," *Minerals Engineering,* vol. 123, pp. 35-48, 2018/07/01/ 2018, doi: https://doi.org/10.1016/j.mineng.2018.04.025.

[124] J. Vind *et al.*, "Modes of occurrences of scandium in Greek bauxite and bauxite residue," *Minerals Engineering,* vol. 123, 04/30 2018, doi: 10.1016/j.mineng.2018.04.025.

[125] J. Kim and G. Azimi, "Recovery of scandium and neodymium from blast furnace slag using acid baking–water leaching," *RSC Advances,* vol. 10, no. 53, pp. 31936-31946, 2020.

[126] X. Zhang, K. Zhou, Y. Wu, Q. Lei, C. Peng, and W. Chen, "Separation and recovery of iron and scandium from acid leaching solution of red mud using D201 resin," *Journal of Rare Earths,* vol. 38, pp. 1322-1329, 12/01 2020, doi: 10.1016/j.jre.2019.12.005.

[127] N. H. Tran *et al.*, "Occurrence and risk assessment of multiple classes of antibiotics in urban canals and lakes in Hanoi, Vietnam," *Sci Total Environ,* vol. 692, pp. 157-174, Nov 20 2019, doi: 10.1016/j.scitotenv.2019.07.092.

[128] H. Qiu *et al.*, "From trace to pure: Recovery of scandium from the waste acid of titanium pigment production by solvent extraction," *Process Safety and Environmental Protection,* vol. 121, pp. 118-124, 2019.

[129] Y. Chen *et al.*, "Highly efficient recovery and purification of scandium from the waste sulfuric acid solution from titanium dioxide production by solvent extraction," *Journal of Environmental Chemical Engineering,* vol. 9, no. 5, p. 106226, 2021.

[130] J. Zhou, S. Ma, Y. Chen, S. Ning, Y. Wei, and T. Fujita, "Recovery of scandium from red mud by leaching with titanium white waste acid and solvent extraction with P204," *Hydrometallurgy,* vol. 204, p. 105724, 2021.

[131] Y. Liu *et al.*, "Extraction behavior and third phase formation of neodymium(III) from nitric acid medium in N,N′-dimethyl-N,N′-dioctyl-3-oxadiglcolamide," *Journal of Radioanalytical and Nuclear Chemistry,* vol. 318, no. 3, pp. 2087-2096, 2018/12/01 2018, doi: 10.1007/s10967-018-6261-y.

[132] G. Gongyi, C. Yuli, and L. Yu, "Solvent Extraction off Scandium from Wolframite Residue," *JOM,* vol. 40, no. 7, pp. 28-31, 1988/07/01 1988, doi: 10.1007/BF03258146.

[133] Q. Ye *et al.*, "Solvent extraction behavior of metal ions and selective separation Sc3+ in phosphoric acid medium using P204," *Separation and Purification Technology,* vol. 209, pp. 175-181, 2019.

[134] W. Zhang, T.-A. Zhang, G. Lv, W. Zhou, X. Cao, and H. Zhu, "Extraction separation of Sc (III) and Fe (III) from a strongly acidic and highly concentrated ferric solution by D2EHPA/TBP," *Jom,* vol. 70, no. 12, pp. 2837-2845, 2018.

[135] P. Zhang, S. You, L. Zhang, S. Feng, and S. Hou, "A solvent extraction process for the preparation of ultrahigh purity scandium oxide," *Hydrometallurgy,* vol. 47, no. 1, pp. 47-56, 1997/11/01/ 1997, doi: https://doi.org/10.1016/S0304-386X(97)00033-9.

[136] A. N. Chekhlov, "Crystal Structure of (2.2.2-Cryptand)lithium Perchlorate," *Russian Journal of Coordination Chemistry,* vol. 29, no. 12, pp. 828-832, 2003/12/01 2003, doi: 10.1023/B:RUCO.0000008393.57920.7d.

[137] J. S. Bradshaw, R. M. Izatt, P. B. Savage, R. L. Bruening, and K. E. Krakowiak, "The design of ion selective macrocycles and the solid-phase extraction of ions using molecular recognition technology: a synopsis," *Supramolecular Chemistry,* vol. 12, no. 1, pp. 23-26, 2000.

[138] T. Moeller, D. F. Martin, L. C. Thompson, R. Ferrús, G. R. Feistel, and W. J. Randall, "The Coordination Chemistry of Yttrium and the Rare Earth Metal Ions," *Chemical Reviews,* vol. 65, no. 1, pp. 1-50, 1965/02/01 1965, doi: 10.1021/cr60233a001.

[139] R. I. Ibrahim, M. K. Oudah, and A. F. Hassan, "Viscosity reduction for flowability enhancement in Iraqi crude oil pipelines using novel capacitor and locally prepared nanosilica," *Journal of Petroleum Science and Engineering,* vol. 156, pp. 356-365, 2017/07/01/ 2017, doi: https://doi.org/10.1016/j.petrol.2017.05.028.

[140] F. Nunes da Silva, M. M. Bassaco, D. A. Bertuol, and E. H. Tanabe, "An eco-friendly approach for metals extraction using polymeric nanofibers modified with di-(2-ethylhexyl) phosphoric acid (DEHPA)," *Journal of Cleaner Production,* vol. 210, pp. 786-794, 2019/02/10/ 2019, doi: https://doi.org/10.1016/j.jclepro.2018.11.098.

[141] S. Agarwal, I. Tyagi, V. K. Gupta, F. Hanifpour, M. Maghsudi, and H. Javadian, "Mo (IV) adsorption from nitric acid media by Di-(2-ethylhexyl) phosphoric acid (D2EHPA) coated silanized magnetite nanoparticles," *Journal of Molecular Liquids,* vol. 218, pp. 346-353, 2016.

[142] A. D. Salman *et al.*, "A selective hydrometallurgical method for scandium recovery from a real red mud leachate: A comparative study," *Environmental Pollution,* vol. 308, p. 119596, 2022/09/01/ 2022, doi: https://doi.org/10.1016/j.envpol.2022.119596.

[143] A. D. Salman *et al.*, "Scandium Recovery Methods from Mining, Metallurgical Extractive Industries, and Industrial Wastes," (in eng), *Materials (Basel),* vol. 15, no. 7, Mar 23 2022, doi: 10.3390/ma15072376.

[144] A. D. Salman *et al.*, "Novel Hybrid Nanoparticles: Synthesis, Functionalization, Characterization, and Their Application in the Uptake of Scandium (III)Ions from Aqueous Media," (in eng), *Materials (Basel),* vol. 13, no. 24, Dec 15 2020, doi: 10.3390/ma13245727.

[145] A. D. Salman *et al.*, "Potential Application of Macrocyclic Compounds for Selective Recovery of Rare Earth Scandium Elements from Aqueous Media," *Journal of Sustainable Metallurgy,* vol. 8, no. 1, pp. 135-147, 2022/03/01 2022, doi: 10.1007/s40831-021-00484-7.

[146] A. D. Salman *et al.*, "Synthesis and surface modification of magnetic Fe3O4@SiO2 core-shell nanoparticles and its application in uptake of scandium (III) ions from aqueous media," *Environmental Science and Pollution Research,* vol. 28, no. 22, pp. 28428-28443, 2021/06/01 2021, doi: 10.1007/s11356-020-12170-4.

Appendix A

Table S1. The CCRD for Sc extraction process and practical experimental values

No	Coded independent variables				Real independent variables				Objective function / dependent variables					
									E (%) K 2.2.2		E (%) DC18C6		E (%) C 2.2	
	X1	X2	X3	X4	MC (mol/L	pH of Sc	Time (min)	Sc (mg/L)	Experimental	Predicted	Experimental /	Predicted	Experimental /	Predicted
1	1	-1	-1	1	0.008	2	6	100	32	36	4.1	4.7	29	30
2	0	2	0	0	0.006	5	9	75	44.3	47	3.3	3.6	43	40
3	0	0	0	0	0.006	3	9	75	39.5	42	3	3.66	38	39.7
4	1	1	1	-1	0.008	4	12	50	89.6	92	5.2	4.8	88.5	90
5	-1	-1	1	1	0.004	2	12	100	8.7	6.2	1	0.9	7.3	10
6	0	0	0	-2	0.006	3	9	25	87.7	80	12.21	10.9	85	87
7	0	0	0	2	0.006	3	9	125	18.4	20.8	2.5	3	18	20
8	1	1	-1	1	0.008	4	6	100	90.8	85	9.11	8.8	88.2	87
9	-1	-1	-1	-1	0.004	2	6	50	10.6	13.8	1.7	2.3	9.4	12
10	-1	1	1	1	0.004	4	12	100	12.1	15	1.4	1.3	11.1	8.4
11	1	-1	1	-1	0.008	2	12	50	50	51	3.1	3.5	48.7	50
12	0	0	2	0	0.006	3	15	75	39	37	2.8	3	38.1	40
13	-2	0	0	0	0.002	3	9	75	5.3	2.1	0.89	0.93	3.5	5
14	0	0	0	0	0.006	3	9	75	39.5	43.8	2.68	3.1	36.7	35
15	-1	1	-1	1	0.004	4	6	100	11	9.7	1.37	1.2	9.4	10
16	1	1	-1	-1	0.008	4	6	50	89	93	7.8	8.5	87	86
17	2	0	0	0	0.01	3	9	75	99.3	99.8	9.6	9.66	96	98
18	0	-2	0	0	0.006	1	9	75	28.3	25	1.2	1.1	27.2	25.8
19	-1	1	-1	-1	0.004	4	6	50	10.6	15.3	2	2.5	7.9	9
20	-1	-1	1	-1	0.004	2	12	50	10	15.6	1.78	2	8.2	8
21	1	-1	1	1	0.008	2	12	100	33	30	4.3	3.2	28.6	26
22	-1	-1	-1	1	0.004	2	6	100	3.1	2.9	0.001	0.003	2.3	3
23	0	0	-2	0	0.006	3	3	75	38.4	32.7	2.5	2	36.5	35
24	-1	1	1	-1	0.004	4	12	50	10.5	14.6	2.1	1.9	7.7	11

25	1	-1	-1	-1	0.008	2	6	50	49.6	32.8	2.3	1.9	45.9	50
26	1	1	1	1	0.008	4	12	100	91.1	89.9	9.13	8	90	94
27	0	0	0	0	0.006	3	9	75	39.5	43.8	2.68	3.1	36	34
28	0	0	0	0	0.006	3	9	75	39.5	43.8	2.68	3.1	36	34
29	0	0	0	0	0.006	3	9	75	39.5	43.8	2.68	3.1	36	34
30	0	0	0	0	0.006	3	9	75	39.5	43.8	2.68	3.1	36	34

Table S2. Comparison between the RM leachate solution and final solution after multi SX (Protocol C**)**

	Elements	**Leachate concentration (mg/L)**		**Final concentration (mg/L)**
Protocol (C)	Al	2376		0
	Fe	4634		5
	Mg	127.5		3.83
	Er	630.9		0.11
	Ca	2104		8.17
	Na	1603		1.22
	Ti	699.6		0.05
	Si	2.93		0.14
	K	18.03		0
	Mn	141.8		0
	Ba	2.4		0
	Ce	9.51		1.86
	Co	2.45		0

	Cr	34.28		0
	Dy	0.37		0
	Eu	0.11		0
	Gd	0.81		1.47
	La	5.17		0
	Pr	1.93		0
	Sc	2.65		28.97
	Sm	1.07		0
	Sr	8.73		0.02
	Tb	0.31		0.09
	Th	1.99		0.07
	Y	3.38		0
	Yb	0.51		0.16
	Zr	10.28		0.4

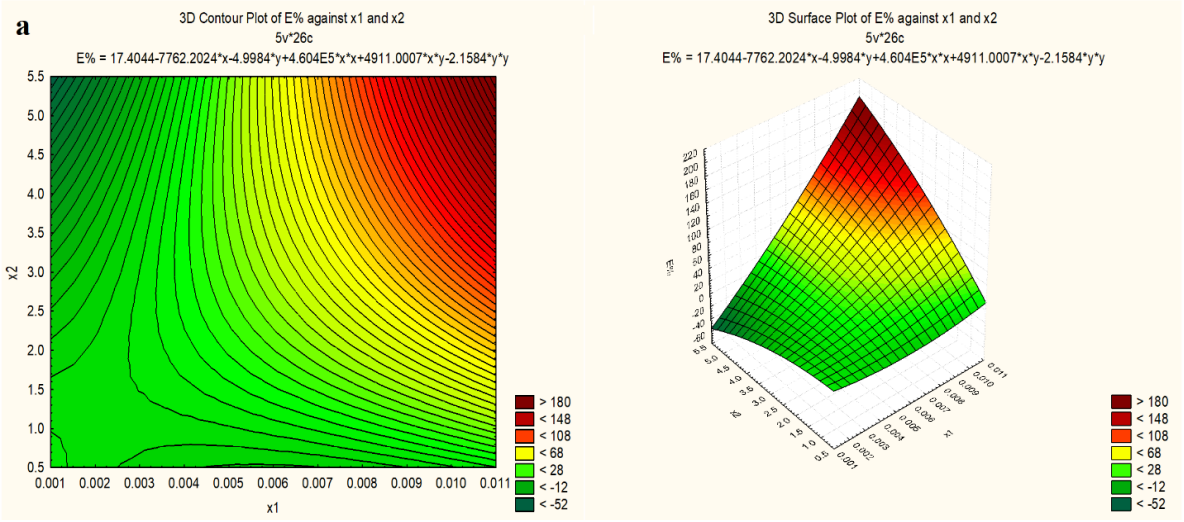
a
3D Contour Plot of E% against x1 and x2
5v*26c
E% = 17.4044-7762.2024*x-4.9984*y+4.604E5*x*x+4911.0007*x*y-2.1584*y*y
x2
x1
> 180
< 148
< 108
< 68
< 28
< -12
< -52
3D Surface Plot of E% against x1 and x2
5v*26c
E% = 17.4044-7762.2024*x-4.9984*y+4.604E5*x*x+4911.0007*x*y-2.1584*y*y
E%
x2
x1
> 180
< 148
< 108
< 68
< 28
< -12
< -52

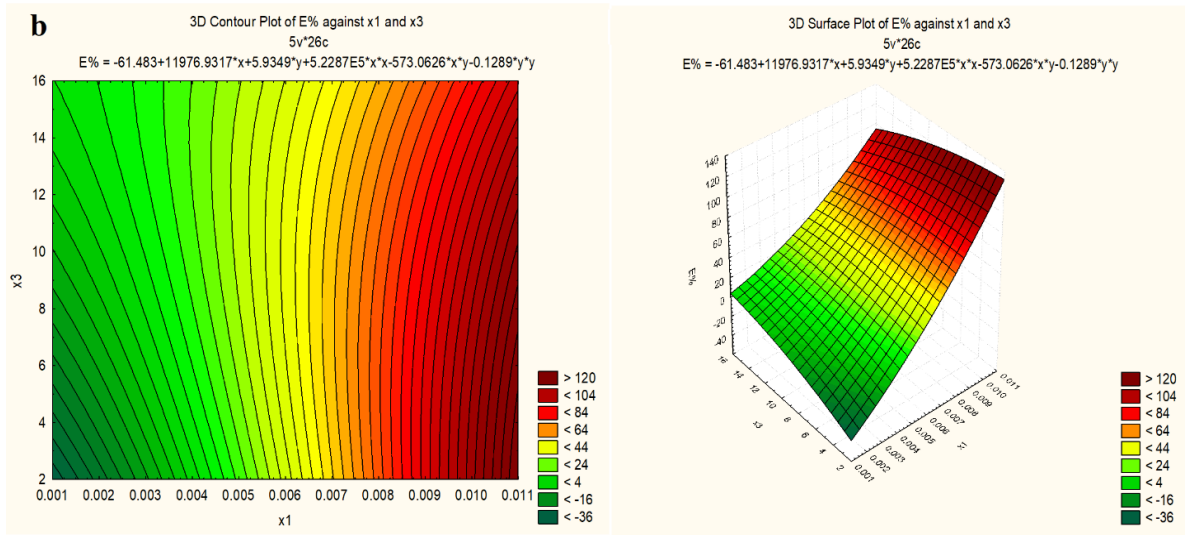
b
3D Contour Plot of E% against x1 and x3
5v*26c
E% = -61.483+11976.9317*x+5.9349*y+5.2287E5*x*x-573.0626*x*y-0.1289*y*y
x3
x1
> 120
< 104
< 84
< 64
< 44
< 24
< 4
< -16
< -36
3D Surface Plot of E% against x1 and x3
5v*26c
E% = -61.483+11976.9317*x+5.9349*y+5.2287E5*x*x-573.0626*x*y-0.1289*y*y
E%
x3
x1
> 120
< 104
< 84
< 64
< 44
< 24
< 4
< -16
< -36

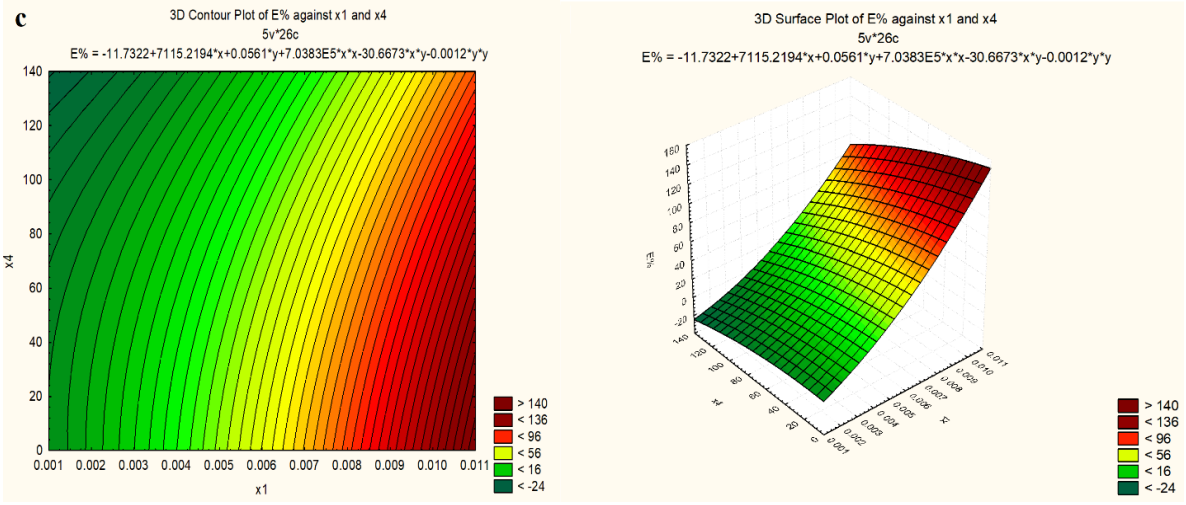
c
3D Contour Plot of E% against x1 and x4
5v*26c
E% = -11.7322+7115.2194*x+0.0561*y+7.0383E5*x*x-30.6673*x*y-0.0012*y*y
x4
x1
> 140
< 136
< 96
< 56
< 16
< -24
3D Surface Plot of E% against x1 and x4
5v*26c
E% = -11.7322+7115.2194*x+0.0561*y+7.0383E5*x*x-30.6673*x*y-0.0012*y*y
E%
x4
x1
> 140
< 136
< 96
< 56
< 16
< -24

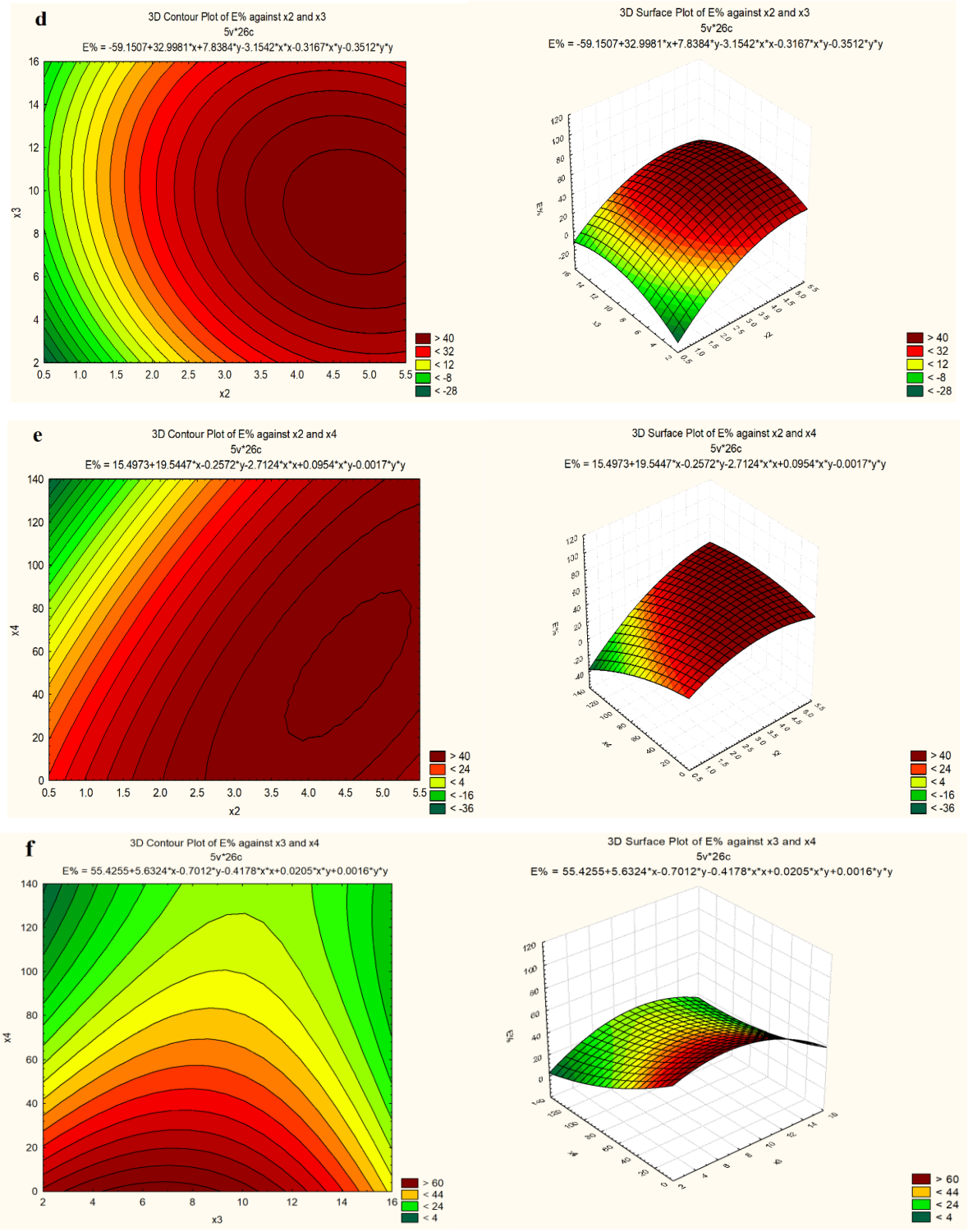

Fig. S1 3D-response surface and contour plot showing the interaction between variables of extraction by K 2.2.2 (a) X1-X2, (b) X1-X3, (c) X1-X4, (d) X2-X3, (e) X2-X4, (f) X3-X4

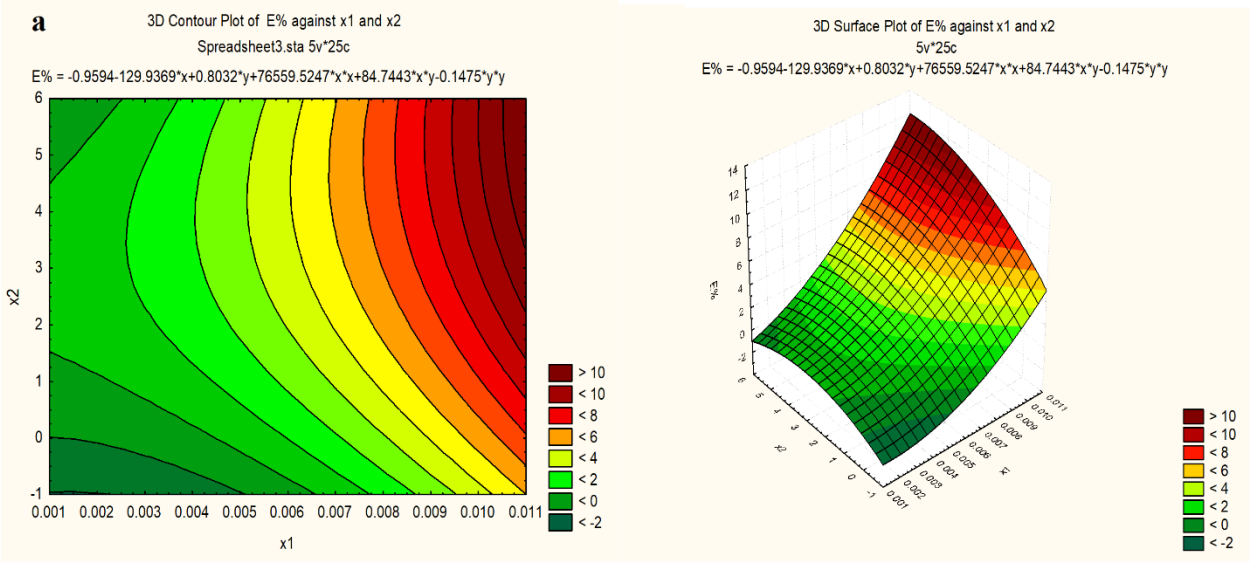
a
3D Contour Plot of E% against x1 and x2
Spreadsheet3.sta 5v*25c
E% = -0.9594-129.9369*x+0.8032*y+76559.5247*x*x+84.7443*x*y-0.1475*y*y
x2
x1
> 10
< 10
< 8
< 6
< 4
< 2
< 0
< -2
3D Surface Plot of E% against x1 and x2
5v*25c
E% = -0.9594-129.9369*x+0.8032*y+76559.5247*x*x+84.7443*x*y-0.1475*y*y
E%
x2
x1
> 10
< 10
< 8
< 6
< 4
< 2
< 0
< -2

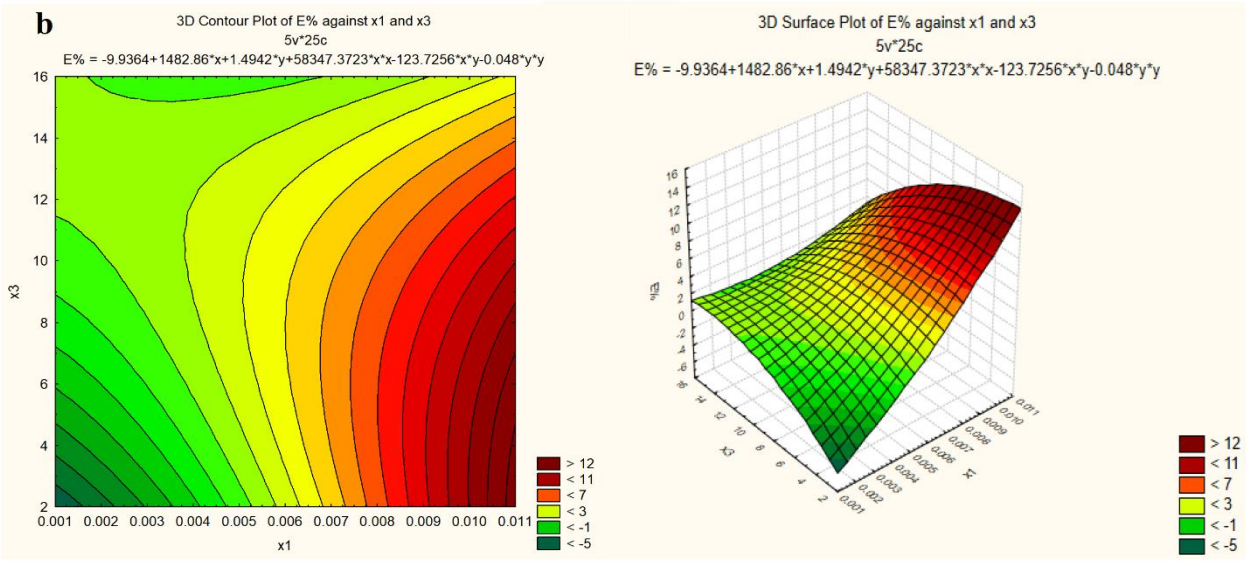
b
3D Contour Plot of E% against x1 and x3
5v*25c
E% = -9.9364+1482.86*x+1.4942*y+58347.3723*x*x-123.7256*x*y-0.048*y*y
x3
x1
> 12
< 11
< 7
< 3
< -1
< -5
3D Surface Plot of E% against x1 and x3
5v*25c
E% = -9.9364+1482.86*x+1.4942*y+58347.3723*x*x-123.7256*x*y-0.048*y*y
E%
x3
x1
> 12
< 11
< 7
< 3
< -1
< -5

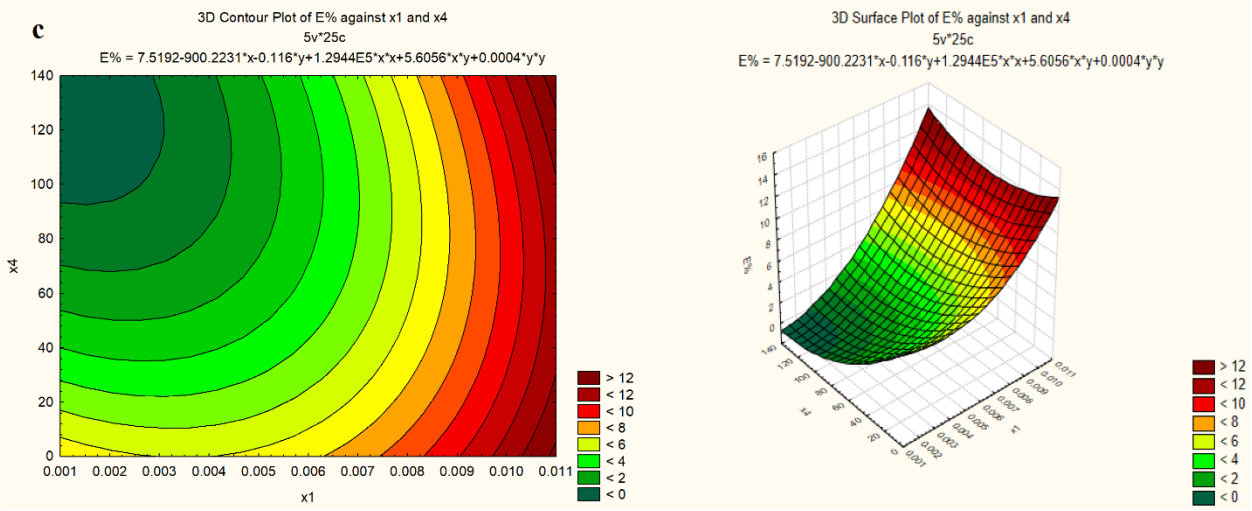
c
3D Contour Plot of E% against x1 and x4
5v*25c
E% = 7.5192-900.2231*x-0.116*y+1.2944E5*x*x+5.6056*x*y+0.0004*y*y
x4
x1
> 12
< 12
< 10
< 8
< 6
< 4
< 2
< 0
3D Surface Plot of E% against x1 and x4
5v*25c
E% = 7.5192-900.2231*x-0.116*y+1.2944E5*x*x+5.6056*x*y+0.0004*y*y
E%
x4
x1
> 12
< 12
< 10
< 8
< 6
< 4
< 2
< 0

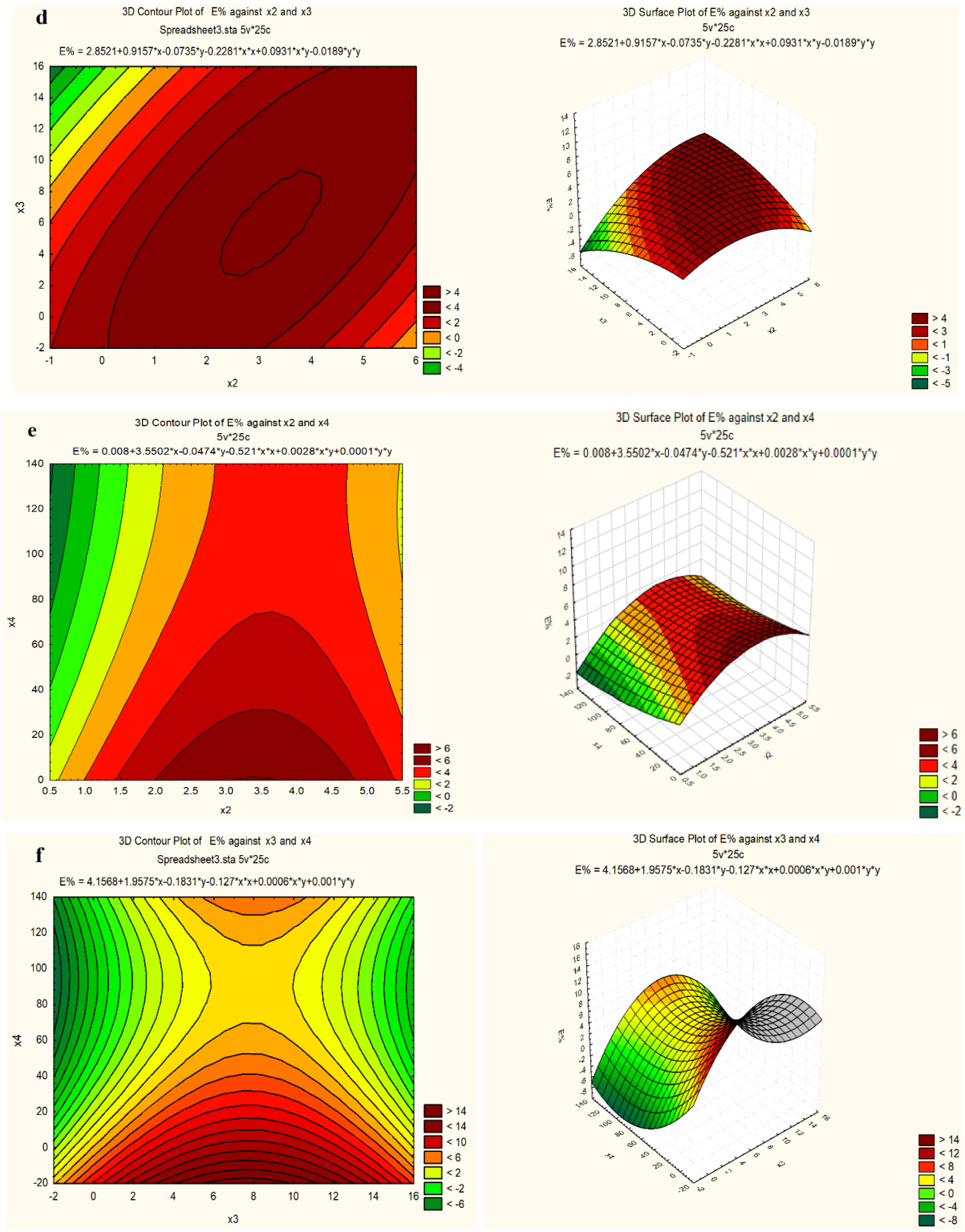

Fig. S2. 3D-response surface and contour plot showing the interaction between variables of extraction by DC18C6 (a) X1-X2, (b) X1-X3, (c) X1-X4, (d)X2-X3, (e) X2-X4, (f) X3-X4

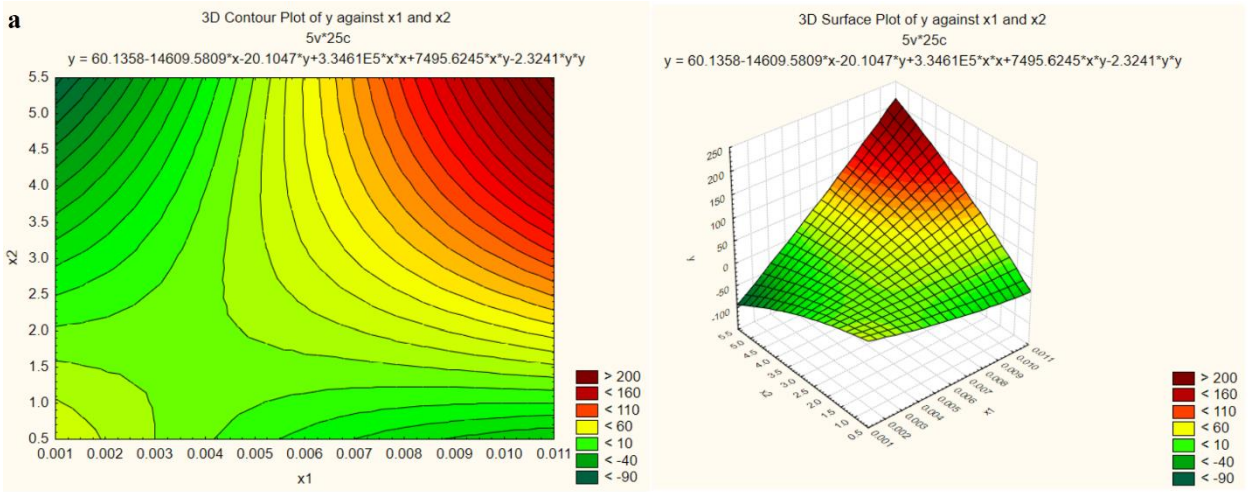
a
3D Contour Plot of y against x1 and x2
5v*25c
y = 60.1358-14609.5809*x-20.1047*y+3.3461E5*x*x+7495.6245*x*y-2.3241*y*y
x2
x1
> 200
< 160
< 110
< 60
< 10
< -40
< -90
3D Surface Plot of y against x1 and x2
5v*25c
y = 60.1358-14609.5809*x-20.1047*y+3.3461E5*x*x+7495.6245*x*y-2.3241*y*y
y
x2
x1
> 200
< 160
< 110
< 60
< 10
< -40
< -90

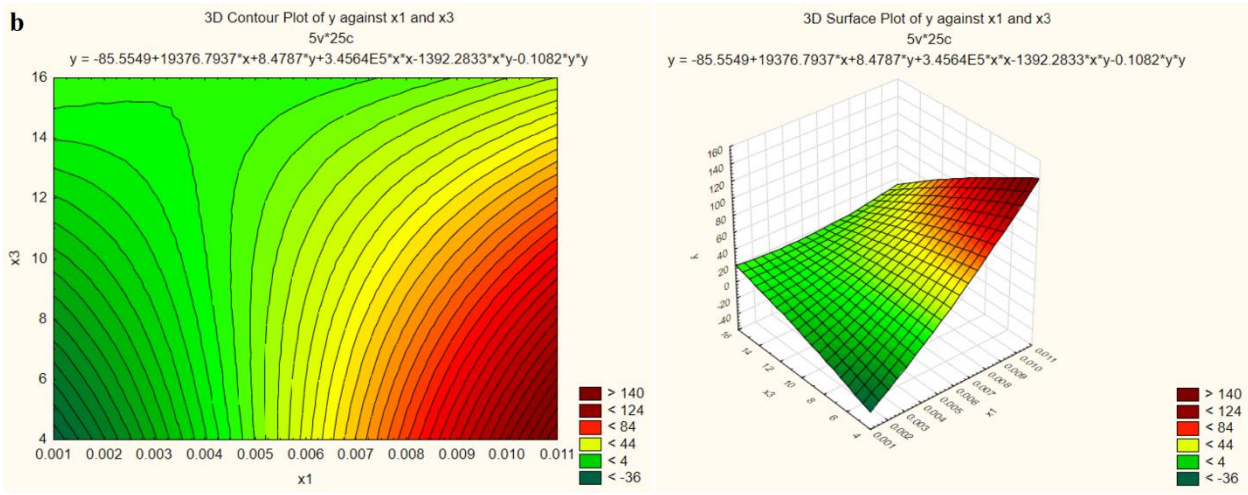
b
3D Contour Plot of y against x1 and x3
5v*25c
y = -85.5549+19376.7937*x+8.4787*y+3.4564E5*x*x-1392.2833*x*y-0.1082*y*y
x3
x1
> 140
< 124
< 84
< 44
< 4
< -36
3D Surface Plot of y against x1 and x3
5v*25c
y = -85.5549+19376.7937*x+8.4787*y+3.4564E5*x*x-1392.2833*x*y-0.1082*y*y
y
x3
x1
> 140
< 124
< 84
< 44
< 4
< -36

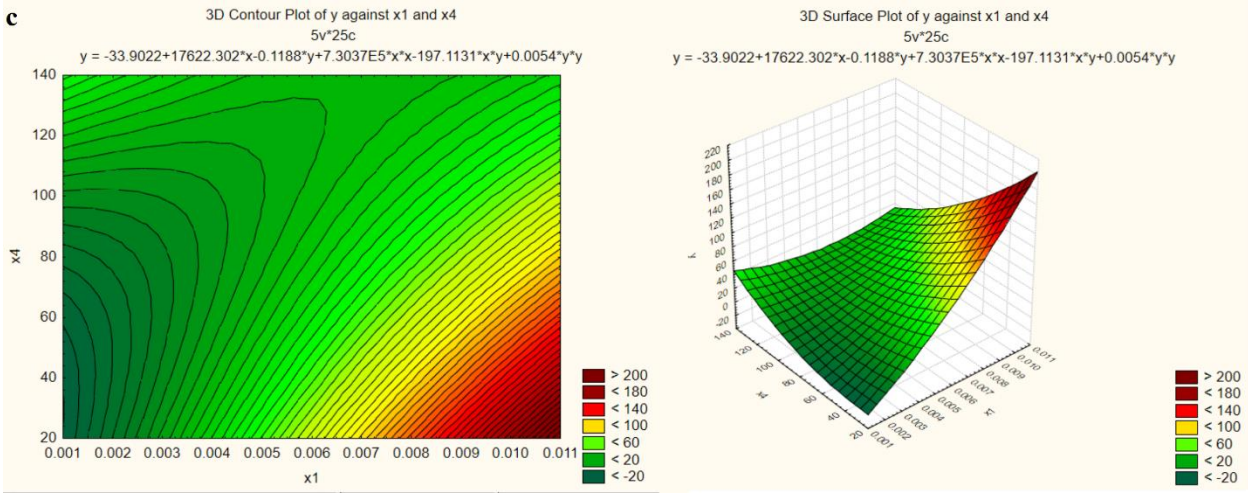
c
3D Contour Plot of y against x1 and x4
5v*25c
y = -33.9022+17622.302*x-0.1188*y+7.3037E5*x*x-197.1131*x*y+0.0054*y*y
x4
x1
> 200
< 180
< 140
< 100
< 60
< 20
< -20
3D Surface Plot of y against x1 and x4
5v*25c
y = -33.9022+17622.302*x-0.1188*y+7.3037E5*x*x-197.1131*x*y+0.0054*y*y
y
x4
x1
> 200
< 180
< 140
< 100
< 60
< 20
< -20

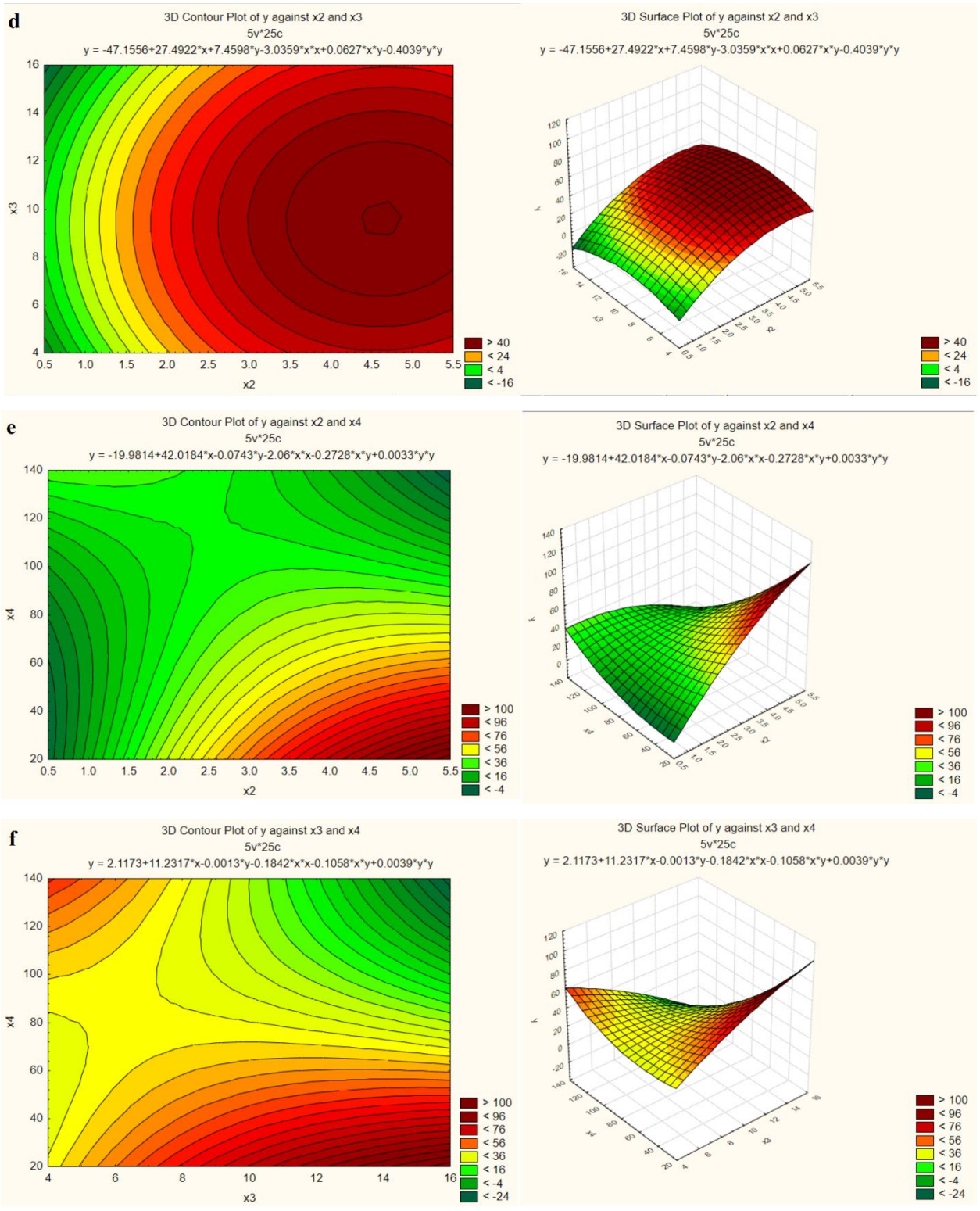

Fig. S3. 3D-response surface and contour plot showing the interaction between variables of extraction by C 2.2(a) X1-X2, (b) X1-X3, (c) X1-X4, (d) X2-X3, (e) X2-X4, (f) X3-X4

Appendix B

Publications related to dissertation:

1. **Salman, A. D**.; Juzsakova, T.;Jalhoom, M. G.;Abdullah, T. A.;Le, P.-C.; Viktor, S.; Domokos, E.; Nguyen, X. C.; La, D. D.; Nadda, A. K.; Nguyen, D. D., A selective hydrometallurgical method for scandium recovery from a real red mud leachate: A comparative study. Environmental Pollution, 2022, 308, 119596. **IF= 9.9.**
2. **Salman, A. D**.; Juzsakova, T.; Rédey, Á.; Le, P.-C.; Nguyen, X. C.; Domokos, E.; Abdullah, T. A.; Vagvolgyi, V.; Chang, S. W.; Nguyen, D. D., Enhancing the Recovery of Rare Earth Elements from Red Mud. Chemical Engineering & Technology 2021, 44 (10), 1768-1774. **IF= 1.7**
3. **Salman, A. D**.; Juzsakova, T.; Mohsen, S.; Abdullah, T. A.; Le, P.-C.; Sebestyen, V.; Sluser, B.; Cretescu, I., Scandium Recovery Methods from Mining, Metallurgical Extractive Industries, and Industrial Wastes. Materials 2022, 15 (7), 2376. **IF= 3.7.**
4. **Salman, A. D**.; Juzsakova, T.; Jalhoom, M.; Ibrahim, R.; Domokos, E.; Al-Mayyahi, M.; Abdullah, T.; Szabolcs, B.; Al-Nuzal, S., Studying the extraction of scandium (III) by macrocyclic compounds from aqueous solution using optimization technique. International Journal of Environmental Science and Technology, 2022, 1-18. **IF= 3.5.**
5. **Salman, A. D**.; Juzsakova, T.; Jalhoom, M. G.; Le Phuoc, C.; Mohsen, S.; Adnan Abdullah, T.; Zsirka, B.; Cretescu, I.; Domokos, E.; Stan, C. D., Novel hybrid nanoparticles: synthesis, functionalization, characterization, and their application in the uptake of scandium (III) ions from aqueous media. Materials, 2020, 13 (24), 5727. **IF= 3.6.**
6. **Salman, A. D**.; Juzsakova, T.; Jalhoom, M. G.; Le, P.-C.; Abdullah, T. A.; Cretescu, I.; Domokos, E.; Nguyen, V.-H., Potential Application of Macrocyclic Compounds for Selective Recovery of Rare Earth Scandium Elements from Aqueous Media. Journal of Sustainable Metallurgy, 2022. **IF= 3.**
7. **Salman, A. D**.; Juzsakova, T.; Ákos, R.; Ibrahim, R. I.; Al-Mayyahi, M. A.; Mohsen, S.; Abdullah, T. A.; Domokos, E., Synthesis and surface modification of magnetic Fe_3O_4@ SiO_2 core-shell nanoparticles and its application in uptake of scandium (III) ions from aqueous media. Environmental Science and Pollution Research 2021, 28 (22), 28428-28443. **IF= 3.5.**